NANYANG TECHNOLOGICAL UNIVERSITY

PROCESSING AND MECHANICAL PROPERTIES OF CARBON NANOTUBE REINFORCED ALUMINUM COMPOSITES

LIAO JINZHI

SCHOOL OF MECHANICAL & AEROSPACE ENGINEERING

2012

PROCESSING AND MECHANICAL PROPERTIES OF CARBON NANOTUBE REINFORCED ALUMINUM COMPOSITES

LIAO JINZHI

School of Mechanical & Aerospace Engineering

A thesis submitted to the Nanyang Technological University
in fulfillment of the requirement for the degree of
Doctor of Philosophy

2012

ABSTRACT

Current and future challenges of aerospace and automotive application have led to design and development of novel materials, which reduce weight combined with improved strength. In recent years, aluminum (Al) composites reinforced by carbon nanotube (CNT) have attracted increasing attention, due to the extraordinary high strength and stiffness of CNTs. In the development of Al-CNT composites, several issues are of significance: (i) successful fabrication process of Al-CNT composites with low processing cost coupled with good mechanical properties; (ii) understanding their structural evolution during the processing; (iii) identifying their mechanical properties using different means. This project aims to synthesize Al-CNT composites coupled with improved strength, reliability and reproducibility in processing and to investigate their mechanical properties.

In this work, Al/Al-CNT composites were synthesized using powder metallurgy (P/M) technique followed by secondary processing. 0-2.0wt.% of CNTs were added as reinforcements. CNT incorporation into the Al matrix simultaneously improved the densification, hardness and tensile strength of the materials. The improved yield strength was attributed to the load partition effect of CNT, thermal mismatch between matrix and CNT, and Orowan strengthening. Besides, a novel Spread-Dispersion (SD) technique has been proposed to produce Al-CNT nanocomposite, and an enhancement in tensile strength of 66% of the Al-CNT nanocomposite was obtained compared with the monolithic counterpart. The separation of CNTs was affected by both the powder mixing and the secondary operation.

Special attention was given to the room- and elevated-temperature tension, nanoindentation and fatigue properties evaluation. It was found that the values of nanoindentation hardness and elastic modulus reached maximum at the 0.5wt.% CNT added to Al samples. The elevated-temperature tensile tests (25-500°) revealed that the incorporation of CNT improved the strength of the composites, but the ductility of the composites continuously decreased with increasing temperature (hot embrittlement). The causes of such a hot embrittlement were attributed to the interfacial segregation, large surface contact area of matrix/CNT, and CNT clusters. Furthermore, fatigue results showed that CNTs could slow fatigue crack propagation by crack-bridging, CNT frictional pullout, and breakage mechanism. At lower CNT content composite (0.5wt.%), fatigue cracks grew tortuously to avoid CNTs, whilst they grew along CNT clusters at higher reinforcement content (2.0wt.%).

In short, Al-CNT composites were successfully processed by an appropriate combination of volume content of the reinforcement, the CNTs and metal powder mixing technique, the subsequent consolidation and secondary processing. Especially at an optimum content of CNT (0.5wt.%), the Al-CNT composites showed significantly improved densification, nanoindentation modulus, hardness, tensile strength at room and elevated temperature, and fatigue resistance (though decreased failure strain) compared with the unreinforced counterparts.

ACKNOWLEDGEMENTS

The author would like to express her most sincere appreciation to her supervisor, Dr. Ming-Jen Tan, for his professional guidance and patient supervision. His working attitude with great effectiveness and strong responsibility is appreciated. Without his insightful criticism and expert guidance, this thesis could not reach its present form.

Many thanks to her co-supervisor, Dr. Idapalapati Sridhar, for his precious advice and encouragement.

Thanks to Dr. David Lee Butler, Dr. Khor Khiam Aik, Dr. Yu Ligen, Dr. Zhou Wei, Dr. Chai Gin Boay for their kind permission to use their equipments.

Thanks to all the technical staffs and students of Materials Laboratory, School of Mechanical and Aerospace Engineering, especially Ms Meiyoke Yong, Mr Pang Jianjun, Dr Yang Hongwang, Mr Yahya Motemani Sharabiani, Mr Sa'Don Bin Ahmad, Mr Leong Kwok Phui, Dr. Liu Qinglin, Dr. Khun Nay Win, Dr Wang Zhiying for their technical assistance and useful discussions.

Thanks are given to all those who helped me during the writing of this thesis.

And most importantly, the author would like to acknowledge Nanyang Technological University, Singapore, for financial support in the form of a graduate scholarship.

CONTENTS

LIST OF ABBREVIATIONS

Al	Aluminum
AMCs	Aluminum matrix composites
CNT	Carbon nanotube
CTE	Coefficient of thermal expansion
Cu	Copper
EDS	Energy dispersive spectrometry
FESEM	Field emission scanning electron microscopy
HRTEM	High-resolution transmission electron microscopy
IFSS	Interfacial shear stress
I/M	Ingot metallurgy
Mg	Magnesium
MMCs	Metal matrix composites
MWCNT	Multi-walled carbon nanotube
Ni	Nickel
OM	Optical microscopy
P/M	Powder metallurgy
RD	Rolling direction
SD	Spread-Dispersion
SEM	Scanning electron microscopy
SPS	Spark plasma sintering
SSA	Specific surface area
SWCNT	Single-walled carbon nanotube
TEM	Transmission electron microscopy
XRD	X-ray diffraction

LIST OF FIGURES

LIST OF TABLES

CHAPTER 1

INTRODUCTION

1.1 Background

Metal matrix composites (MMCs) have been the object of a significant and sustained research and design effort in the past three decades [1]. The primary support for these composites has come from the aerospace industry for airframe and spacecraft components. MMCs combine metallic matrix properties (ductility and toughness) with reinforcement properties (high strength and high modulus), leading to greater strength in shear and compression and higher service temperature capabilities [2]. The high performance of MMCs has made them attractive candidate materials for aerospace, automotive, recreation industries and other structural applications.

Current and future challenges of aerospace and automotive application have led to design and development of novel materials, which reduce weight combined with improved strength, and there have been continuous efforts endeavored in this area. Compared with the conventional macro- and micro-reinforcements, like SiC, Al_2O_3, B_4C, ZrO_2, Y_2O_3, etc, the nano-scale reinforcements exhibit some advantages, like smaller inter-particle spacing and higher interfacial contact area. In recent years, extensive interest has been attracted to nano-reinforcement composites. No other nano-filler, however, has gained as much attention as that of carbon nanotubes (CNTs).

Since the first observation of CNTs in 1991 [3], work carried out in recent years has revealed the intriguing mechanical, electrical and thermal properties of these novel molecular scale wires [4-29]. Due to the intrinsic strength of carbon–carbon sp^2 bond and their special structure, CNTs have extraordinary high mechanical strength and stiffness. Experimental measurements have indicated that single-walled nanotubes (SWCNTs) have Young's moduli ranging from 1 to 5TPa, and multi-walled nanotubes (MWCNTs) show an average value of 1.8TPa [5]. Additionally, CNTs possess relatively low density, varying from 1.2g/cm^3 for SWCNTs and up to 1.8g/cm^3 for MWCNTs [5]. These give CNTs a high specific strength of 55.55GPa/(mg/m^3) and high specific modulus of 555.55GPa/(mg/m^3) [5], which make them ideal nanoscale reinforcement phase in composites. In a sense they may be the next generation of carbon fibers.

Many researchers have endeavored to develop advanced CNT based composites using metallic, polymeric and ceramic matrices. However, in CNT reinforced composite materials, the development of metallic-CNT composites are far less than that of polymeric-CNT ones. This is quite surprising considering that metals are the most commonly used structural materials in today's world [26]. The slower development of metallic-CNT composites is mainly due to the fact that MMCs are significantly more difficult to be produced compared with polymeric matrix composites. In metallic-CNT composites, the most commonly used metal materials are aluminum (Al), nickel (Ni), copper (Cu) and magnesium (Mg). Amongst them Al and its alloys are the most widely used materials as the metal matrix in recent years. This is mainly attributed to several reasons: firstly, the low density of Al alloys, which is the first requirement in most applications; secondly, they are cheaper compared with other low density alloys; thirdly,

Al alloys are very well-known alloys due to their high use in several industries, from aeronautics and automotive to leisure. Their excellent behavior, from different points of view, i.e., specific strength and stiffness, corrosion resistance, machinability and workability, is very well known and can be modified in order to satisfy different applications [30].

Although there has been increasing effort on the development of CNT reinforced Al composites (Al-CNT) [15-16, 25, 31-33], only a few improvements on Al-CNT composites have been reported, which is mainly attributed to the processing difficulties and lack of understanding of the strengthening mechanisms, and most importantly, cost. The establishment of an appropriate and economical processing practice for CNT reinforced Al nanocomposites is still a challenge. Furthermore, to date, the majority of the mechanical properties evaluation on Al-CNT bulk composite has been only focused on the tensile tests at room temperature. There is limited report on other mechanical properties of these composites, such as nanoindentation, high temperature tensile properties and fatigue resistance, etc. Further work in the evaluation on these properties would be of value.

1.2 Objective:

Accordingly, the main objectives of this project form two parts:

(1) Synthesis of Al-CNT composites coupled with improved strength, reliability and reproducibility in processing.

(2) Investigation the mechanical properties of the Al-CNT composites.

1.3 Scope

Based on the objectives of this study, the scope of this work consists of:

(1) Fabrication of Al-CNT composites using powder metallurgy (P/M) technique. The processing-microstructure-properties relationships between Al-CNT composites will be studied.

(2) CNT evolution during composite fabrication process will be studied.

(3) Al-CNT composite fabricated by a simple Spread-Dispersion (SD) process will be discussed.

(4) Local mechanical properties of Al-CNT specimens will be detected by nanoindentation.

(5) Room-temperature tension tests of Al-CNT composites will be conducted.

(6) Elevated-temperature tension tests of Al-CNT composites will be conducted.

(7) Fatigue tests of Al-CNT composites will be conducted.

The novelty of this project is:

- Al-CNT composites to be developed are novel materials which have potential to be used in commercial application, such as aerospace industry, automotives parts, household products, sport utilities, etc.
- Investigation of the mechanical properties of the novel Al-CNT composites.

1.4 Organization

The present thesis is divided into 11 chapters. The first chapter briefly introduces MMCs and CNTs and brings out the advantages and limitations of Al-CNT composites. The available reports on the current development of Al-CNT composites have been reviewed in Chapter 2. Chapter 3 describes the experimental details. Detailed analysis of the processing-microstructure-properties relationships and strengthening mechanisms are made in Chapter 4. Chapter 5 studies the CNT evolution in the powder metallurgy processing. In Chapter 6, well-dispersed CNTs reinforced Al matrix composite fabricated by a novel Spread-Dispersion (SD) process is stated. Chapter 7 studies the nanoindentation behavior of Al-CNT composites. Chapter 8 studies the elevated-temperature tensile behavior of the Al-CNT composites. Chapter 9 studies the fatigue behavior of the Al-CNT composites. Finally, the conclusions and recommendations for future work are presented in Chapter 10 and 11, respectively.

1.5 Summary

This chapter provides a background on the existing problems that are encountered in the development of carbon nanotube reinforced aluminum matrix composites. The objectives of this research work are stated, and the scope of the work is given. The thesis organization is described in the final section of this chapter.

CHAPTER 2

LITERATURE REVIEW

2.1 Aluminum (Al) & Al Composites Basics

2.1.1 Background

Aluminum is the most abundant metal in the Earth's crust, and the third most abundant element, after oxygen and silicon, making up about 8.2 % by weight of the Earth's solid surface [34]. Aluminum is too reactive chemically to occur in nature as the free metal. The most important source of aluminum is bauxite, which provides with over 99 % of the metal [34]. The basic physical properties of aluminum are displayed in Table 2-1.

Among the most striking characteristics of aluminum is its versatility. The range of physical and mechanical properties that can be developed from refined high-purity aluminum to the most complex alloys is remarkable. The properties of aluminum that make this metal and its alloys the most economical and attractive for a wide variety of uses are appearance, light weight, fabricability, physical properties, mechanical properties, and corrosion resistance. Aluminum has a density of 2.7g/cm^3, approximately 1/3 of steel (7.83g/cm^3), copper (8.93g/cm^3). Aluminum has good corrosion resistance. The exposed surface of aluminum combines with oxygen to form an inert aluminum oxide film protecting further oxidation. By appropriately treated, aluminum can resist corrosion by water, salt and other environmental factors. Besides, aluminum exhibits other excellent

physical properties, like excellent electrical and thermal conductivity. Aluminum is nonferromagnetic, a property of importance in the electrical and electronics industries [35]. Aluminum is of high machinability and workability. The attractive properties of the aluminum alloys have made them widely used in a variety of industries including transport, food preparation, energy generation, packaging, architecture, and electrical transmission applications.

Table 2-1. Basic properties of aluminum.

Atomic Symbol	Al
Atomic Number	13
Atomic Weight	26.98154
Density	2.6989 g/cm^3
Hardness, Vickers	15
Elastic Modulus	68 GPa
Shear Modulus	25 GPa
Atomic Radius	143.1 pm
Electron Configuration	3s23p1
Melting Point	660 °C
Boiling Point	2519 °C
Thermal Conductivity	210 W/m · K
Specific Heat Capacity	0.900 J/g · °C

2.1.2 Aluminum Metal Matrix Composites

Metal matrix composites (MMCs) have been extensively studied since many years, and the primary support has come from the aerospace industry for airframe and spacecraft components [36]. MMCs combine metallic properties (ductility and toughness) with ceramic properties (high strength and high modulus), leading to greater strength in shear and compression and higher service temperature capabilities [2]. The high performance of MMCs has made them attractive candidate materials for aerospace, automotive, recreation industries and other structural applications.

MMCs generally consist of two components: one is the metal matrix and the other is the reinforcement. The matrix is the monolithic material providing a support into which the reinforcements are embedded. Numerous metals have been used as matrices. The most important have been light metals such as aluminum, magnesium or titanium, and cobalt and cobalt-nickel alloys, and copper alloys and superalloys.

The reinforcement is embedded into the matrix. MMCs reinforcements can be generally divided into five major categories: continuous fibers, discontinuous fibers, whiskers, wires and particulate (including platelets). Typical reinforcement materials are oxides, carbides and nitrides which are used because of their excellent combinations of specific strength and stiffness at both ambient temperature and elevated temperature [36].

For a long period of time, aluminum and its alloys were some of the most widely used materials as the matrix in MMCs, both in research and development and in industrial

applications. This is mainly attributed to several reasons: First, the low density of aluminum alloys, which is the first requirement in most applications. Second, they are cheaper compared with other low density alloys (such as Mg or Ti). Third, aluminum alloys are very well-known alloys due to their high use in several industries, from automotive and aeronautics to leisure. Their excellent behavior, from different points of view, i.e., strength, ductility, corrosion, is very well known and can be modified in order to satisfy different applications [30]. Among various reinforcements, the widely used particle for reinforcing Al alloys is SiC_p and Al_2O_3, due to their low cost and wide range of available grades.

The major advantages of aluminum metal matrix composites by comparison with the unreinforced materials are as follows [37]:

- Greater strength
- Improved stiffness
- Improved high temperature properties
- Enhanced and tailored electrical performance
- Improved abrasion and wear resistance
- Improved damping capabilities

2.2 Carbon Nanotube (CNT) Basics

2.2.1 Family of Carbon

Until 1980's, it was accepted that diamond and graphite are the only two physical forms of pure carbon. Their atoms were covalently bonded. Diamond crystallizes in cubic unit cell and it has two interpenetrating FCC structure in which the atoms are connected by covalent bonds [38], see Figure 2-1(a). It is a good insulator since it has no free electrons [38]. Graphite crystallizes in a layer or sheet structure. The carbon atoms in the layer are connected together in a hexagonal structure by covalent bonding as diamond [38], see Figure 2-1(b). It has high electrical conductivity since it has free electrons. The layers are connected by van der Walls forces.

In 1985, C_{60} was found. It was spherical in shape and formed a ball with 32 faces, called buckerminsterfullerence or buckyball in short, see Figure 2-1(c). After this discovery, other spherical shape buckyball with different molecules, C_{36}, C_{70}, C_{76} and C_{84} were also found. They consist of hexagons and pentagons. The above new allotropes of carbon family are recognized as the fullerenes. The unique geometric construction of carbon atoms exist not only in the buckyball shape, but also found to be existence as cylinder shape. They are carbon nanotubes (CNTs), see Figure 2-1(d). The family of carbon is shown in Figure 2-1.

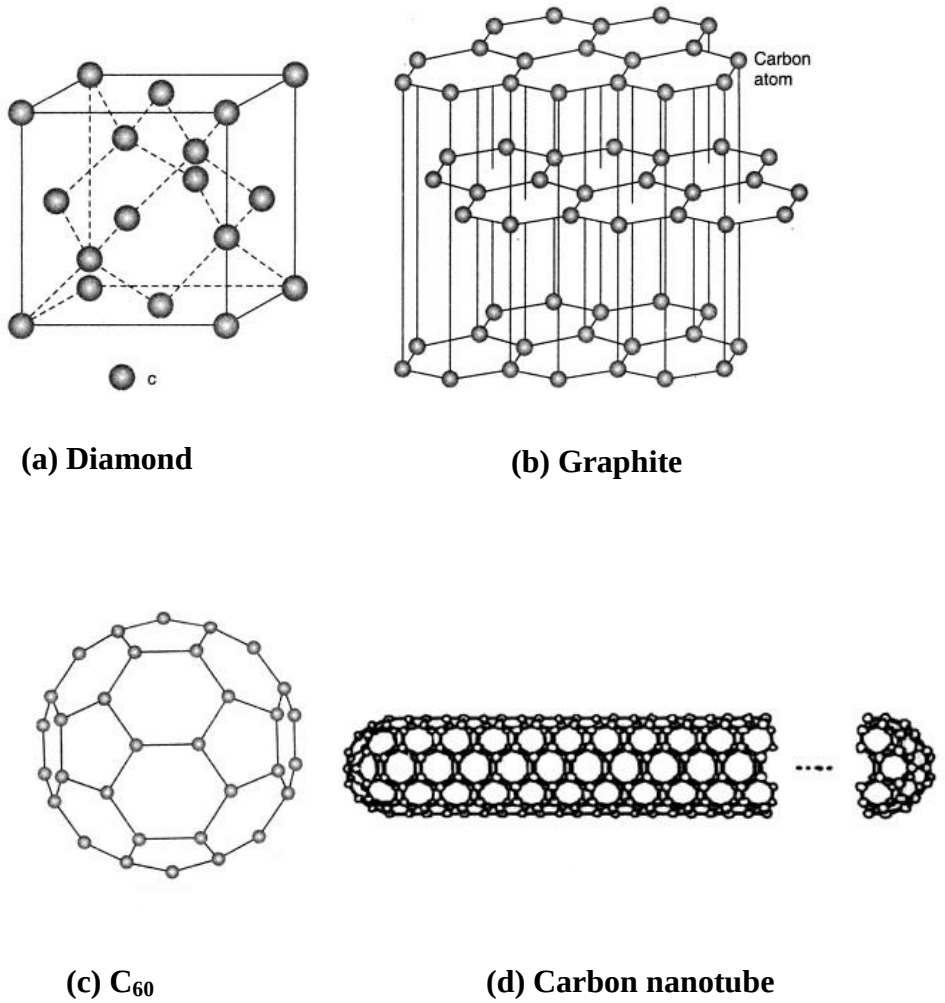

(a) Diamond **(b) Graphite**

(c) C_{60} **(d) Carbon nanotube**

Figure 2-1. Allotropy of carbon [38].

2.2.2 CNTs

The first observation of nanotubes was made at the negative end of the electrode during the arc discharge production of fullerenes. Japanese researcher Iijima [3] used high resolution TEM to observe these multi-wall carbon nanotubes (MWCNTs) and first published them, which was immediately recognized as an important novel material and attracted long and continuous interest on them in the last two decades. Consequently the discovery of single-walled nanotubes was made in 1993 [39-40]. The atomic structure of a CNT can be visualized (imagined) as a lay of graphene (a single atom thick graphite), rolling up into a seamless nanometer-sized cylinder. CNTs are also called buckytubes. Different types of CNTs can be produced by rolling up the graphene in certain direction. The main types are armchair (n,n), zig-zag (n,0), and chiral (n,m), as shown in Figure 2-2.

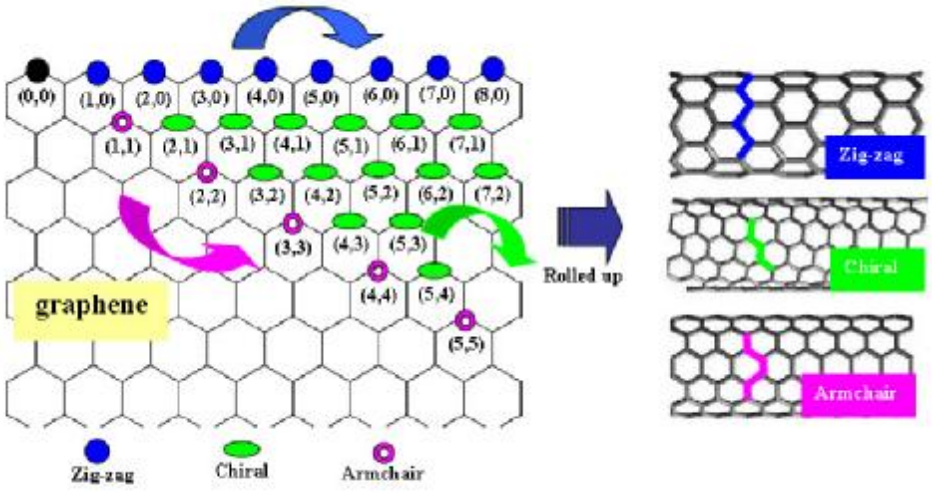

Figure 2-2. Different types of CNTs can be produced by rolling up the graphene in certain direction. The main types are armchair (n,n), zig-zag (n,0), and chiral (n,m) [41].

These nano-wires consists single-walled nanotubes (SWNTs), double-walled nanotubes (DWNTs) and multi-walled nanotubes (MWNTs). SWCNTs are tubes of a lay of graphite rolling up into a cylinder with two ends capped. Likewise, DWCNTs have double lays of graphites, and MWCNTs have more than two lays. High resolution transmission electron micrographs (HRTEM) of SWCNT, DWCNT and MWCNT are shown in Figure 2-3 (a) to (c) [42-44], respectively.

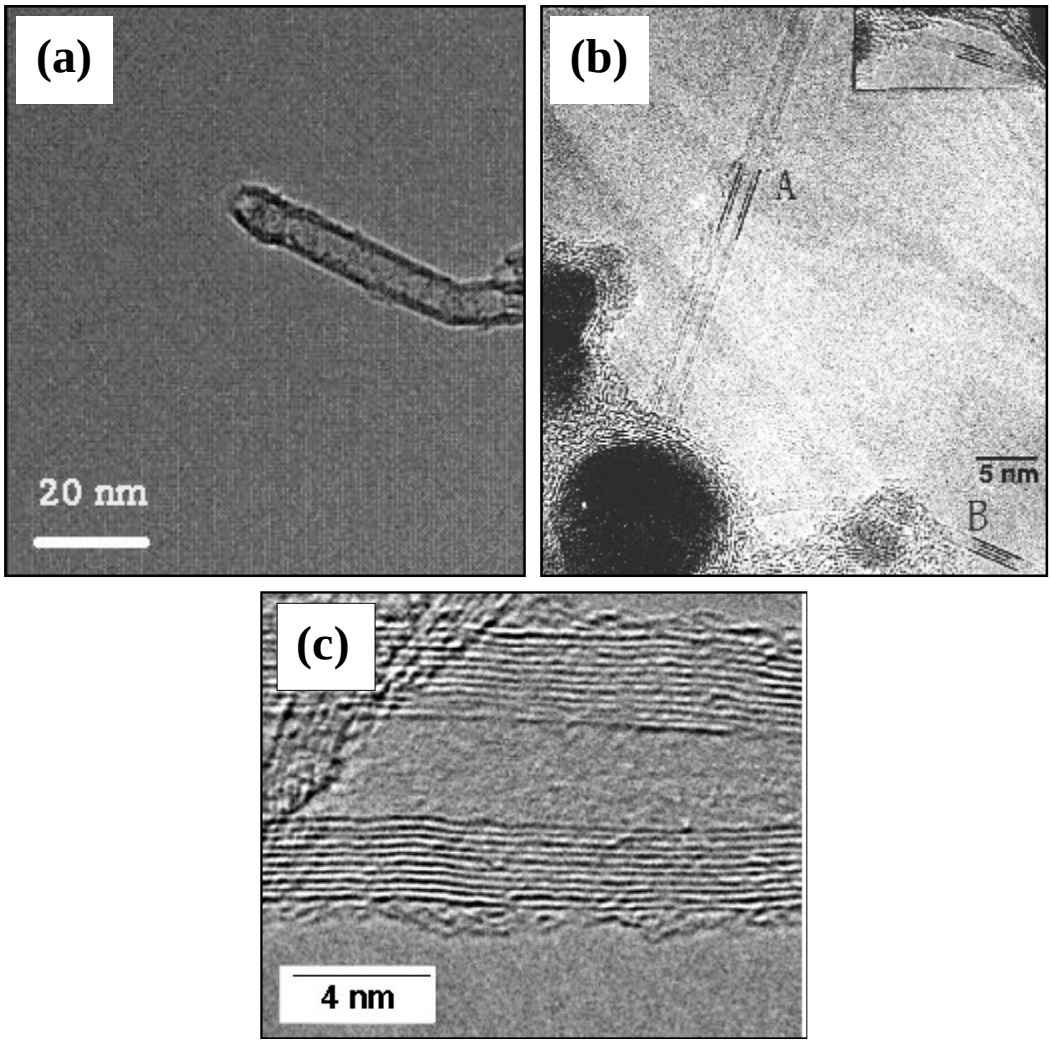

Figure 2-3. HRTEM images of (a) SWCNT [42]; (b) DWCNT [43]; and (c) MWCNT [44].

Fundamentally, CNTs are chemically bonded with sp^2 bonds, an extremely strong form of molecular interaction, which determine the extra-high strength and stiffness of the CNTs. Experimental measurements have indicated that SWCNTs have Young's moduli ranging from 1 to 5TPa, and MWCNTs show an average value of 1.8TPa [5]. Additionally, CNTs possess relatively low density, varying from 1.2g/cm^3 for SWCNTs and up to 1.8g/cm^3 for MWCNTs [5]. These give CNTs a high specific strength of 55.55GPa/(mg/m^3) and high specific modulus of 555.55GPa/(mg/m^3), which make them ideal nanoscale reinforcement phase in composites [5]. Further, compared to the traditional micrometer-sized reinforcements, such as carbon fiber and SiC_p, the deformation characteristics of nanotubes are also intriguing. Carbon fiber are stiff but brittle and act as rigid rod, while CNTs are elastic and can be readily bent, buckled, twisted, flattened or tangled without breaking (Figure 2-4), so CNTs are flexible, remaining in arbitrary shapes when bending in composites [45]. In a sense they may be the next generation of carbon fibers.

The novel properties of CNTs make them potentially useful in many applications in electronics, optics, catalyst and other fields of materials science [4-7, 9-12, 46-47]. One attractive application is that CNTs act as fiber reinforcements in composite materials, due to their remarkable mechanical and geometrical properties (extremely high Young's modulus and rupture strength, high aspect ratio, nanometre-range diameter). Since the last decade, many researchers have endeavored to develop advanced CNT based composites using metals, polymers and ceramic matrix phases [15-16, 19, 21, 28, 48-62].

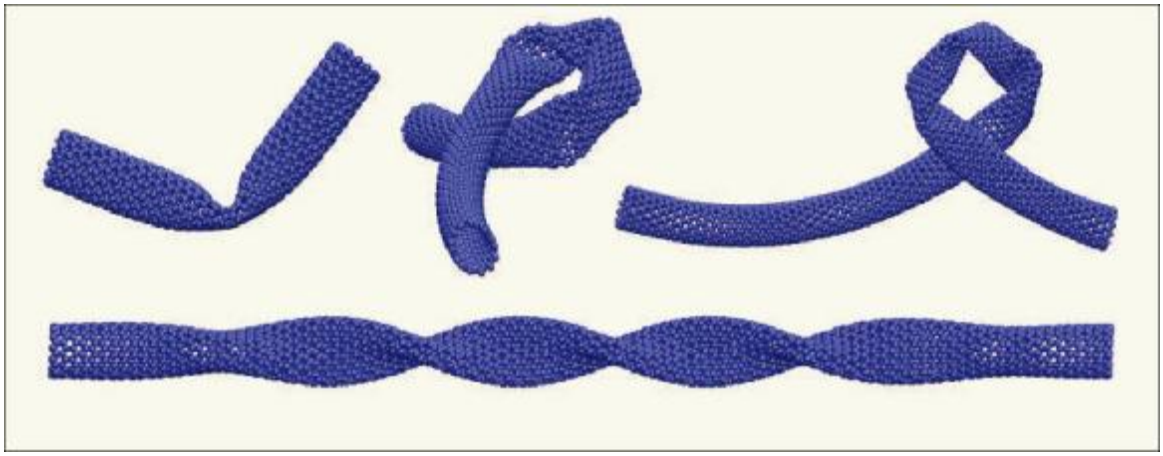

Figure 2-4. The deformation characteristics of CNTs [45].

2.3 CNT Reinforced Al Composites

2.3.1 Background

In the current development of metal matrix composite materials, the reinforcements used have decreased in size from macro-, over meso- and micro- to the nano-scale over time [47]. Compared with the conventional reinforcements, like SiC, Al_2O_3, B_4C, ZrO_2, etc, the nanoscale reinforcements exhibit some advantages, like smaller inter-particle space and higher interfacial contact area. In recent years, extensive interest has been attracted to nano-reinforcement composites. No other nano-filler, however, has gained as much attention as that of carbon nanotubes due to the attractive strength and stiffness of the tubes. The attractive mechanical and geometrical properties of CNT have been described in previous section. Table 2-2 provides a comparison of the physical and mechanical properties of CNT and some most commonly used discontinuous reinforcements. By comparison, it can be seen that CNT has low density, low thermal expansion, while

extra-high stiffness and strength (Table 2-2), which make them attractive fillers in composite materials.

Table 2-2. Characteristics of some commonly used discontinuous reinforcements [63-65].

Reinforcement	Density (g/cm^3)	Thermal expansivity (10^{-6}/°C)	Strength (MPa)	Young's modulus (GPa)
CNT	1.2-2.6	-1.5 (SWCNT)	100,000	1,400
Al_2O_3	3.98	7.92	221 (1090 °C)	379 (1090 °C)
Al_3Ti	3.3	—	—	217
AlN	3.26	4.84	2069	310 (1090 °C)
B_4C	2.52	6.08	2759 (24 °C)	448 (24 °C)
C	2.18	-1.44	—	690
MgO	3.58	11.61	41 (1090 °C)	317 (1090 °C)
Si	2.33	3.06	—	112
SiC	3.21	5.4	—	324 (1090 °C)
Si_3N_4	3.18	1.44	—	207
SiO_2	2.66	<1.08	—	73
TiB_2	4.5	8.28	—	414 (1090 °C)
TiC	4.93	7.6	55 (1090 °C)	269 (24 °C)
WC	15.63	5.09	—	669 (24 °C)
ZrB_2	6.09	8.28	—	503 (24 °C)
ZrC	6.73	6.66	90 (1090 °C)	359 (24 °C)
ZrO_2	5.89	12.01	83 (1090 °C)	132 (1090 °C)

The potential applications of CNTs in metal matrix composites have been widely reported in recent years [15-17, 20-24, 27-28, 33, 49-50, 66-68]. However, in all CNT reinforced composite materials, i.e. polymeric, ceramic and metallic matrix composites, the metallic-CNT composites are the least investigated ones, with respect to polymeric and ceramic-CNT composites. Figure 2-5 shows the number of journal articles published on CNT-reinforced composites in the last decade [26]. It can be clearly seen that majority of the research has been carried out on reinforcement of polymers by CNTs [26]. This can be attributed primarily to the relative ease of polymer processing, which often does not require high temperatures for consolidation as needed for metals and ceramic matrixes [26].

In metallic-CNT composites, the most commonly used metal materials are aluminum (Al), nickel (Ni), copper (Cu) and magnesium (Mg), and amongst them Al based composites are the ones that draw most attention in recent years [26]. This is due to the attractive physical and mechanism properties of Al, that is, high stiffness and strength, combined with low density as mentioned earlier. Although there has been increasing effort on the developments Al-CNT composites [15-17, 20-24, 27-28, 33, 49-50, 66-68], the improvement in strength is not satisfactory. In the following subsections, Al-CNT composites processing, microstructure and mechanical properties would be discussed, and its challenges and potential would be brought out.

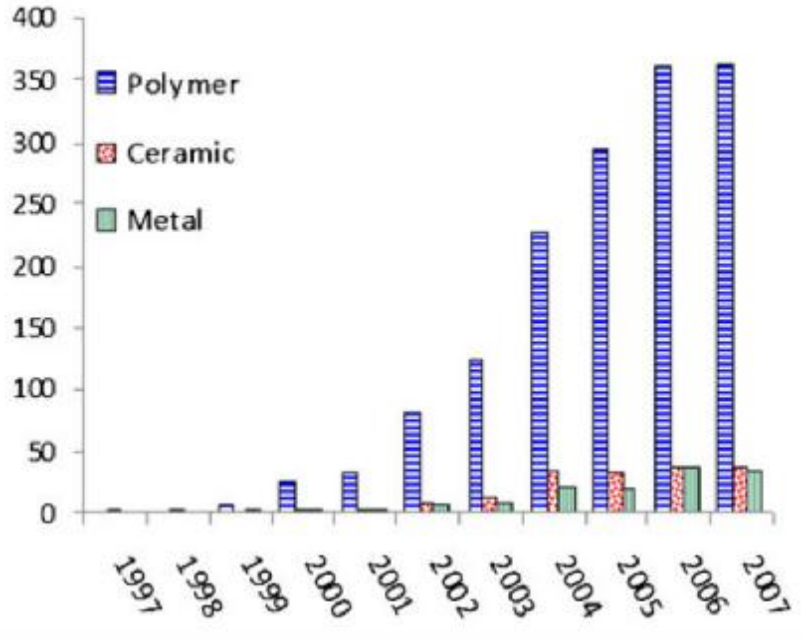

Figure 2-5. Number of publications on CNT reinforced polymer, ceramic and metal matrix composites [26].

2.3.2 Al-CNT Composite Processing

The potential applications of CNTs in MMCs, especially aluminum matrix composites (AMCs), have been widely reported in recent years [15, 17-19, 24, 31, 48, 69-74]. A range of manufacturing methods have been used to obtain the CNT reinforced aluminum matrix (Al-CNT) composites. Figure 2-6 displays the proportion of the various synthesis methods adopted from the year 1998 to 2010.

From Figure 2-6, it can be seen that P/M is the most popular and widely used technique, around two thirds of the total processing routes. Although many other novel methods were attempted, such as electro-deposition [75], cold spraying [76] and sputtering [77-78],

they have been limited by the complicated preparation process, associated with the constraint of equipment availability and high cost. In contrast, P/M has its attraction in being simple, versatile and economical. It avoids the segregation problem associated with casting due to the difference of density, particle size, and the flow characteristics between the constituents. It is also well known that the aluminum powder metallurgy offers components with low density, long-term performance reliability, mechanical and fatigue properties, corrosion resistance, high thermal and electrical and conductivity; and most of the current Al-CNT composites are fabricated by P/M and significant enhancement in stiffness and strength have been obtained [19, 25, 71-72]. Here, fabrication of Al-CNT composites using P/M technique would be discussed in detail, and other fabrication methods, i.e. casting, roll bond, spray forming and pressureless infiltration would be discussed in brief.

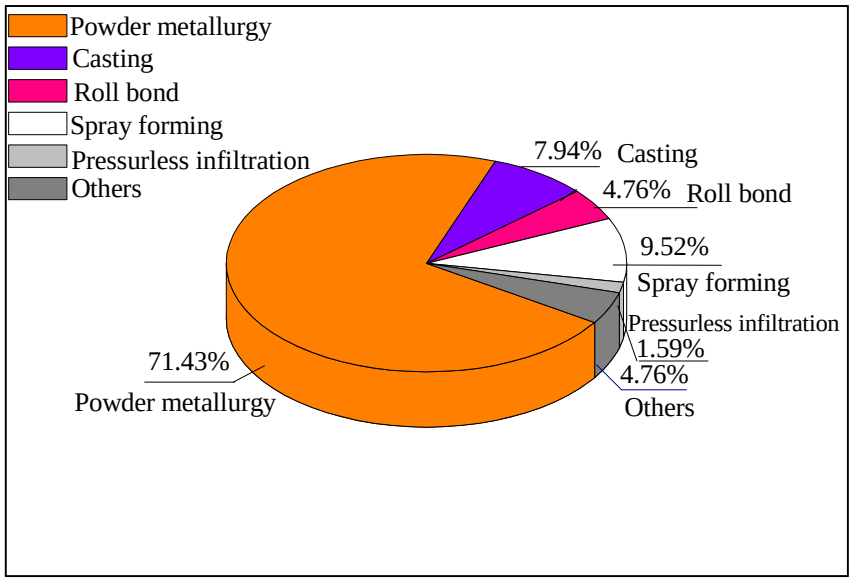

Figure 2-6. Percentage of the processing techniques for fabricating Al-CNT composite (source: Scopus, as of 1st October 2010).

2.3.2.1 Powder Metallurgy (P/M) Process

There are many manufacturing methods to obtain the CNT reinforced Al matrix composite. Among these synthesis methods, the conventional P/M is the most commonly used due to its simplicity, effectiveness and economic advantage. Figure 2-7 illustrates the schematic P/M route, which starts with initial component powders. General P/M route for making MMCs includes [79]:

(i) Blending and mixing;

(ii) Consolidation, e.g. compaction and sintering, hot pressing, isostatic pressing (cold/hot);

(iii) Secondary processing e.g. extrusion, rolling, equi-channel angular extrusion (ECAE);

(iv) Final machining and finishing.

Fully dense high performance alloys and composite can be produced with uniform microstructure by P/M.

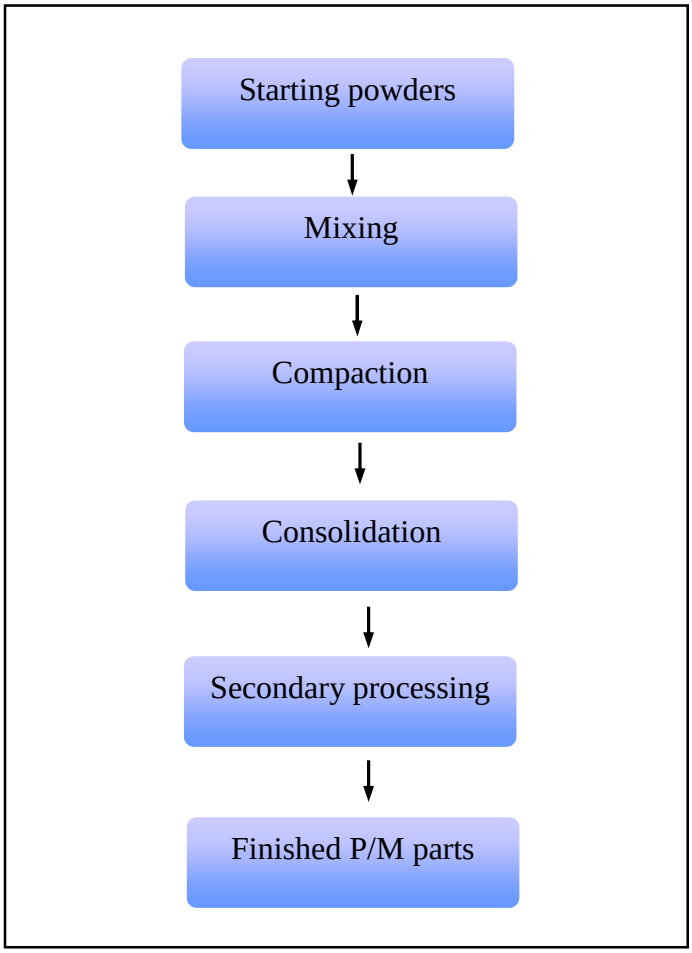

Figure 2-7. The general schematic diagram of P/M.

The manufacturing procedure for producing the Al-CNT composite requires multistage processes. Table 2-3 presents a comprehensive summary of the various experimental work reported on the Al-CNT composite by P/M. The available information on the mixing, consolidation as well as secondary processing, mechanical properties including tensile/compressive strength, ductility and hardness are also included. To take advantage of the extraordinary mechanical properties of CNT as reinforcement, many aspects related to the P/M process should be carefully considered. In the following sections, the process variables of P/M stages are discussed in detail.

Table 2-3. Summary of processing routes and mechanical properties of P/M Al-CNT composite.

Chronological references	CNT content	Powder mixing	Consolidation Secondary processing.	Experimental density (g/mm^3)	$\sigma_{0.2}$ (MPa)	σ_{UTS} (MPa)	Ductility (%)	HV hardness	Remark
Kuzumaki *et al* [74] 1998	0	Al and CNTs powder were stirred in ethanol at 300rpm for 0.5h and immediately dried.	Hot pressing and hot extrusion.	-		89	-	-	-
	5					84	26		
	10vol.% CNT					80	18		
George *et al* [5] 2005	1	Ball milling	Cold compaction, inert gas sintering and hot extrusion.	-	80	141	-	-	-
	2vol.% SWCNT				90	134			
George *et al* [5] 2005	0.5	Same as ↑	Same as ↑	-	86	134	-	-	-
	2vol.% MWCNT				99	138			
He *et al* [73] 2007	Pure Al	-	Pressing, vacuum sintering at 640℃	2.69	-	140	-	0.15GPa	-
	Al-1wt.%Ni-5 wt.% CNT	Ball milling	Pressing, vacuum sintering at 640℃	2.48	-	213	-	0.32GPa	-
	Al-1wt.%Ni-5 wt.% CNT	In situ grown CNT in Al powder	Pressing, vacuum sintering at 640℃	2.50	-	398	-	0.65GPa	-
Deng *et al* [80] 2007	2024Al-1wt.%CNT	-	Cold isostatic pressing and subsequent hot extrusion.	-	-	-	-	-	The enhancement due to the bridging and pulling-out role of CNTs in the Al matrix composite.
Esawi *et al* [31] 2008	0	Planetary mill at 300rpm, no milling media.	Hot roll compaction followed by sintering: vacuum furnace at 300℃, for 3h then air furnace 550℃ for 45 min.	2.687	70	128	25	-	-
	0.5			2.66	100	148	18		
	1			2.65	70	105	7		
	2% CNT			2.59	-	62	2		
Esawi *et al* [32] 2009	0	Planetary ball milling with argon atmosphere and agitated using a planetary ball mill at 200rpm for 3h.	The milled powder mixture was compacted and hot-extruded at 500℃ with extrusion ratio of 4:1.	-	-	284 (Annealed 500℃, 10h)	8.6	-	CNTs act as void nucleation sites during tensile testing. In addition, both CNT pullout and CNT inner tube

	2wt.% MWCNT					345	5.7		slippage were observed.
	0	Planetary ball milling with argon atmosphere and agitated using a planetary ball mill at 200rpm for 6h.	Same as ↑	-	-	348.5 (Annealed 500℃, 10h)	8.4	-	-
	2wt.% MWCNT					348	7.9		
R. Pérez *et al* [33] 2009	0	Mechanically milled for 5h in a high energy mill in arrrgon atmosphere (pure Al was not milled).	Powder mixture was compacted, vacuum sintered at 823K for 3h, hot extruded with extrusion ratio of 16.	-	105	159	-	-	Amorphization of the outer-shells of CNTs; Al_4C_3 was detected by XRD.
	0.25								
	0.5				138	180			
	0.75				-	-			
	1				147	191			
	1.25				167	218			
	1.5				-	-			
	1.75wt.%				189	243			
Choi *et al* [25] 2009	0	High-energy ball milled 6h, ball-to-powder weight ratio 15:1 at 500rpm for 6h	Ball milled powders were containerized and hot-rolled at 480C.	2.68	262	-	-	-	CNTs were uniformly dispersed.
	1.5			2.67	386				
	3			2.67	483				
	4.5			2.65	610				
	6.0vol.%			--	-				
Kwon *et al* [19] 2009	0	CNTs were dispersed into Al powders as assistance of natural rubber. The rubber was evaporated by heat treated at 500C.	Spark plasma sintering at 600℃, and hot extrusion at 400℃.	-	-	85	18	22	Al_4C_3 was formed on the grain boundary during sintering, and implanted into matrix during extrusion.
	5vol.%CNT					194	10	52	
Morsi *et al* [49] 2010	0	SPEX milling (for 60 min and 90 min respectively) was conducted under an argon atmosphere with a ball to powder ratio of 5:1 using 1.5 wt.% of methanol as a process control agent	Compacted and spark plasma extruded (SPE) using a ram speed of 6.3mm/s and varying extrusion onset temperatures (for extrusion temperature at 442℃.	-	-	375 (Compression)	79	-	No carbide was detected by XRD.
	2.5wt.% CNT					415 (Compressio)	86		

Joo *et al* [20] 2010	0	Planetary ball milling	High pressure torsion (HPT) at 200℃ to consolidate the powders.	-	-	255	25	-	Majority of the CNT/Cu reinforcements are located at grain boundaries.
	5vol.%					510	9		
Morsi *et al* [50] 2010	2.5wt.%	SPEX milling under argon atmosphere for 2h.	-	-	-	-	-	91	Formation of carbides at temperatures as low as 400℃.
	5.0wt.% CNT							107	
Choi *et al* [24] 2010	Pure Al	Al-Si powder was first ball milled at 500rpm for 18h under an argon atmosphere. The milled Al–5wt.%Si powders were further ball milled by adding 3vol.% MWCNT for 6h under the same conditions.	Powder mixture was can-contained and hot rolled at 480℃.	-	-	400	13	-	-
	Al–5wt.%Si					460	9		
	Al–5 wt.%Si -3vol.% MWCNT					520	6		

(I) Mixing

Powder mixing is the primary step in P/M to ensure a uniform distribution of a multi-powder system, with different particle size, shape, density and other characteristics [82]. CNT agglomeration within the metal matrix is a predominant problem, due to the strong van der Waals forces of attraction between these long and thin wires. CNT agglomeration in the matrix generates defects in matrix and also causes inhomogeneity to the mechanical properties of the composites. In order to overcome this, various powder mixing methods have been used [15, 19, 71, 73, 83]. Different powder mixing techniques are presented in Figure 2-8. From the literature, mechanical alloying of the CNTs and Al powder is the one most commonly used. Aside from this method, other efforts have been made, like solvent mixing, medium-assisted mixing, in-situ growing. These mixing techniques are presented in Figure 2-8.

(a) Mechanical Alloying (MA)

The most common approach for dispersing CNTs in metal matrices reported is mechanical alloying (MA). MA is an effective method to mix the powders in the desired proportion. As reported, different types of milling equipment have been used to produce mechanically alloyed Al and CNT powders, like shaker mills (such as SPEX mills) [49-50], planetary ball mills [20, 71], attritor mills [84], and so forth. Mechanical alloying with appropriate controlled parameters has been proven to be an effective technique on the de-agglomeration and homogeneous dispersion of CNTs into the metal powders. The various MA conditions include alloying time, intensity, ball-to-powder ratio to obtain the effective dispersion of CNTs within the matrix, also maximum retention of the CNT

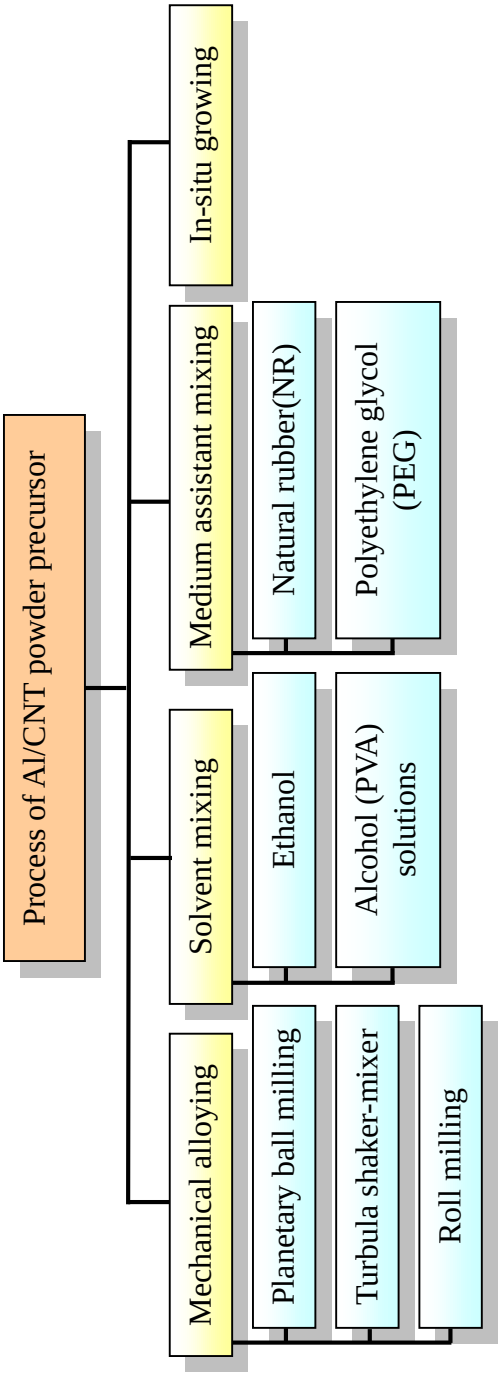

Figure 2-8. Overview of the technologies to process of Al/CNT powder precursor for P/M technique.

structure. It is suggested that a suitable selection of the size of CNTs and Al powders, combined with appropriate milling parameters, would allow uniformly distributed CNT reinforcements thereby ensuring improved and consistent properties of the resultant composites.

One issue in the planetary ball milling processing is the gravity separation, i.e. light CNT powders would be on the upper part of the Al powders due to density difference. Besides the density difference, the surface properties and the large difference in geometries and difference in fraction, also limited the homogenous-distribution of CNTs in the Al powders. It has been reported [19] that even in the slurry-based processes, the dispersion of CNTs were limited, because of the large difference of zeta potential [19], and the spherical shape and resultant surface curvature of the metal powders. It is supposed that, instead, smaller sized metal particles with flat-shape would assist a more even distribution of the nano-scale tubes. The spherical Al powder could be flattened by mechanical milling (MM) before mechanical alloying (MA) with CNTs. This suggestion was realized by Choi *et al* [24]; they applied a specific ball milling process which could significantly enhance the CNT dispersion: firstly, Al-Si metal powder was ball milled at 500rpm for 18h under an argon atmosphere to minimize the metal particle size; secondly, the milled Al-Si powders were further ball-milled by adding 3vol.% MWCNT for 6h under the same conditions. The powder mixture was canned and hot-rolled at 480℃. CNTs were separated and uniaxially aligned along the rolling direction. The tensile strength of the Al-5Si-3MWCNT was enhanced 13% compared with counterpart Al-5Si alloy.

As mentioned earlier, the milling time, intensity and ball-to-powder weight ratio should be carefully controlled in order to ensure the intact structure of CNT. Improper mixing would lead to poor dispersion and as a result low enhancement of strength and also inconsistent products. This can be directly attributed to the clustering of CNTs at higher addition. It should be noted that in ball milling process, it does not mean that the longer milling time would give the better dispersion effect. Long milling time could lead to metal powder cold weld and increased particle size. Therefore, CNTs embedded in the cold-welded particles become difficult to disperse. Esawi *et al* [32] have reported that longer mechanical alloying time did not help to improve the tensile strength of the Al-CNT composites compared with the counterpart monolithic Al. In practice it is difficult to estimate the optimum milling time, at which alloying occurs and the CNT of every Al particles is the same as the desired proportion. At present, the proper selection of MA condition to obtain good CNT dispersion in metal matrix is quite challenging.

(b) Solvent Mixing

It has been reported that CNTs could form a stable suspension in solvents, such as ethanol, acetone or dimethylformamide (DMF) [85-86]. Based on this, there have been some attempts to mix CNTs and metal powders within a solvent, herewith called “solvent mixing”. Solvent mixing hereby is different from wet grinding. In wet grinding, metal powder mixtures are milled with a liquid medium and the liquid only facilitates milling but does not take part in alloying with the powder [87]. But in solvent mixing, the solvent plays a role in dispersing CNT.

There have been some reports introducing solvent mixing technique, through which CNTs and metal powder were dissolved and mixed within a specific solvent. For example, Kuzumaki *et al* [74] have dispersed CNT in Al powder by stirring a Al/CNT mixture in ethanol for 30min and dried immediately in a vacuum furnace. Deng *et al* [80] first dispersed CNTs into liquid ethanol, followed by mixing the CNT-ethanol suspension with 2024Al powders. Subsequently the CNT-2014Al-ethanol mixture was ball milled for 1h. Agarwal *et al* [6] dispersed CNTs in a polyvinyl alcohol (PVA) solution, then Al powder was added, followed by spray drying. However, in these cases, the mechanical properties of the resultant Al-CNT composites were not improved significantly.

The latest breakthrough in solvent mixing was obtained by Wang *et al* [27]. In their study, 2wt.%CNTs were first dispersed in ethanol using an ultrasonic shaker, and then Al powders were added. The mixture was simultaneously mechanical stirred and sonicated for 30min. The ethanol was evaporated in an oven for 24h. The mixture was then ball milled for various times, i.e. 12, 24, 48 and 72h. They reported that homogeneous distribution of the CNTs was observed within the Al matrix.

However, in solvent mixing cases, one main problem is that CNTs tend to re-agglomerate on the surface of the matrix particle when the mixing solvent is dried. This is because the repellent functional groups existing on the surface of CNTs and the solution would no longer work once the solution has evaporated. Moreover, these methods have been constrained for large quantity production, therefore the sample size and bulk fabrication are limited.

(c) Medium-assisted Mixing

The medium-assisted mixing is novel and interesting, and different from traditional powder mixing routes. This method is somewhat like injection molding, which is widely used in mixing ceramic powder and binder. In injection molding, both ceramic powder and the polymeric binder (thermoplastic types) are combined into a homogeneous mixture; and once the part is molded, the thermoplastic binders are chemically or thermally removed from the powder mixture, so that the part can be sintered to high density. There have been attempts in trying to take advantage of the injection molding to disperse the CNTs in Al which a mixing medium acts as a binder and is subsequently removed once the Al powder and CNTs are mixed.

For example, Kwon *et al* [19] have used a nanoscale dispersion (NSD) method, in which the CNTs were dispersed into Al powders, with the assistance of natural rubber. The rubber was evaporated by heat-treating at 500℃. CNTs were observed at the grain boundary and grain growth did not occur due to the pinning effect of the CNTs. According to Kwon's group, this method has greatly improved the mechanical property of Al-CNT composite, i.e. the addition of 5vol.% CNTs increased the tensile strength to about thrice that of monolithic Al.

However, in the medium-assisted mixing method, one issue that should be considered is the residue of the mixing medium. It is difficult to thoroughly remove the residue which could result in void defect in the consolidated material; also the process to remove the residue increases the processing complexity and cost.

(d) In-situ Growing

A break through in the mechanical property improvement of Al-CNT composites was made by He *et al* [73] in 2007 using an in-situ CNT synthesis technique. They synthesized CNTs in-situ Al powders through chemical vapor deposition (CVD). The powder mixture was subsequently consolidated by pressing and sintering. The resultant Al-5wt.%CNT-1wt%Ni composite showed extremely high strength and hardness, 184% and 330% higher than the counterpart monolithic Al, respectively. This remarkable strengthening is caused by the dispersion strengthening of the homogeneously dispersed CNTs, see Figure 2-9 [73]. Besides, the retention of the perfect structure by in-situ sythesis gives the CNTs their extreme hardness (62–150GPa) [73]. Till now, the results obtained by He *et al*. [73] are still the best reported improvement in Al-CNT composites, but it is limited by the availability of equipment and high cost.

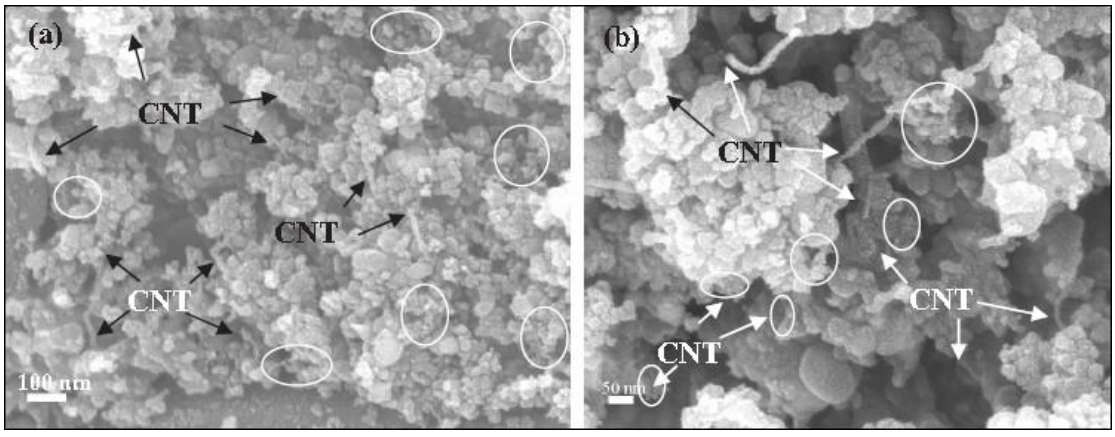

Figure 2-9. (a) SEM image of a CNT(Ni)–Al composite powder; (b) enlarged SEM image of several typical CNTs (indicated by arrows) dispersed in Al powder. CNTs were homogeneously dispersed within Al powder by in situ synthesis of CNTs [73].

(II) Consolidation

The consolidation process is critical for the quality of the resultant product. It determines the density, the grain size and component condition of the composite. The as-reported consolidation techniques of P/M Al-CNT components mainly are (i) sintering, and (ii) severe plastic deformation consolidation (SPD).

(a) Sintering

Sintering of the green compact is carried out in a controlled atmosphere (vacuum, argon, nitrogen, etc) at about 70% of the melting temperature (in Kelvin), to consolidate the mechanically-bonded powders into a coherent body having the desired service properties [82]. The various parameters in sintering are:

(i) Sintering atmosphere

(ii) Temperature

(iii) Holding time

(iv) Heating and cooling rate

Most sintering processes for Al-CNT composites have been carried out in conventional furnaces with vacuum or protective inner atmosphere. For example, He *et al* [73] used pressing and vacuum sintering (640°C, 3h) to obtain bulk Al-CNT composite. George *et al* [5] cold compacted the ball-milled Al/CNTs powder, and sintered them in an inert gas environment (nitrogen) for 45min at 580℃. Beside conventional sintering, spark plasma sintering (SPS), a comparatively new densification technique, has also been explored for fabrication of Al-CNT composite [19]. The rapid heating and applied pressure of the SPS

would also be effective in providing specimen with small grain size and high density. Kwon *et al* [19] used spark plasma sintering (SPS) to densify the Al-CNT powder mixture. Figure 2-10 shows micrographs of the transverse and longitudinal cross sections of the SPS compact [19]. The sintered compact has high density of 96.1% and grain growth did not occur during sintering. The high density is mainly attributed to the reduced atmosphere from the use of a carbon mold, and the small grain size is due to the pinning effect of CNTs and the restrain from the alumina layer of Al powders [19].

However, a common phenomenon in sintered compacts is that the CNTs are likely to be repulsed to the grain boundary during the manufacturing process. When the quantity of CNT increases, CNT agglomerat and cluster at the grain boundary, resulting in the deterioration of the strength of the material. Evidence of copious CNT at the grain boundary regions and triple points of the matrix has been shown by various researchers [19, 26].

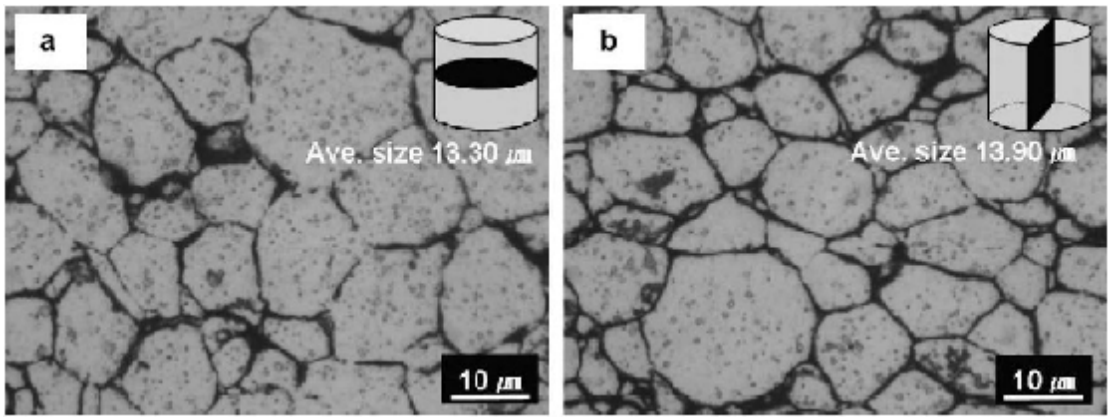

Figure 2-10. Micrographs of (a) transverse cross section and (b) longitudinal cross section of Al–CNT sintered compact (after SPS) [19].

(b) Severe Plastic Deformation Consolidation (SPD)

Severe plastic deformation consolidation (SPD) can be applied both for consolidation powder, and deformation of solid bulk material [20]. SPD consolidation relies on plastic deformation of individual particles, rather than diffusion, to achieve bonding and thus can be carried out at much lower temperatures [88]. For sample, hot extrusion, hot pressing and hot isostatic pressing (HIP) can be used for consolidation of powders to get near theoretical density. Grain boundary sliding is assumed to be the one of the main densification mechanisms in severe plastic deformation consolidation [89].

Kuzumaki *et al* [74] fabricated Al-CNT composite by hot extrusion of powder compacts at 600℃. In a study by Deng *et al* [90], 2024Al-1wt.%CNT composite was fabricated by cold isostatic pressing followed by hot extrusion. In both studies, the tensile strength of the resultant composites were not apparently improved. This may be due to the clustering of CNTs from improper powder mixing in the earlier step.

(III) Post Consolidation Processing

The consolidated composite can be used in the as-consolidated condition, or it can undergo secondary processing to achieve some desirable geometry or/and property. It is well-known that secondary processing with severe compression forces is favorable to attain high density and prefect matrix-reinforcement bonding of the resultant product. The commonly used secondary processes are extrusion and rolling, due to their simplicity, substantial material deformation and obtained texture. The secondary processing applied to Al-CNTs composite are usually carried out at high temperature [69-70, 81, 91-92], in

order to reduce the forming forces and to prevent cracks occurring due to the decreased ductility of Al-CNT composites.

It is suggested that by the application of secondary processing, the matrix deforms in a plastic manner and the plastic flow could break the CNT-clusters and re-distribute the CNTs in the matrix. It also improves the density and CNT orientation. In addition, the compressive forces from secondary processing are expected to exert a better contact of the matrix-CNT interface, leading to better load transfer. Furthermore, CNTs can act as obstacles to dislocation movement in metals, so that plastic deformation is not uniform in the matrix. Orowan loops also are expected to exert a back stress on dislocation sources during the plastic deformation from the secondary processing [93]. Similar studies have also reported [69-70, 81, 91-92] that CNTs are re-distributed and preferentially oriented with the matrix during rolling, leading to improved mechanical properties of the composite.

Besides powder metallurgy technique, there are also other fabrication methods, like casting, roll bonding and spray forming, which would be outlined in the following subsections briefly.

2.3.2.2 Casting

The melting point of Al is comparatively low, 660.32°C, which is suitable for casting. Li and co-workers have tried to synthesize Al-CNT composites by high pressure die casting [16]. In their study, 0.05wt.% MWCNTs were weighted and then wrapped in Al foil to

form a ball. Four balls containing MWCNTs were set on the entrance of the die as shown in Figure 2-11. The molten Al alloy (Al239D) was pushed into the die by the piston with a high velocity. Because of the small cross section at the entrance, the melt is accelerated to a high speed (as fast as 250m/s), which leads to a turbulent flow in the die and could help the dispersion of MWNTs [16]. In the tensile testing, tensile stress and the elongation at fracture were both increased by addition of the 0.05wt.% MWNTs. Improvement of the mechanical properties was claimed due to the advanced mechanical properties of the carbon nanotubes. But only 0.05wt.%MWCNTs were added in their study, no attempt was made to increase the CNT content by them. It may be due to the poor Al-CNTs wettability, high viscosity of Al and strong agglomeration of CNTs with increasing fraction in the matrix.

In another study by Lim *et al* [28], they fabricated MWCNT reinforced Al alloy composite via friction stir processing. They reported that multi-walled microstructure survived the thermo-mechanical conditions imposed during processing. But no detail about the casting temperature and processing atmosphere were mentioned in their report. The temperature stability of SWCNT is estimated to be up to 2800°C in vacuum and about 750°C in air [94], and above 480°C in air for MWCNTs [95]. In the stir casting process, a completely uniform distribution could not be achieved when regularly tangled nanotubes were used as the base material, but they suggested that multiple passes may be required to further improve the dispersion of nanotubes in the matrix.

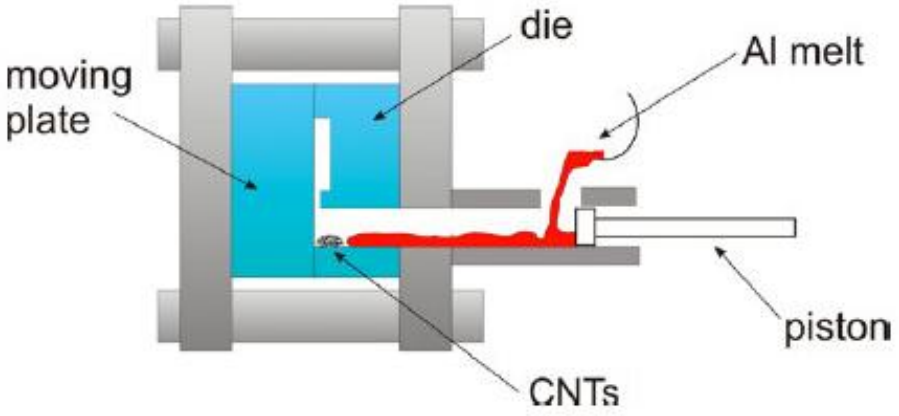

Figure 2-11. Schematic of high pressure die casting technique [16].

2.3.2.3 Roll Bonding

The roll bonding process was developed by Saito *et al* [96] with the purpose of refining grain size in metal alloys. Later roll bonding was also applied for some metal composites [92, 97-99]. In roll bonding process, several layers of metal foils were roll bonded to form a single strip of composite. A solid-state bond between the original individual metal pieces is formed during to the severe compressive pressure. Lahiri *et al* [91] has synthesized Al-CNT via roll bonding. In their study, commercially pure Al foils of 40μm thickness were used. CNTs were ultra-sonicated in acetone for 30min and sprayed on Al-foil with a hand atomizer and dried. Four layers of Al foils with intermediate three layers of sprayed CNTs were stacked together and rolled in a cold rolling machine. The schematic of the roll bond process is shown in Figure 2-12. Uniform distribution of CNT has been observed from the Al-2vol.%CNT composite foil delaminated surface, but with high CNT fraction, Al-9.5vol.%CNT composite, agglomerated CNTs were observed, as shown in Figure 2-13 [91]. From the experimental results, they concluded that CNTs play

a dual role in strengthening mechanism depending on their degree of dispersion in the aluminum matrix [91]. Uniformly dispersed CNTs enhance the elastic modulus of the composite by behaving like a homogeneous structure and resisting the plastic deformation at lower stress. Agglomerated CNT clusters for high CNT concentration behave as the precipitates and do not enhance the elastic modulus of the composite. CNT clusters inhibit the dislocation flow and results in an increased dislocation density with the increasing CNT content. As a result thecomposite gets strengthened by strain hardening [91].

In another fabrication of CNT reinforced Al alloy composite via roll-bonding study by Salimi *et al* [69], they reported that MWCNTs with diameters >30 nm and >30 walls were retained during four consecutive rolling operations at 50% reduction. Though the roll bonding process was reported as a effective methods to disperse CNTs, one limitation of this method is the size of the roll-bonded sample is small (see Figure 2-12). Bulk structural materials seem difficult to be synthesized using this method.

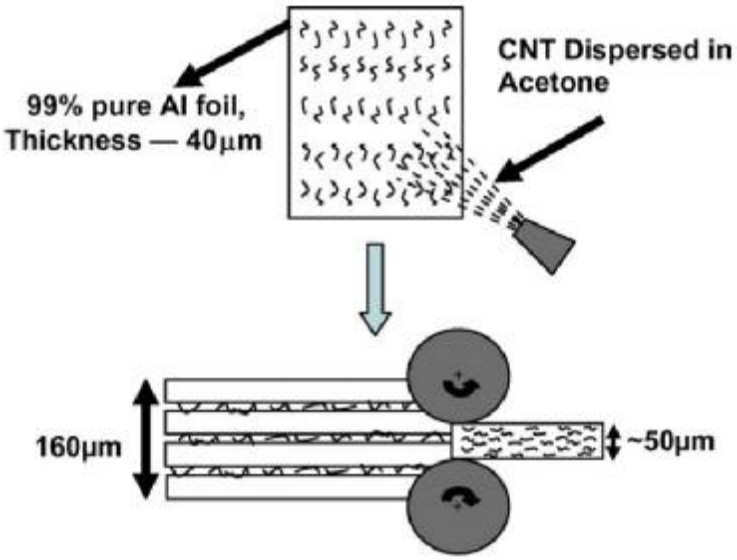

Figure 2-12. Schematic of composite preparation through roll-bonding process [91].

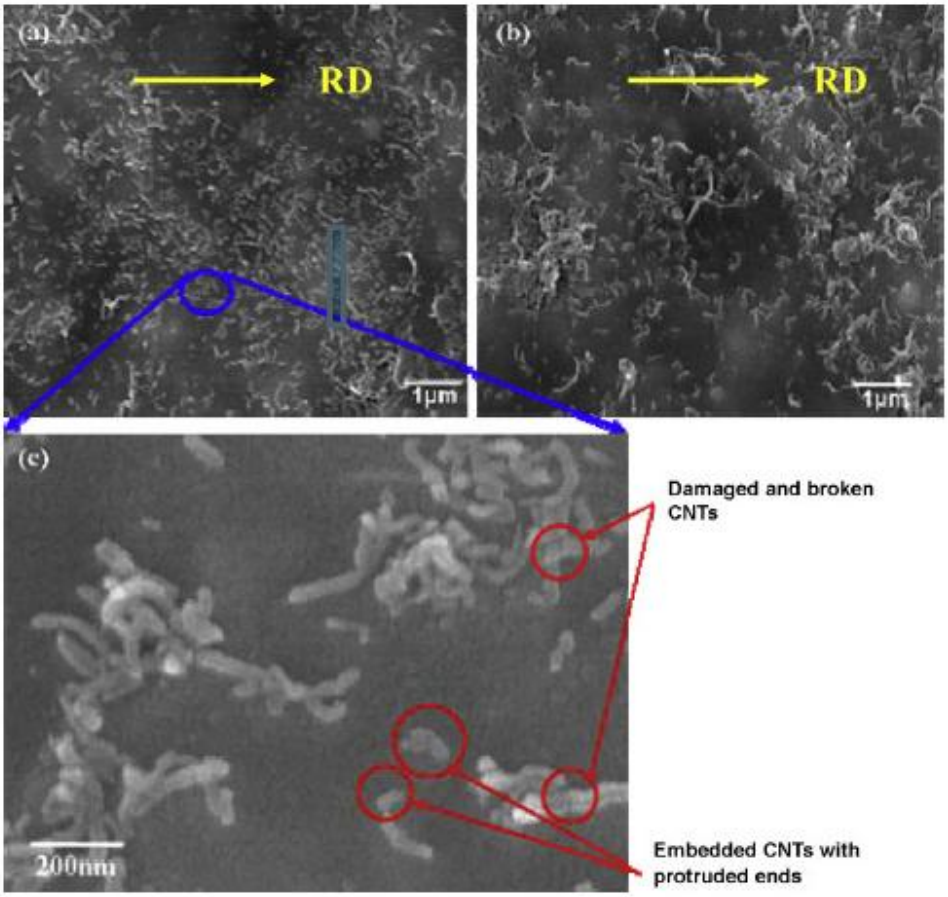

Figure 2-13. SEM images of (a) Al–2vol.%CNT composite foil delaminated surface showing uniform dispersion of CNTs, (b) Al–9.5vol.%CNT composite foil delaminated surface showing agglomeration of CNTs, and (c) Al–2vol.%CNT delaminated surface at high magnification showing protruded end of CNTs and CNT breakage [91].

2.3.2.4 Spray Forming

The research group of Agarwal used plasma spray forming (PSF) to fabrication Al-Si alloy reinforced MWCNTs [53, 100-103]. The nanocomposite exhibits retention and homogenous distribution of MWCNTs in Al–Si matrix. In their study, spherical pre-alloyed Al–Si powder with and without 10 wt.% MWCNT were deposited on rotating

6061 aluminum mandrel to fabricate freestanding cylindrical nanocomposite structures by plasma spray forming (PSF) [102]. The cylindrical sample of 0.635mm thickness was obtained and tensile specimens were machined from the master sheet, see Figure 2-14 [102]. They reported an improvement in elastic modulus of 78% in CNT composite as compared to Al matrix. They computed the effective elastic modulus of the Al-CNT composite using Rules of Mixture (ROM) using the following equation. Fracture in Al–Si matrix adjacent to interfacial SiC layer formed on MWCNT surface was observed [102]. One disadvantage of the spray forming process is that there were porosities left. It needed post-spraying sintering to eliminate the porosities left in the as-sprayed samples [103].

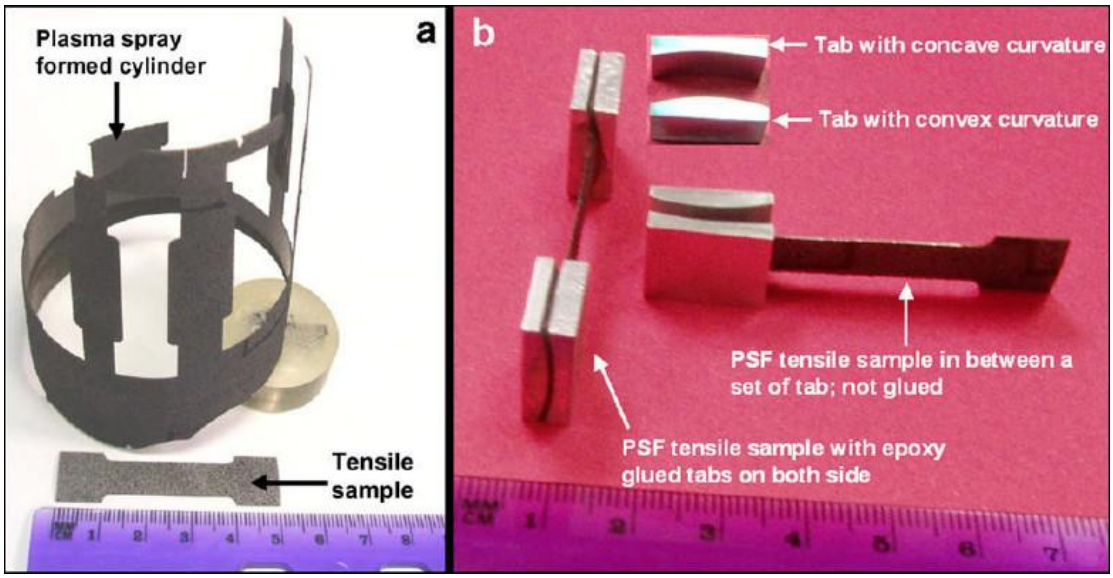

Figure 2-14. (a) Tensile samples machined out from the spray formed cylindrical Al–CNT nanocomposite structures and (b) aluminum tabs on the grip sections of tensile samples for facilitating the gripping during the testing [102].

There are a few studies using other processing routes to fabricate Al-CNT composites, like electrodeposition by Takashi *et al* [75]. The electrodeposition is primarily used for formation of thin composite coatings with a reported thickness of 20 to180μm [26]. Zhou *et al* [104] have synthesized Al composites reinforced with CNT (0-20vol.%) via pressureless infiltration, and the wear properties of the resultant composites were studied. They reported that the wear rate of the composite decreased steadily with the increase of CNTs content in the composite due to self-lubrication and unique topological structure of CNTs.

2.3.3 Mechanical Properties and Strengthening Mechanisms

At present, the measurements of the mechanical properties of Al-CNT composites have been reported mainly by tensile tests, and in the literature good tensile strength was realized only with the low content of CNTs (less than 2wt.%). With increasing content of CNTs, the tensile strength decrease. For example, in a study by Esawi *et al* [31], they reported that Al-CNT composite exhibited a decreasing tensile strength with increasing addition of CNTs (> 0.5wt.%), see Figure 2-15(a). Meanwhile, Al-CNT composite exhibited a decreasing tensile elongation compared with the monolithic Al, see Figure 2-15(b). Evidence of the decreased ductility of Al-CNT composite is given in most reports [5, 19, 50, 74]. A summary of the reported tensile strength as a function of CNT content is presented in Figure 2-16. The influence of CNT content is discussed in section 6.

Table 2-3 presents a comprehensive summary of the studies reporting the mechanical

properties of Al-CNT composite. The available information on the mixing and consolidation routes, mechanical properties including tensile/compressive strength, modulus, and hardness are also provided. It is worthwhile to consider the strengthening mechanisms in these composites. Based on the geometry and physical properties of CNTs, three main strengthening mechanisms are proposed: (i) load transfer, (ii) Orowan mechanism, and (iii) thermal mismatch. It should be noted that the improved tensile strength is presumably due to a simultaneous combination of several contributing factors. These mechanisms are related to each other and in most cases they operate simultaneously.

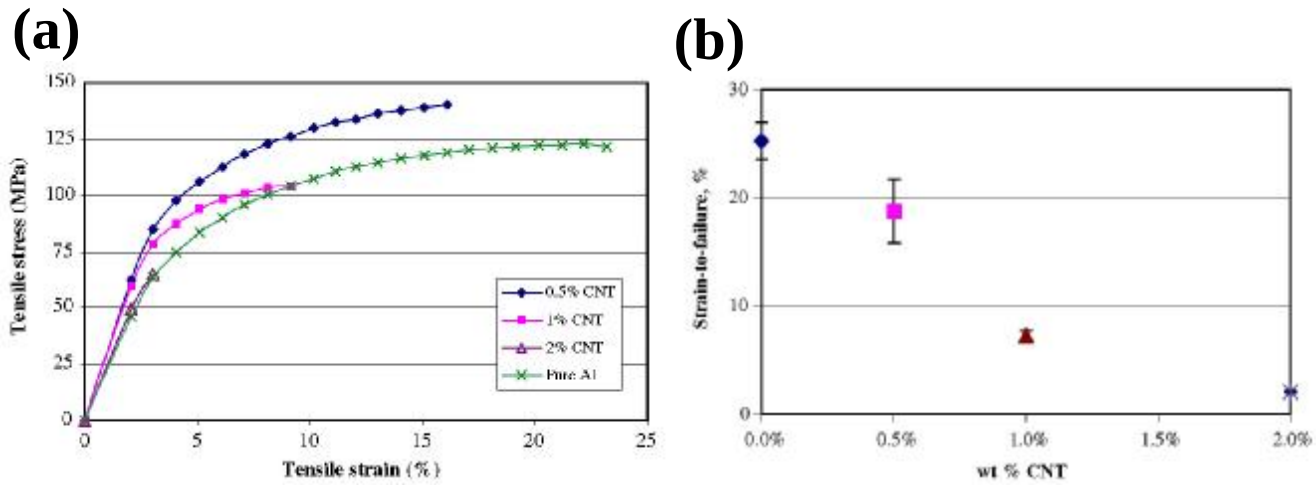

Figure 2-15. (a) Typical stress–strain curves for various wt.% Al–CNT samples; and (b) average strain-to-failure for the different wt.% CNT–Al, ductility decreasing with increasing wt.% CNT [31].

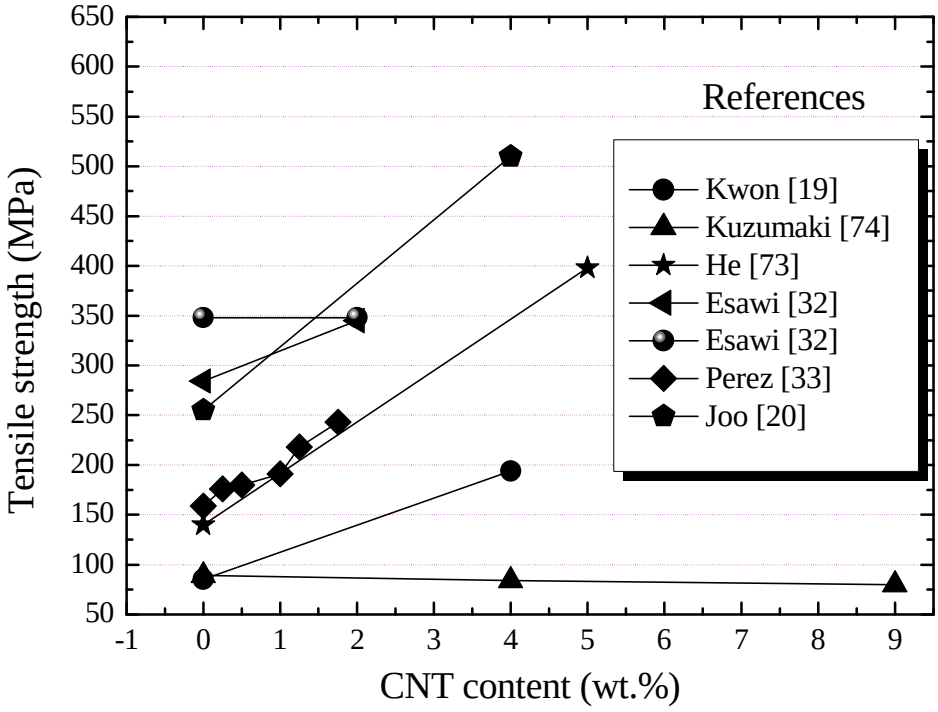

Figure 2-16. P/M Al-CNT composite tensile strength as a function of CNT content.

2.3.3.1 Load Transfer

During loading Al-CNT composite, load partition is realized by the matrix/fiber interfacial shear stress (IFSS). A strong interface or good adhesion, would promote load transfer efficiency and, consequently, enhancing the strength of the composite. The interfacial behavior is critical to the mechanical properties of MMCs, such as tensile strength, stiffness, toughness, ductility, fatigue, creep behavior, and etc. Generally there are three types of adhesion mechanisms between two surfaces [105], that is, (i) chemical bonding, (ii) mechanical interlocking, and (iii) physical bonding, which are presented below.

(1) Chemical Bonding

Regarding the chemical reaction between Al/CNT, there is no consensus. At present, the CNT/matrix chemical reaction and interfacial bonding are still largely unconfirmed.

There have been reports on the formation of Al_4C_3 on the Al/CNT interface [33, 50]. In annealing experiments conducted on the 5.0wt.% CNT-Al powder at temperatures ranging from 300℃ to 500℃, Morsi *et al* [50] reported that Al_4C_3 is evident at temperatures of 500℃, and there also appears to be a trace at 400℃. Ci *et al* [78] reported the formation of nanometric Al_4C_3 at the open ends of nanotubes and the amorphous surface layers at annealing temperatures as low as 500℃ by TEM. Although TEM is a powerful tool at the nano-scale, it can only be selective rather than representative. Besides TEM, there are some studies examining the existence of carbide by XRD [33, 50]. However, it is difficult to detect the existence of carbide due to the low content of CNT (thus the low quantity formation of the carbide), and even it is not clear whether the carbide is formed from CNT or from contamination.

Even if the chemical formation of Al_4C_3 is existent; it is difficult to assess its contribution to bond strength. Kwon *et al* [19] suggested that the formation of Al_4C_3 is viewed as beneficial. According to them, the aluminum carbide was generated during the sintering process (see Figure 2-17), and was implanted into the aluminum matrix during the extrusion process. Such implanted aluminum carbides would conjoin the Al matrix and the CNTs more strongly.

Contrary opinion argues that the formation of Al_4C_3 is detrimental, since it is brittle,

resulting in poor interfacial bonding, poor load transfer and easier fiber pull-out. For example, it has been reported by Kim *et al* [106] that the formation of Al_4C_3 during spark plasma sintering was attributed to the poor wear performance and decreased hardness of the composite. The formation of Al_4C_3 brittle phases leads to reduction of strength and the premature failure of the composite was also reported in carbon fiber reinforced Al-based matrix composites [107].

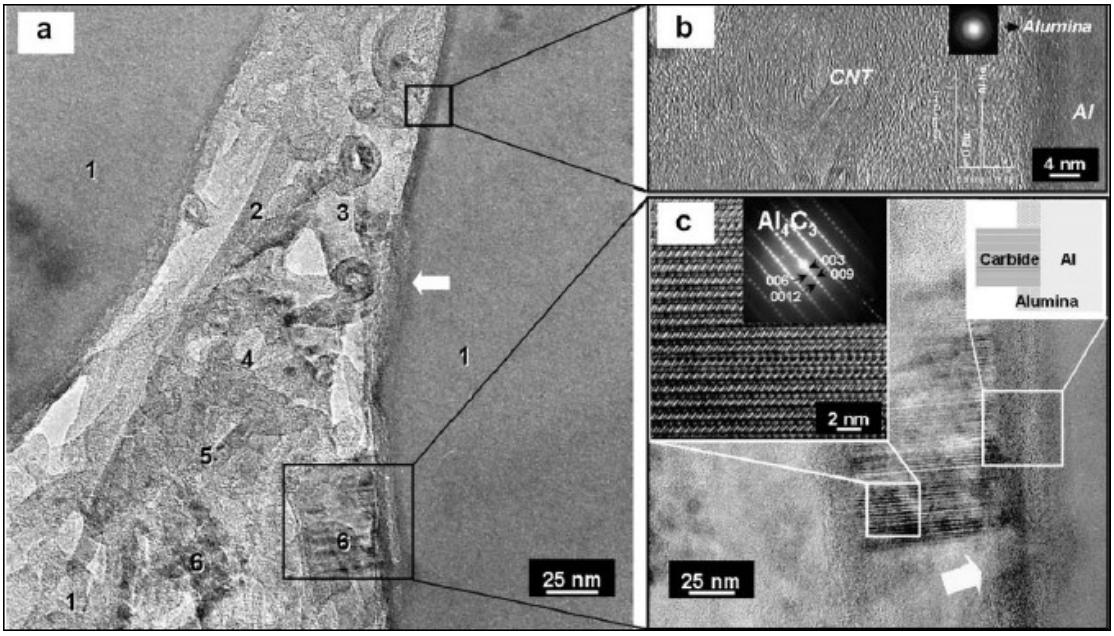

Figure 2-17. TEM micrographs of the grain boundary layer of the sintered compact. (a) Micrograph of the entire grain boundary; (b) the region between the CNTs and Al matrix; (c) the region of Al_4C_3 phase [19].

(2) Mechanical Interlocking

In the load transfer process, when the fiber is about to be pulled out, first, the intact coalescence structure between CNT and Al is shelled off, then the mechanical

interlocking comes into action. For mechanical interlocking, adhesion is promoted mechanically by a large interfacial area, i.e. surface roughness, friction interlocking and dovetail interlocking [105]. Several contributing factors for Al/CNT interfacial bonding would be discussed in brief and these factors facilitate load transfer.

(a) For the CNT *per se*, the irregularities and protrusions on the tube surface serve as mechanical anchors, locking the matrix. In addition, the inherent characteristics of CNT, i.e. large aspect ratio (up to 132,000,000:1) as well as high specific surface area (as high as 178 m^2/g), distorted tubes and roughened surface, would facilitate mechanical interlocking.

(b) For the surrounding matrix, the applied normal compression stresses arising from thermal shrinkage and processing constraint, promote the interfacial shear stress between CNTs and matrix, resulting in good load transfer ability. CNTs experience physical constraint from the P/M process. There also exists a compressive stress on the CNT cross surface, resulting from the thermal mismatch of the coefficient of thermal expansion (CTE) between the matrix and CNTs. This will be discussed in detail in section 2.3.3.3

(c) For the case of MWCNT, the local regions of pressure or defects in the outer wall increase the sliding resistance with the wall next to it, leading to a larger force to pullout the inner wall. Outer wall containing local defects, especially the fractured end, would lead to a "stick-slip behavior" [108], resulting in additional energy for wall pullout. It has been reported that topological defects, commonly Stone-Wales

defect, are unavoidably generated during synthesis and increase during the subsequent mixing process [109]. Mechanical bonding may preferably occur in these local defects regions [110].

(3) Physical Bonding

As all adhesive bonds involve molecules in intimate contact, physical bonding will occur. Physical bonding is mainly a result of the van der Waals forces (electric dipole interactions). This intermolecular attraction forces is weak in the CNT reinforced composite system (0.08-5 kJ/mol), much lower than primary chemical bonds (covalent or ionic) across the interface (60-1100kJ/mol). It may be negligible in the load transfer mechanism.

2.3.3.2 Orowan Mechanism

In general, the yield strength of a composite material is the stress required to operate dislocation sources, and it is governed by the presence and magnitude of the obstacles obstructing the dislocation movement [93].

Orowan strengthening, caused by the resistance of closely spaced hard particles to the passing of dislocations, is important in aluminum alloys [93]. Orowan mechanism requires a small inter-particle spacing, thus it is not significant in the macro- and micro-sized particle reinforced composites. In contrast, it becomes more favorable in the nano-scale CNT reinforced composite, due to the small filler size and small inter-particle spacing. Further, rod shape reinforcement would cause more effective strengthening

mechanism than spherical shape reinforcements [111]. However, as mentioned earlier, since CNTs are mostly found repulsed and clustered to the grain boundary in the manufacturing process, there are some doubts whether Orowan strengthening exists in these cases.

2.3.3.3 Thermal Mismatch

CNTs have a coefficient of thermal expansion approximately of ~$1\times 10^{-6}\,K^{-1}$, which is considered to be the same as graphite; while commercially pure Al exhibits a much greater coefficient of thermal expansion of $23.6 \times 10^{-6}\,K^{-1}$ [5]. Hence, there exists a thermal mismatch of the CTE between the matrix and CNTs, when the composite cools down from the fabrication temperature. The radial stress, σ_{therm}, applied on the CNT cross surface arcing from thermal shrinkage could be obtained from [112]:

$$s_{therm} = \frac{\left(a_f - a_m\right)\Delta T}{\frac{1+g_m}{2E_m} + \frac{1-2g_f}{E_f}} \qquad (2\text{-}1)$$

Where γ is the Poisson's ratio, E is elastic modulus and ΔT is the temperature difference. From Equation (2-1), it can be seen that: (i) if $\alpha_f > \alpha_m$, σ_{ther} would be positive, that means there is tensile stress on the interface; (ii) Conversely, if $\alpha_f < \alpha_m$, σ_{therm} would be negative and there is compressive stress on the interface [112]. For CNT reinforced Al matrix system, the latter is applicable. Thermal contraction of the matrix exerts a compressive stress (thermal shrinkage) on the particle surface. This radial compressive stress is beneficial to the enhancement of friction between CNTs and matrix phase.

Again, when the components are subjected to a temperature change, such as cooling from

the processing temperature, thermal stresses around the nanoparticles large enough to cause plastic deformation are generated in the matrix, especially in the interface region [93]. The dislocation density generated in the close vicinity of CNTs would lead to work hardening of the matrix, hence improving the strength.

In summary, the dominant strengthening mechanism in the Al-CNT composites are deemed to be the load partition effect of CNT, thermal mismatch between matrix and CNT, and Orowan strengthening.

2.3.3.4 Other Contributing Factors

The manufacturing procedure for producing the Al-CNT composite requires multistage processing. It should be noted that the final quality of the resultant composite is determined by an appropriate combination of volume content of the reinforcement, the CNTs and metal powder mixing technique, the subsequent consolidation and secondary processing, heat treatment, etc. By selecting a proper combination of the above affecting factors, the expected strengthening mechanisms could be achieved.

2.3.4 Volume Content

CNTs have been incorporated in Al composites mainly for the purpose of enhancing the mechanical properties of the composite. Theoretically, according to the basic Rule of Mixtures, the Al-CNT composite mechanics in such a system should increase at a rate predicted by the linear rule- of-mixtures based on fiber volume fraction and the strength of the matrix and fiber. Whereas in practice, they almost exclusively employ relatively

low loadings (0–5wt.%) within the Al matrix, see Figure 2-16, because with higher volume fraction of CNTs, the mechanical properties drop. Most reports show that the optimum tensile strength was obtained with an CNT content less than 5wt.%. Even at the low content of CNTs (less than 2wt.%), the expected strength of the composite was far from realized as compared with theoretical calculation. It indicates the particular high strength of CNTs was not transferred into the composites. This is due to the intricate entanglements of long and smooth CNTs and resulting agglomeration. With higher volume fraction of CNTs, the inter-CNT spacing decreases, and CNTs naturally agglomerate, resulting in the decreasing mechanical properties.

From the literature, although a comparatively high volume fraction of CNTs can be successfully incorporated into Al matrix by high energy ball milling [25], however, a portion of the CNTs were damaged and became amorphous during the high energy ball milling, leading to the volumetric change (decrease) of the final products.

2.3.5 CNT Evolution

With respect to composite processing, one critical issue is the microstructure evolution of CNTs during P/M processing. It have been reported that in micro-size particle reinforced MMCs, such as Al_2O_3 and SiC, considerable amount of damage to the particulates was associated to the cold or hot-rolling [113-114].

The morphology and structure of the CNTs were experimentally observed to be damaged by the severe impacting forces during ball milling. According to Pierard *et al* [115], with increasing milling time the CNTs will progressively lose its tubular structure; and after a

long milling time, 50h, the tubular structure would completely disappear and the formation of multi-layered polyaromatic material are observed. Agglomerated CNTs are difficult to separate without damage by physical force. The high energy mechanical alloying inevitably damages the CNTs and destroys their tubular structure, which is detrimental to the overall mechanical properties [71].

2.3.6 Challenges and Potentials of Al-CNT Composites

2.3.6.1 Challenges

(1) Engineering Challenges

Although there have been a wide range of studies on CNT-reinforced Al matrix composites, attainment of the expected improvement of properties, in particular their mechanical properties, have not been largely realized. The key challenges include:

(i) Improving dispersion degree

(ii) Understanding and enhancing load transfer (interfacial bonding)

(iii) Optimizing volume content

(iv) Determining the most expeditious processing technique

Firstly, one of the key problems is the clustering of CNTs in the metal matrix. Optimum strength and ductility is obtained when CNTs are uniformly distributed throughout softer matrix. CNT agglomeration in the matrix generates defects in matrix, which is detrimental to the mechanical properties of the composites. Meanwhile, it is also difficult to directly assess the dispersion effect. Till now only indirect methods, i.e. mechanical property testing, allow an estimation of the dispersion degree.

Secondly, load transfer efficiency is one of the essential factor that must be fulfilled to take advantage of the high Young's modulus of the CNT. The understanding of interfacial bonding as applied to CNT is not very clear. As mentioned earlier, despite observations of carbide being formed at the interface, there are different opinions on the formation and function of the carbide and the resulting bond strength.

Thirdly, in practice, a relatively low addition of CNTs (0–5wt.%) was used within the Al matrix. With higher volume fraction of CNTs, the inter-CNT spacing decreases, and the CNTs increasingly agglomerate, resulting in the decreasing mechanical properties. A better way to incorporate larger content of CNT into the matrix with corresponding improvement in the mechanical performance will be of value.

Fourthly, the adoption of a processing method to produce bulk Al-CNT composite with low cost and energy saving, while maintaining good composite quality is important. Though some novel and effective composite synthesis methods were introduced, these usually increase the processing complexity and cost.

There are also other problems, like the difficulty of aligning the CNTs within the matrix. The fillers have a range of misorientation angles even after extrusion. The misaligned CNTs influence the load-transfer efficiency. In comparison, randomly-oriented fibers will result in isotropic mechanical properties, but at reduced levels of improvement [116]. Further, to date, the majority of the mechanical properties evaluation of Al-CNT bulk composite has been on the room temperature tensile and compressive tests. There is limited report on other properties, such as thermal and electricity conductivity, fatigue,

creep, wear resistance, corrosion resistance and other elevated temperature properties. Further work in the evaluation on these properties would be of value.

(2) Cost Challenges

Bulk production of CNTs with low cost still cannot be realized at present. Compared to other commonly used reinforcements, the cost of CNT is much higher, retail prices of around U$1.5 per gram of as-produced MWNTs as of March 2010 (Shenzhen Nanotech Port Co. Ltd, China). Also there are a lot of suppliers in the market with varying quality. The development of new techniques to produce high quality CNT at low cost is also essential.

(3) Safety Issues

Another problem is the manipulation and safety of CNTs. Though nano-scale materials have attracted increasing interest, it is still not clear the impact of nano-materials to human beings by inhalation or skin-contact. Whether the nano-materials add contamination to the environment, e.g. water, is also not clear. How to safely and environment-friendly take advantage of the nano-scale CNT needs more attention.

With these concerns, it is not yet feasible to use the Al-CNT composite for industrial application. Up to now, the CNTs/AMCs are at a research stage and there has been no report on industrial applications. In comparison the commonly used reinforcement materials, like SiC, Al_2O_3, B_4C, ZrO_2, are economically more attractive than CNTs due to their availability, high strength and stiffness, consistent production, and more importantly.

2.3.6.2 Potential and Applications

Although the exact strengthening mechanisms of the Al-CNT composite are not yet very clear, as well as the processing challenges and other concerns, there appears to be a number of beneficial effects from CNTs contributing to the overall performance increase. Table 2-4 provides a comparison of P/M Al-CNT composites and other conventional Al composites [33]. It can be seen that P/M Al-CNT composites show improved strength compared to counterpart Al alloys.

In actual applications, high-strength and light-weight structural components are crucial. Though for the available literature on CNT reinforced Al based composites, most of the matrices used were pure Al, if the strengthening effect of CNT in pure Al matrix is good, they can be applied to Al alloys, like Al2024, Al2124, Al60601. As the ease of the synthesis and continuous decreasing cost of CNTs, CNT reinforced composites have good potential to be used in commercial application, such as aerospace industry, automotives parts, household products, sport utilities, etc, and bulk/large products in future is not impossible.

Table 2-4. Comparative results from data found in the literature for monolithic Al and Al-CNT composites [33].

Al alloy and composite	$\sigma_{0.2}$ (MPa)	σ_{UTS} (MPa)	HV hardness
Al-0.00wt.%MWCNT	105	159	49.2
Al-0.25wt.%MWCNT	137	176	47
Al-0.50wt.%MWCNT	138	180.7	54.9
Al-1.00wt.%MWCNT	147	191.5	59.3
Al-1.25wt.%MWCNT	167.1	218.8	60.3
Al-1.75wt.%MWCNT	189.2	243	73

2.4 Summary

This chapter described the Al and CNT basics. The available reports on CNT reinforced Al system composites produced by various fabrication methods were reviewed. The strengthening mechanisms that contribute to the Al-CNT composites, as well as CNT content and evolution during composite fabrication process were addressed. Finally, the challenges which ensue in realizing CNT as filler in Al composites were discussed from the point of processing, cost considerations and safety manipulation. The following conclusions can be made:

(1) The procedure for producing the Al-CNT composite is a multistage process. The final quality of the resultant composite is determined by an appropriate combination of volume content of the reinforcement, the CNTs and metal powder mixing technique, the subsequent consolidation and secondary processing, etc. By selecting a proper combination of the affecting factors, the

expected strengthening mechanisms can be achieved.

(2) There are various strengthening mechanisms that may occur in CNT reinforced Al matrix composites, including load transfer, Orowan mechanism and thermal mismatch. Some of these mechanisms are related to each other and in practice, they operate simultaneously.

(3) The challenges of the P/M Al-CNT composite lie on the (i) dispersion degree, (ii) load transfer (interfacial bonding), (iii) volume content, (iv) CNT alignment, and (v) processing technique. Up to now, the CNT/AMCs are still at a research stage and their full potential is yet to be realized.

CHAPTER 3

EXPERIMENTAL PROCEDURE

Operating procedures of the experiment are documented to understand how the individual equipment operates and contributes to the whole experiment. The details and the equipments used are recorded in this chapter.

3.1 Composite Synthesis

3.1.1 Materials

Aluminum (Al) powders were used as the matrix material and multi-walled carbon nanotubes (CNTs) were used as the reinforcement phase.

Aluminum Powders

The gas atomized Al powder was supplied by Henan Yuan Yang Aluminum Industry Co. Ltd, China. The average size of the Al powder is approximately 5μm, with purity >99%. The detailed specifications of the as-received Al powder are shown in Table 3-1, and Figure 3-1 shows the powder size distribution diagram. Sample micrographs of the as-received Al powders are shown in Figure 3-2.

Table 3-1. Specifications of as-received Al powder.

Material	Production method	Density (g/cm^3)	Purity (%)	Diameter (μm)
Al powder	Gas atomization	2.7	>99	5

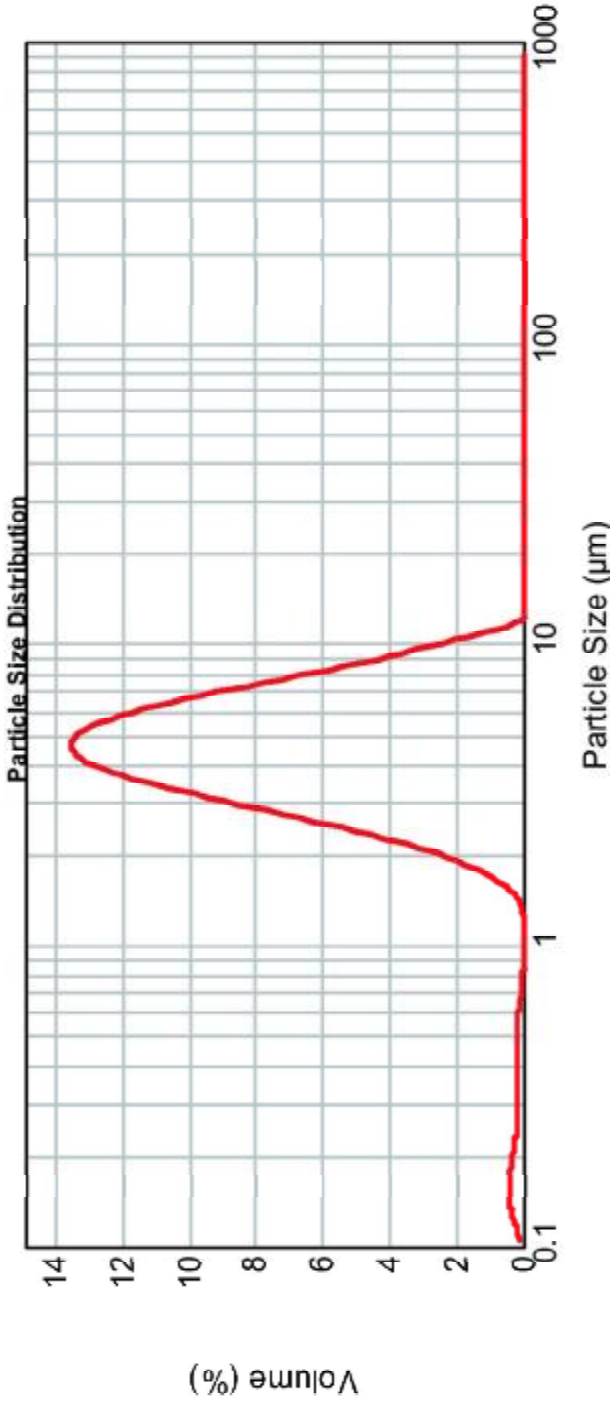

Figure 3-1. Aluminum particle size distribution diagram. The average size of the Al powder is approximately 5µm.

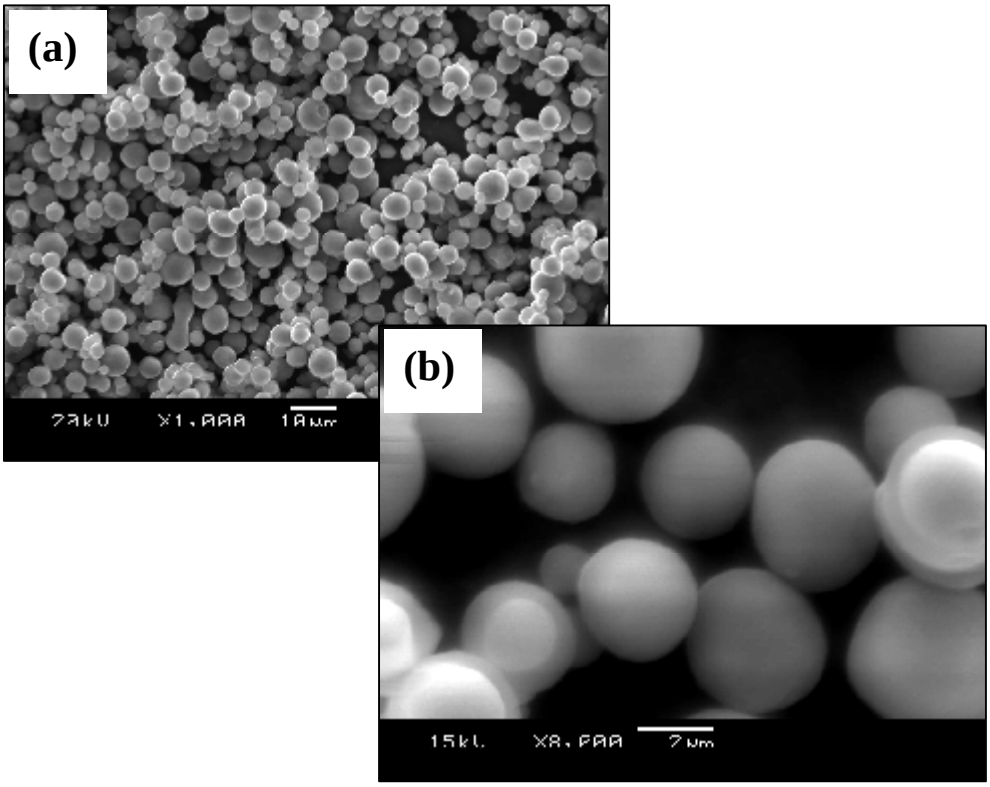

Figure 3-2. SEM images of as-received Al powder: (a) low magnification, and (b) high magnification.

CNTs

CNTs were supplied by Shenzhen Nanotech Port Co. Ltd (NTP), China. The CNTs were fabricated by chemical vapor deposition (CVD) method. The detailed specifications of the as-received Al and CNTs powders are shown in Table 3-2. Figure 3-3 illustrates the Raman spectra of the as-received CNTs. As is clear from Figure 3-3, there were two peaks at ~ 1320cm^{-1} (D band) and the other at ~ 1580cm^{-1} (G band). The G band is assigned to zone center phonons of E_{2g} symmetry, showing the original graphitic structure of CNTs. On the other hand, the D band is assigned to K-point phonons of A_{1g} symmetry, indicating the disorder features of the graphite.

Sample micrographs of the as-received CNTs are shown in Figure 3-4 and 3-5. As shown in Figure 3-2, it can be seen that CNTs agglomerate together. This is due to the intricate entanglements of long and smooth CNTs and resulting agglomeration due to strong van der Waals forces of attraction between them. In the high-resolution image, no amorphous carbon layer is visible on the outer surface of the nanotube.

Table 3-2. Specifications of as-received CNTs.

Material	Production method	Density (g/cm^3)	Purity (%)	External diameter	Length (μm)	Special surface area (m^2/g)
CNT_S	Chemical vapor deposition	2.2	>95	50-100 nm	5-15	200-250

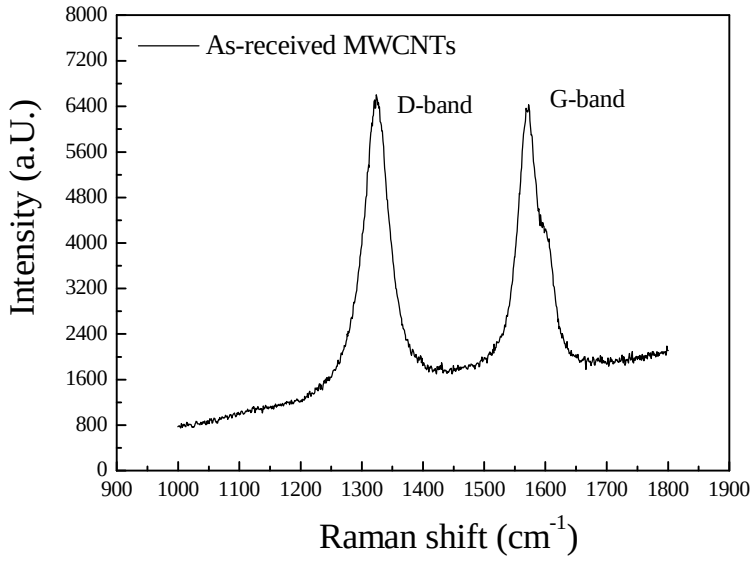

Figure 3-3. First-order Raman spectra of the as-received CNTs.

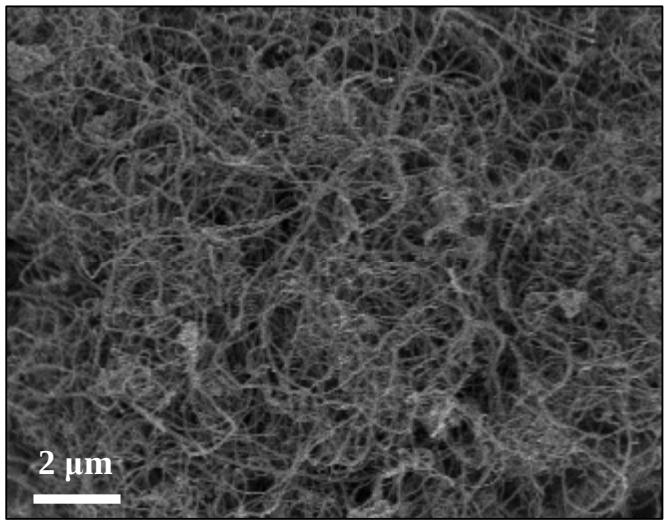

Figure 3-4. FESEM image of as-received CNT powder.

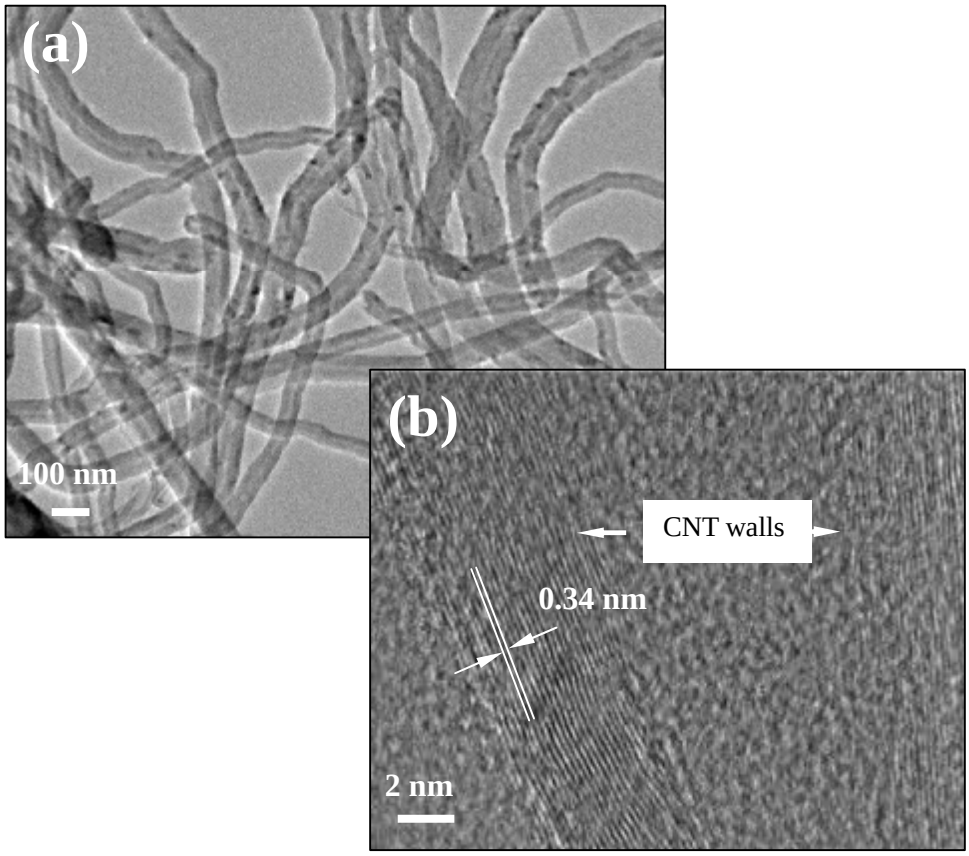

Figure 3-5. TEM image of as-received CNT: (a) low magnification and (b) high magnification; the distance between the CNT walls is 0.34nm.

3.1.2 Processing

Aluminum composites with 0-2.0wt.% loading of CNTs were synthesized by powder metallurgy (P/M) technique and combined with secondary processing. The detailed processing procedure would be discussed in Chapter 4.

This study would also provide a simple technique to produce Al-CNT nanocomposites - Spread-Dispersion (SD) method. The detailed SD procedure would be discussed in Chapter 5.

3.2 Physical and Mechanical Properties Testing

In order to investigate the effect of CNTs on the physical and mechanical properties of the composites, samples were machined from the master samples and their density, microhardness, nanoindentation, room- and elevated-temperature uniaxial tensile properties and fatigue resistance were tested and analyzed.

3.2.1 Density Measurement

The experimental density of the composites was obtained by Archimedes' method. Three density measurements were made on randomly selected samples for statistical analysis. The theoretical density of the composites was calculated by the Rule of Mixture:

$$r_c = r_{Al}(1-V_{CNT}) + r_{CNT}V_{CNT} \quad (3\text{-}1)$$

And the porosity percentage of the composites was calculated by:

$$p = (1-\frac{r_a}{r_{Al}(1-V_{CNT}) + r_{CNT}V_{CNT}})\times 100 \quad (3\text{-}2)$$

where p is the porosity percentage of the composite; ρ_c is the theoretical density of the composite; ρ_a is the actual density of the composite; ρ_{Al} and ρ_{CNT} is the density of Al and CNT, respectively; V_{Al} and V_{CNT} is the volume fraction of Al and CNT respectively.

3.2.2 Microhardness

Micro-Vickers hardness tests were performed using 100 grams load. Ten random points were measured for statistical analysis.

3.2.3 Nanoindentation Tests

In order to investigate the local mechanical properties of the tensile-fractured specimens, nanoindentation tests were conducted. The detailed nanoindentation tests would be discussed in Chapter 7.

3.2.4 Room-temperature Uniaxial Tensile Tests

In order to investigate the effect of CNTs on the strength and ductility of the composite, room-temperature uniaxial tensile tests were carried out on the monolithic Al and Al-CNT composites. Tensile I-shape specimens were machined from the master sheet with a dimension of 11mm × 4mm × 1.5mm (length × width × thickness). The uniaxial high temperature tensile tests of Al/Al-CNTs were performed using Instron 8502 testing machine. Tensile test was conducted under room temperature with strain rate of 1 x 10^{-3}/s. Unless specifically noted, all the strains reported in this thesis are engineering strain rather than true strain.

3.2.5 Elevated-temperature Uniaxial Tensile Tests

In order to investigate the effect of CNTs on the strength and ductility of the composite at elevated temperature, elevated-temperature uniaxial tensile tests were carried out on the monolithic Al and Al-CNT composites. Tensile I-shape specimens were machined from the master sheet with a dimension of 11mm × 4mm × 1.5mm (length × width × thickness).

The elevated-temperature tensile tests of Al/Al-CNTs were performed using Instron 8502 testing machine equipped with an electrical resistance furnace chamber. Tests were performed at ambient temperatures of 25, 200, 300, 400 and 500°C, with strain rate of $1x10^{-3}$/s. Test temperature was monitored by a thermocouple close to the gauge length of the specimen. Temperature varied between ±3°C.

3.2.6 Fatigue Tests

Room temperature tension-tension fatigue tests were conducted of the Al/Al-CNT composites. I-shape specimens were machined from the as-rolled sheet with a dimension with a gauge length of 11mm. The specimens were tested at peak stresses of 100, 110, 120, 130, 140 and 150MPa. The stress ratio (R) is 0.1 and frequency is 5Hz. Stress ratio is the ratio between the minimum stress to the maximum stress in one cycle of loading in a fatigue test.

3.3 Characterization

3.3.1 Optical Microscopy

Microstructure of the Al/Al-CNT specimens was characterized under a Carl Zeiss optical microscopy (OM). Samples were sectioned from the master materials, and mounted, then grinded using metal bonded diamond discs, followed by polishing down to 1μm diamond paste. The OM sample preparation was done following the standard metallographic procedure. Samples were cleaned in acetone or ethanol before etching. Flick's reagent (i.e. 10ml HF, 15ml HCl and 90ml H_2O) was used to etch the specimen to reveal the grain boundary.

3.3.2 SEM

Scanning electron microscopy (SEM) was also employed in the characterization of microstructures and fracture surface of the specimens. Both normal SEM and filed-emission scanning electron microscopy (FESEM) were used. Normal SEM was performed on a JEOL, JEM-5600 and FESEM investigation was performed on a JEOL, JEM-7600. Energy dispersive spectroscopy (EDS) connected to the SEM was used to examine the chemical composition of the second phases present in the material. Before SEM, all samples were gold-sputtered.

3.3.3 TEM

Transmission electron microscopy (TEM) was done on a JEOL, JEM-2010 TEM, operating at 200kV. TEM specimens were prepared by sectioning the samples into slices

from the bulk material by a low speed diamond saw. The samples were manually ground to approximately 100μm using diamond discs before mechanical polishing to a thickness of about 80μm using diamond paste (1μm). Thin samples were then punched into 3mm diameter discs, followed by followed by electrochemically polished down to an electron transparent thickness less than 100nm using twin-jet polishing with a 20vol.% nitric acid and 80 vol.% methanol mixture under -20℃.

3.3.4 Raman Spectroscopy

Raman spectroscopy (Renishaw RM1000) was utilized to understand the quality of CNTs. Raman spectra were excited with a 633nm helium–neon (He–Ne) laser. The Raman spectra were baseline corrected using linear function and the peak shapes were fitted by a Gaussian function.

3.3.5 XRD

X-ray diffraction (XRD), which employed a Philips XRD-PW-1831 diffractometer, with Cu K_α radiation, was used to determine the phase composition of the testing specimens, operating at 20kV, 30mA.

3.4 Summary

This chapter provides an overview of the experimental procedures and techniques used in this work. The processing of CNT reinforced Al composites by powder metallurgy techniques combined with secondary process are outlined. The methods used to

characterize the microstructure, physical and mechanical properties of the materials are stated.

CHAPTER 4

PROCESSING, MICROSTRUCTURE AND ROOM TEMPERATURE TENSILE STRENGTH OF AL/CNT COMPOSITES

4.1 Introduction

As mentioned in Chapter 2, only a few improvements on CNT reinforced aluminum (Al) matrix composites have been reported [15, 16, 25, 31-33], which is mainly attributed to the processing difficulties and lack of understanding of the strengthening mechanisms, and most importantly, cost. The establishment of an appropriate and economical processing practice for CNT reinforced Al composites is still a challenge.

Accordingly, the aim of this study is to fabricate CNT reinforced Al composites coupled with improved strength, and reliability and reproducibility in processing. The composites were synthesized using powder metallurgy (P/M) technique combined with secondary processing. The microstructure and mechanical properties of the composites as well as the CNT microstructure evolution were characterized. Attempts were made to understand the strengthening mechanism.

4.2 Experimental

4.2.1 Processing

Aluminum powder and 0.5, 1.0, 2.0 wt.% CNTs were used. Monolithic Al and Al-CNT composites were synthesized by P/M technique and combined with hot extrusion and hot rolling. For the comparison purpose monolithic Al sample (without CNTs) was also fabricated. The fabrication process for Al/Al-CNT composites is presented in Figure 4-1. The detailed procedure is presented below:

(i) Powder mixing

Measured amounts of CNTs (to achieve a weight fraction of 0.5, 1.0 and 2.0%) were mixed with Al powder in a plastic jar and the mixture was blended by ball milling.

(ii) Compaction

The Al-CNT mixture was cold compacted under 20 tons by a hydraulic pressing machine for 5 min. Molybdenum disulfide (MoS_2) lubricant was used in order to reduce the frictional forces, and aluminum foil was used to surround powders when compacting.

(iii) Sintering

The green-compacts were then vacuum-sintered at a temperature of 530°C with a holding time of 3.5h. Natural cooling was applied.

(iv) Extrusion

The sintered cylindrical samples of 30mm diameter and 22mm length were hot extruded into a cylindrical rod of 10mm diameter at 520°C with an extrusion ratio of 9:1. The extrusion process was carried out at 5mm/sec.

(v) Rolling

To obtain full density, the hot-extruded rods were hot rolled. These extruded rods were hot rolled at 500°C to 85% reduction to give a 1.5mm plate.

4.2.2 Room-temperature Uniaxial Tensile Tests

Tensile I-shape specimens were machined from the as-rolled sheet with a dimension of 11mm × 4 mm × 1.5mm (length × width × thickness). Details of the tensile tests were described in Chapter 3.

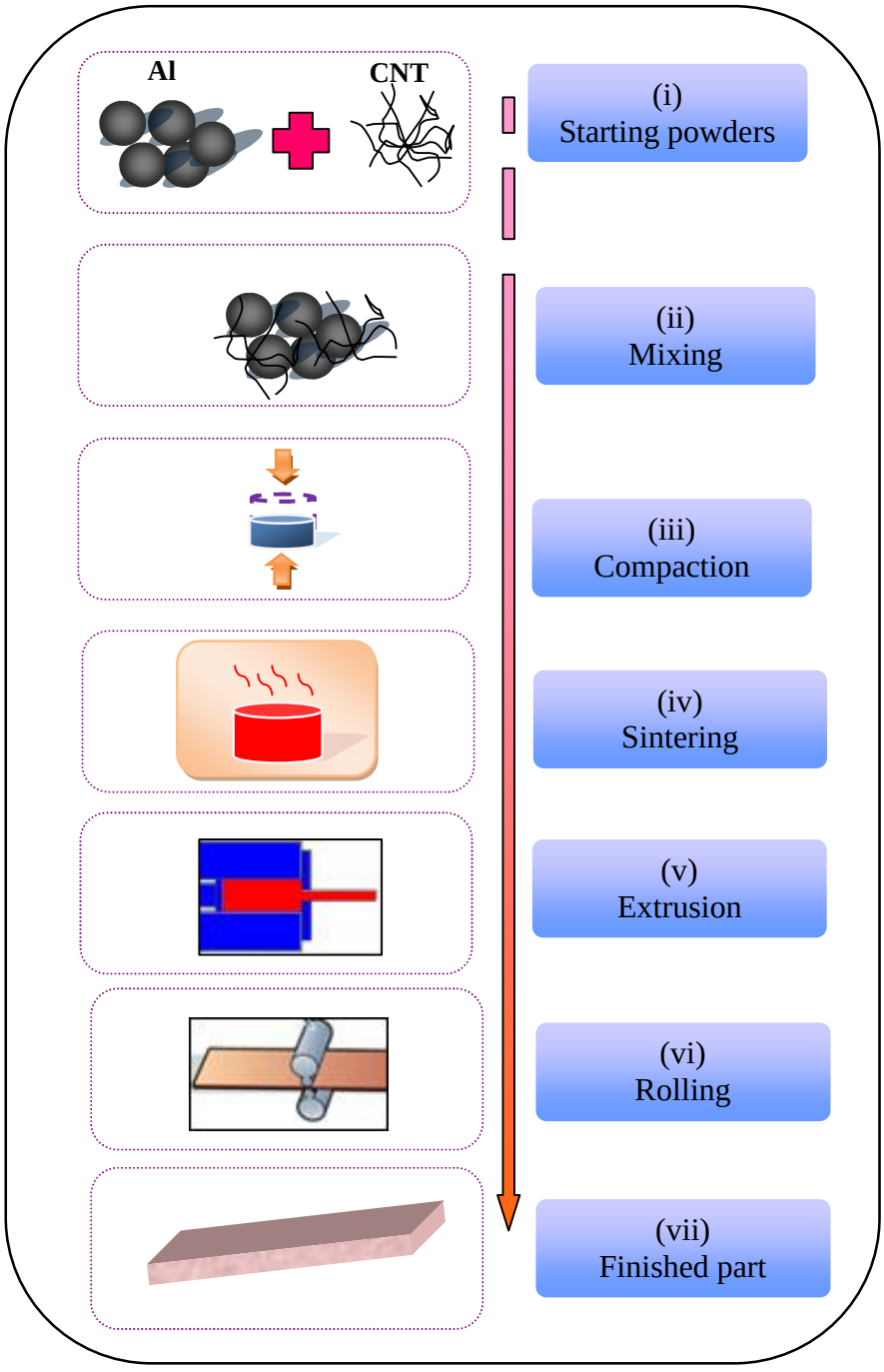

Figure 4-1. Fabrication procedure for Al/Al-CNT composites.

4.3 Results

4.3.1 Powder Mixture

SEM micrographs of the mixed Al/CNT powders are shown in Figures. 4-2. It can be seen that the individual CNT was embedded within the Al powders, although it was likely that the round shape of the metallic powder was difficult for the CNTs to embed in. Some CNT clusters were still found amongst the Al powders.

Raman spectroscopy revealed complementary information on the evolution of CNTs after powder mixing. Figure 4-3 illustrates the Raman spectra of the as-received CNTs as well as the post mixed CNTs. As clearly from Figure 4-3, there were two peaks at ~1320cm^{-1} (D band) and the other at ~1580cm^{-1} (G band). By comparison of the I_D/I_G ratios of these spectra, it could be seen that this ratio varied (see Figure 4-3). The as-received CNTs had the lowest I_D/I_G ratios of 0.858 (this was produced from their production growth and treatment after growth [9]). The I_D/I_G ratios progressively increased to 0.994 of the low energy ball-milled CNTs. The I_D/I_G ratio represents the defect density in graphitic structures. The amount of defects apparently increased in the CNTs after powder mixing.

In addition, the G-band shift of the roll-milled CNTs to a large wavenumber could be observed. In this study, it is suggested that the shift of G band contributed to the residual strain in the CNTs, which was the result from the mechanical alloying. When a strain is applied to them, the interatomic distances of the CNTs change, hence the vibrational frequencies of some of the normal modes change, resulting in a Raman peak shift [4]. The larger the strain that the CNT experiences, the larger the Raman peak shifts [120]. The

residue stress in the mechanical alloyed CNTs was substantial, as G-band shift of the roll-milled CNTs was evident.

The I_D/I_G ratios, as well as the G-band shift of the post-mixing sample are presented in Table 4-1, corresponding to Figure 4-3. Further observed from Figure 4-3, for the CNTs after roll-milling, the G-band not only shifted towards higher wavenumbers, but also became broaden and decreased in amplitude. The narrow sharp G-peak in the as-received state became multi-peak features in the mechanical alloyed CNTs (see the enlarged detailed G-bands inset in Figure 4-3). The broadening and shortening of the G-band again confirmed the severe disruption of the graphite structure after mechanical alloying. It was noted that, however, the intensity in the Raman spectra amplitude of the roll-milled sample apparently decreased. This indicated a dilution effect of CNTs.

Presently, however, there is no valid methodology to grade the CNT dispersion. Besides the directly visualized evaluation (though not representative), indirectly measurement of mechanical properties is another way. If the dispersion is good, the mechanical properties will be improved by comparison with the pure metal. The mechanical properties of the Al/Al-CNT composites will be discussed later.

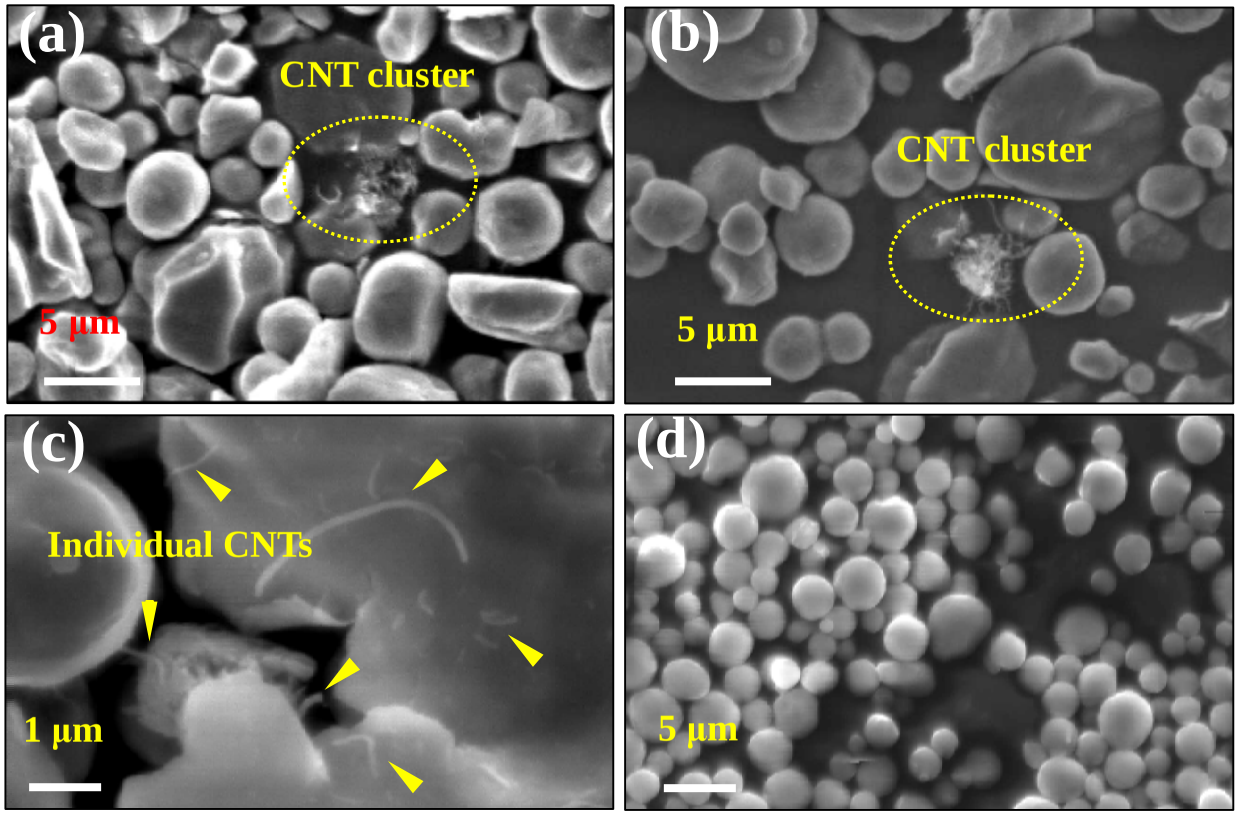

Figure 4--2. SEM micrographs of the Al and CNTs powders after mixing. Some clusters of CNTs could still be observed in (a) and (b); while (c) some individual nanotube spread into the Al powders as arrows indicated; (d) most of the Al powders remained unchanged (round-shape and same size) after mixing.

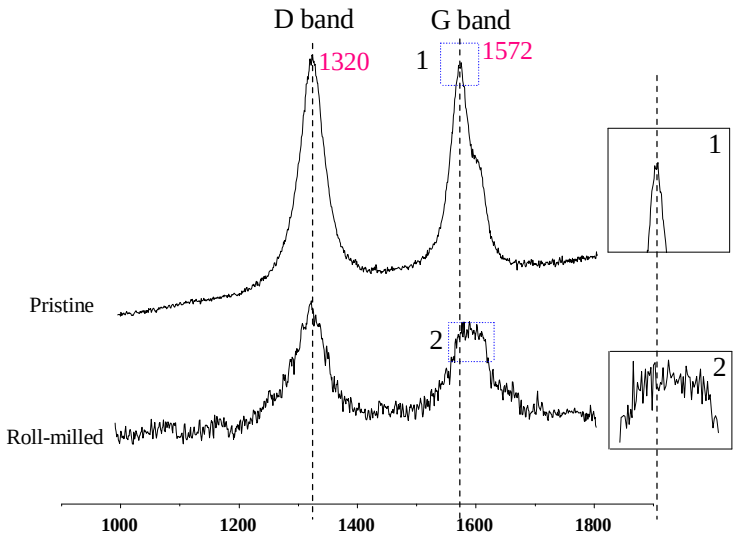

Figure 4-3. Comparison of first-order Raman spectra of as-received CNTs, and CNTs after powder mixing. Note that G mode shifted and broadened after mixing.

Table 4-1. I_D/I_G ratio and G-band shift of the as-received and post-mixed CNTs.

CNTs	As-received	Roll-milling
I_D/I_G	0.858 (±0.2)	1.10 (±0.3)
Position of G band (cm^{-1})	1572	1590

4.3.2 Composite Consolidation

Figures 4-4 (a) - (c) show the photographs of the consolidated Al-CNT composites at the as-sintered, as-extruded and as-rolled stage respectively, and Figures 4-5 (a) - (c) display the microstructure of the corresponding consolidated composites as shown in Figure 4-4. Equiaxed grains were observed in the as-sintered sample. These spherical grains were

elongated subjected to the severe plastic deformation in hot-extrusion process (see Figure 4-5(b)). Meanwhile, the plastic flow led to the alignment of CNTs along the extrusion direction. The size of the grain was further refined by hot-rolling, down to 0.2μm (see Figure 4-5(c)). It can be seen that the plastic deformation has significant effect on refining the matrix grains and condense the materials. The grain size of the consolidated composites at different P/M stage is shown in Figure 4-6.

The XRD profile of the as-received Al powders and the as-sintered Al-CNT composite is shown in Figure 4-7. From Figure 4-7, it can be seen that the X-ray diffraction spectrum of the as-sintered Al-CNT composites did not reveal the presence of either alumina or aluminum carbide. But it is noted that the absence of aluminum carbide may be due to the low content of it and also due to the limit resolution of the XRD.

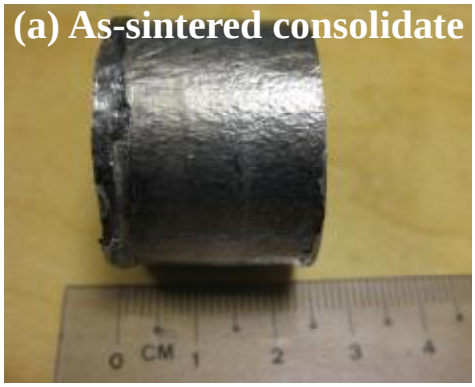

Figure 4-4. Photographs of the consolidated samples: (a) as-sintered consolidate; (b) as-extruded consolidate; and (c) as-rolled consolidate.

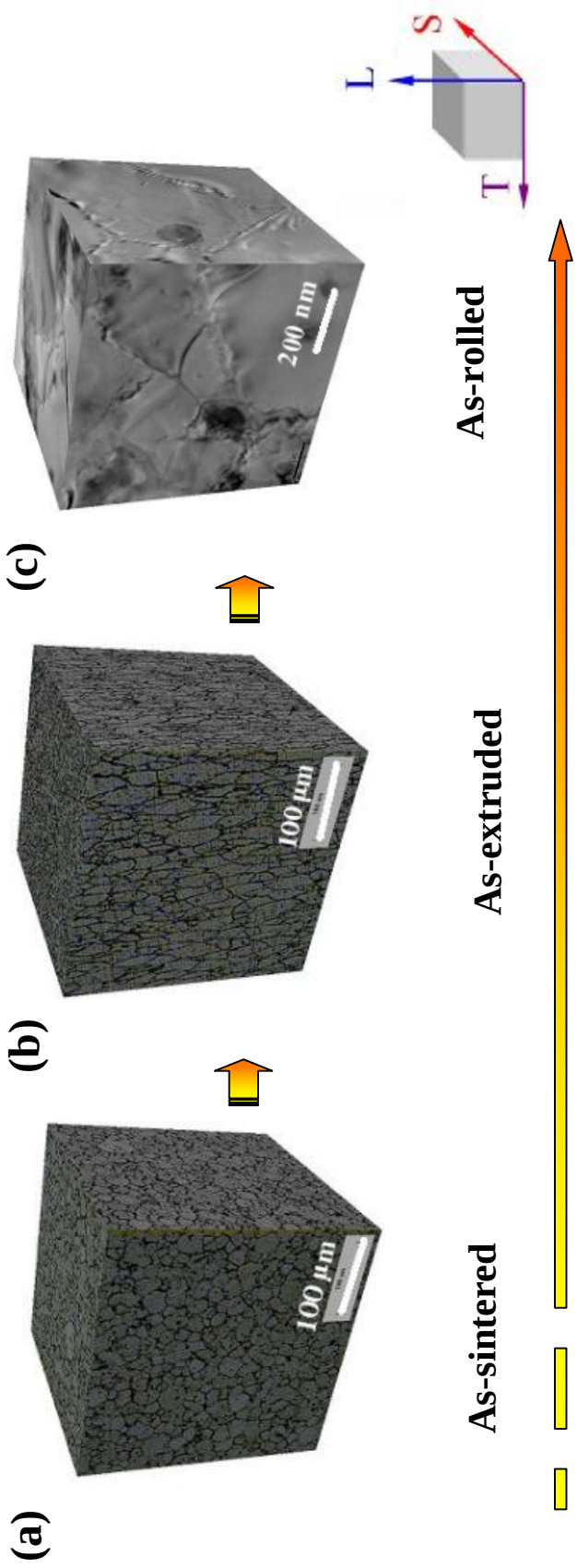

Figure 4-5. Stereoscopic microstructure of the consolidated Al-CNT nanocomposites: (a) optical image of the as-sintered; (b) optical image of the as-extruded; and (c) TEM image of the as-rolled specimen.

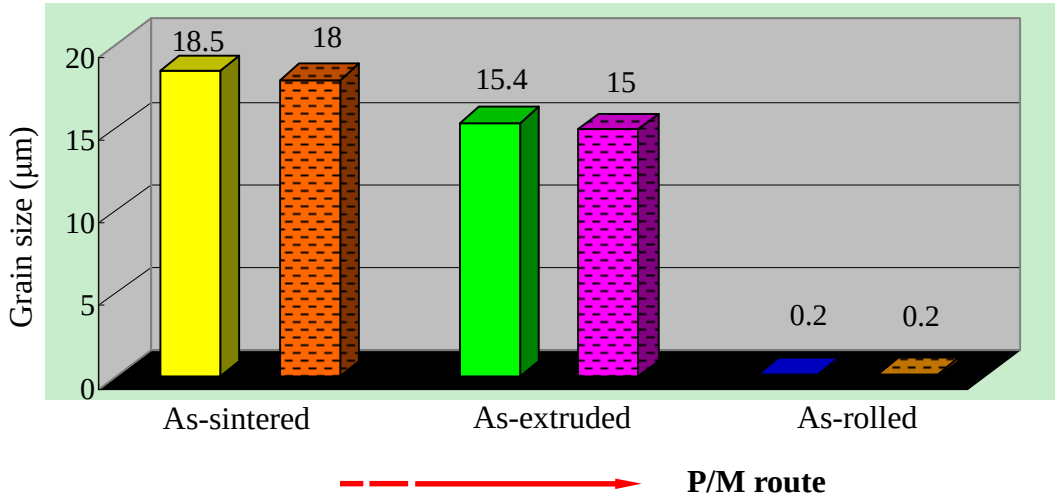

Figure 4-6. The grain size of the as-sintered, as-extruded and as-rolled Al-CNT composites.

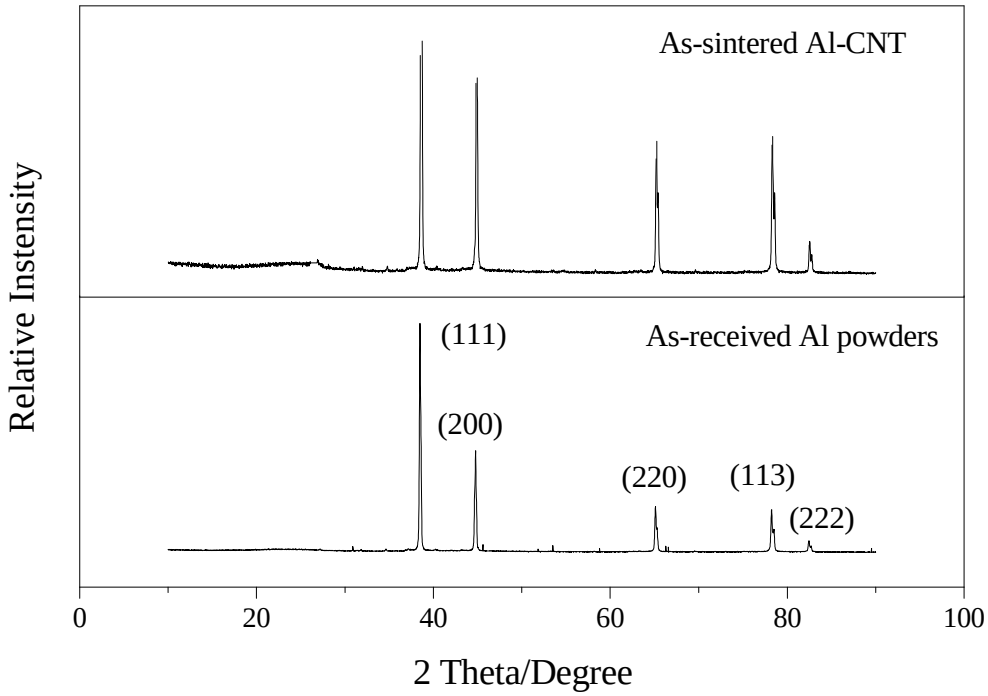

Figure 4-7. Comparison of the XRD profile of as-received Al powder and the as-sintered Al-0.5CNT composite.

4.3.3 Density

The physical and mechanical properties of the final as-rolled monolithic Al and its composites are shown in Table 4-2. The densities of the Al/Al-CNT materials are close to the theoretical ones, which indicates full densification, and superior to most Al products reported. The relative density of Al composites with CNT was higher than that of monolithic Al (without CNT). It is suggested that CNTs helped to improve the matrix densification by filling the microvoids of the Al particles. The Al-0.5CNT has the greatest value of relative density; whilst with higher CNT content, i.e. 1.0wt.% CNT, the densification of the composite decreased. It is because the excess CNTs which remain after filling the microvoids form conglomerates, which interrupt the sintering and deteriorate the consolidation [106].

4.3.4 Microhardness

The microhardness results of Al/Al-CNT composites are presented in Table 4-2. A significant improvement in the hardness of the composites is observed with the incorporation of CNTs. An addition of 0.5wt.% CNT can enhance the hardness by 33%, and an enhancement of 42% was obtained by adding of 1.0wt.% CNT. This indicates that CNTs have a significant effect on the localized plastic deformation of the Al matrix.

4.3.5 Tensile Behavior

The tensile test results of the as-rolled Al/Al-CNT composites are given in Table 4-2. As seen from Table 4-2, a simultaneous increase in 0.2% proof stress, ultimate tensile strength and elongation was found for the CNT reinforced composites. The tensile

strength increased with increasing fraction of CNTs. The strength reached maximum when the 2.0wt.% CNTs were added, as an enhancement as high as 45% was obtained compared with the monolithic Al.

Table 4-2. Physical and mechanical properties of Al/Al–CNT composites.

Materials	Density			Hardness (HV)	σ_{yield} (MPa)	σ_{UTS} (MPa)	Ductility (%)
	Theoretical density (g/cm^3)	Experimental density (g/cm^3)	Relative Density (%)				
Monolithic Al	2.70	2.65	98.26	42.30	121	138	19
Al-0.5CNT	2.68	2.77	103.17	56.29	173	189	17
Al-1.0CNT	2.67	2.70	101.27	60.49	185	198	15
Al-2.0CNT	2.63	2.66	100.95	60.39	189	200	11

4.4 Discussion

4.4.1 Synthesis and Microstructure of Al/Al-CNT Composites

Monolithic Al and Al-CNT composites were successfully obtained by the P/M technique combined with the secondary processing. Density measurement results show that near fully-dense composites were obtained, whose density maintained at a similar level to that of pure Al, due to the low density of CNT. This is attractive for Al application as lightweight structural materials. From the microstructure characterization, no pores in the composites produced were observed (see Figure 4-5(c)). For most Al solid products, voids commonly exist. One main reason is because the strong oxide layer (Al_2O_3) surround on

the surface of Al particles. The oxide barrier prevents the solid state diffusion of Al powder during sintering. In this study, the post processing, i.e. hot extrusion and rolling, however, have been effectively used to achieve full densification and mechanical properties superior to wrought ingot metallurgy (I/M) and normal P/M product in Al alloys. Voids remaining in the sintered samples were eliminated due to the severe plastic deformation in hot extrusion process. The matrix and the reinforcement were also brought into intimate contact with each other by the compressive stress from extrusion and rolling, and hence resulted in more uniformly distributed and well coupled reinforcement in the matrix. It is suggested in this study that the severe deformation from secondary processing has had a positive effect on CNT dispersion and orientation and consequently enhanced mechanical properties. The values of mechanical strength of the Al-CNT composite after sintering, extrusion and rolling are provided in Figure 4-8. The strength of the corresponding pure Al is also presented to provide a better comparison. Compared to the monolithic Al under the same process history, the strength enhancements of the Al-CNT composites are: 5.2% (as-sintered), 10.3% (as-extruded), 35% (as-rolled), see Figure 4-8. It can be seen that secondary processing has further improved the composite strength. It has been explained that by the application of secondary processing, the matrix deforms in a plastic manner and the plastic flow could break the CNT-clusters and re-distribute the CNTs in the matrix. It also improves the densification and CNT orientation. In addition, the compressive forces from secondary processing are expected to exert a better contact of the matrix-CNT interface, leading to better load transfer. Furthermore, CNTs can act as obstacles to dislocation movement in metals, so that plastic deformation is not uniform in the matrix. Orowan loops also are expected to exert a back stress on dislocation sources during the plastic deformation from the secondary

processing [93]. Similar studies have also reported [69, 91-92] that CNTs are re-distributed and preferentially oriented with the matrix during rolling, leading to improved mechanical properties of the composite. In addition, secondary processing led to further structural refinement of the Al matrix (see Figure 4-8), and this would benefit the mechanical properties of the composites. Although the Al/CNT wettability is poor, extensive TEM characterization shows that the CNT is in good contact with the Al matrix due to the nanosize of the reinforcement and the sound synthesis method (see Figure 4-9).

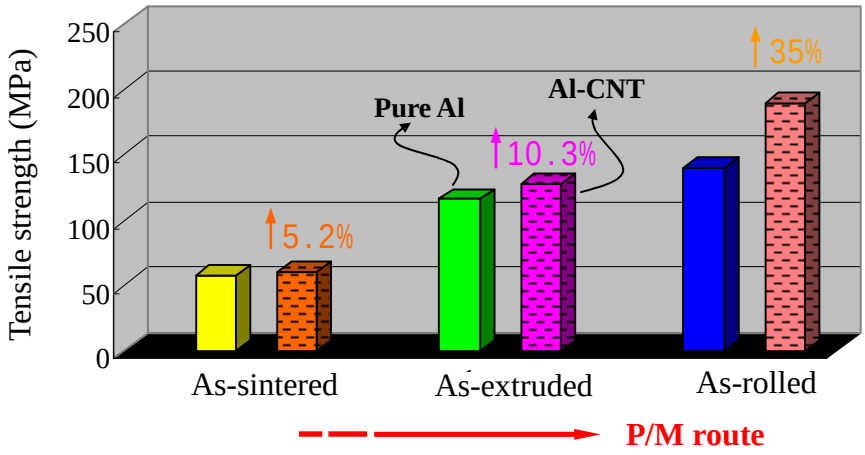

Figure 4-8. Compression yield strength of the as-sintered Al-CNT composite, and tensile strength of the hot-extruded and hot-rolled Al-CNT composite. Arrows show the strength enhancement of Al-CNT composite compared to the counterpart monolithic Al.

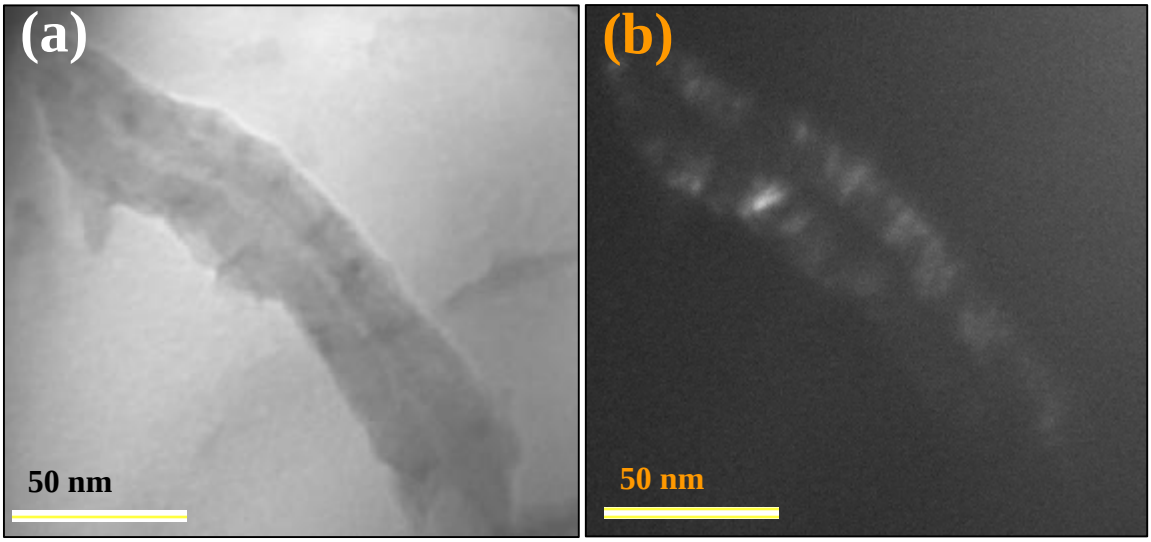

Figure 4-9. TEM images of CNT imbedded in the aluminum matrix (a) bright-field (BF) and (b) dark-field (DF).

4.4.2 Mechanical Behavior

The yield strength of a composite material is the stress required to operate dislocation sources; it is governed by the presence and magnitude of the obstacles which impede the free motion and/or generation of dislocation [93]. In the present CNT composites, the yield stress of those composites were clearly enhanced compared with the counterpart monolithic Al, especially for 2.0wt.% CNT composite, an enhancement of 56% was obtained than monolithic Al (see Table 4-2). Based on the physical properties of CNTs, several strengthening mechanisms were considered hereby: (i) Orowan strengthening; (ii) enhanced dislocation density due to the thermal mismatch between the reinforcement and the matrix; and (iii) load-partition effect of the reinforcement. They are discussed below:

4.4.2.1 Orowan Strengthening

In general, the yield strength of a composite material is the stress required to operate dislocation sources, and it is governed by the presence and magnitude of the obstacles obstructing the dislocation movement [93]. Orowan strengthening, caused by the resistance of closely spaced hard particles to the passing of dislocations, is important in aluminum alloys [93]. Orowan mechanism requires a small inter-particle spacing, thus it is not significant in the macro- and micro-sized particle reinforced composites. In contrast, it becomes more favorable in the nano-scale CNT reinforced composite due to the small filler size and small inter-particle spacing at a given volume content. Further, rod-shape reinforcement would cause more effective strengthening mechanism than spherical shape reinforcements due to the resultant closer inter-particle spacing. Kelly [121] reported that rod-shape reinforcement resulted in around two times as much strengthening effect as that of the spherical ones of the same volume fraction. The small fiber-spacing is beneficial because fiber can bridge cracks throughout the matrix.

4.4.2.2 Thermal Mismatch

CNTs have a coefficient of thermal expansion approximately of ~$1\times 10^{-6}\,K^{-1}$, while purity Al exhibits a much greater coefficient of thermal expansion of $23.6 \times 10^{-6}\,K^{-1}$ [5]. Hence there exists a thermal mismatch of the CTE between the matrix and CNTs, when the composite cools down from the synthesis temperature. During thermal cycling, i.e. sintering-cooling, hot extrusion-cooling and hot rolling-cooling in this study, there would be a higher dislocation density near the reinforcement CNTs due to the thermal mismatch. For rod-shape reinforcements, the enhanced dislocation density, r^{CTE}, which is assumed

to be entirely due to the residual plastic strain developed due to the thermal mismatch of matrix and reinforcement on cooling from the elevated processing temperatures, can be estimated as [122],

$$r_{CTE} = \frac{10fe}{b(1-f)}\frac{1}{D} \tag{4-1}$$

with D designating the diameter of the CNT, while f stand for the volume fraction of the reinforcement; e is the misfit strain due to the different CTE between matrix and reinforcement. It can be seen that with decreasing diameter of the reinforcement, higher dislocation density will be produced at a given reinforcement content. This is especially applicable for the small scale CNT.

Again, when the components are subjected to a temperature change, such as cooling from the processing temperature, thermal stresses around the nanoparticles large enough to cause plastic deformation are generated in the matrix, especially in the interface region [93]. The dislocation density generated in the close vicinity of CNTs would lead to work hardening of the matrix, hence improving the strength.

It is also noted that during plastic deformation, i.e. extrusion and rolling, the distribution of dislocation within the matrix is not homogeneous; there is a higher dislocation density near the reinforcement. Dislocations are obstacles for other dislocations. Once the dislocation has become pinned or restricted, an extra force is required to overcome the restrain forces. This results in a corresponding increase in yield stress. There is a correlation between dislocation density and yield strength following the Taylor relationship [123],

$$\Delta s_y = Gb\sqrt{r_\perp} \quad (4\text{-}2)$$

where G is the shear modulus, b is the Burgers vector, and $r_\perp$ is the dislocation density. Enhanced dislocation density was easily found in the matrix. As shown in Figure 4-10, dislocations pile up in the matrix.

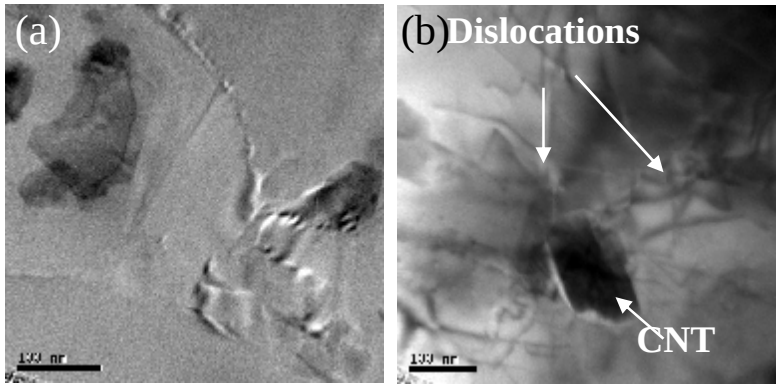

Figure 4-10. TEM characterization shows the as-rolled (a) monolithic Al, and (b) Al-0.5CNT composite, where dislocations pile up in the matrix of the composite.

4.4.2.3 Load partition

The tensile force was transferred to the fiber by the matrix/fiber interfacial shear stress (IFSS). A strong interface or good adhesion, would promote the load transfer efficiency and, consequently, enhancing the strength of the composite. Generally there are three types of adhesion mechanisms between two surfaces, that is, (i) physical bonding, (ii) chemical bonding and (iii) mechanical interlocking [124]. Physical bonding is mainly a result of the van der Waals forces, which is weak in the CNT reinforced composite system. The chemical bonding arising from the chemical reaction of aluminum and CNTs is not

established; also it is difficult to assess its contribution to bond strength even the chemical bonding exists. For mechanical interlocking, adhesion is promoted mechanically by a large interfacial area, that is, surface roughness, friction interlocking and dovetail interlocking [124]. In this study, this is deemed to be the main contribution to the load transfer, and in what follows, several contributing factors for Al/CNT mechanical interlocking would be quantitatively and qualitatively discussed.

Ⅰ Effects of CNT Interfacial Bonding

The thin and long CNT has a large aspect ratio of up to 132,000,000:1, which is significantly larger than any other material. The high-aspect-ratio structures are beneficial to the mechanical interlocking of CNTs with the matrix. Further, CNTs possess an enormous specific surface area (SSA) being several orders of magnitude larger than conventional macro- and mico-fillers [47]. An external SSA of CNTs is as high as 178m^2/g [125]. The high surface area in contact would beneficially facilitate load transfer.

On close examination of the surface of CNT, it could be observed that irregularities and protrusions existed on the tube surface (Figure 4-11). These surface asperities served as mechanical anchors, locking the matrix. Based on the above, the inherent characteristics of CNT *per se*, that is, large aspect ratio as well as high specific surface area, distorted tubes and roughened surface, which would lead to a better interfacial bonding with the matrix.

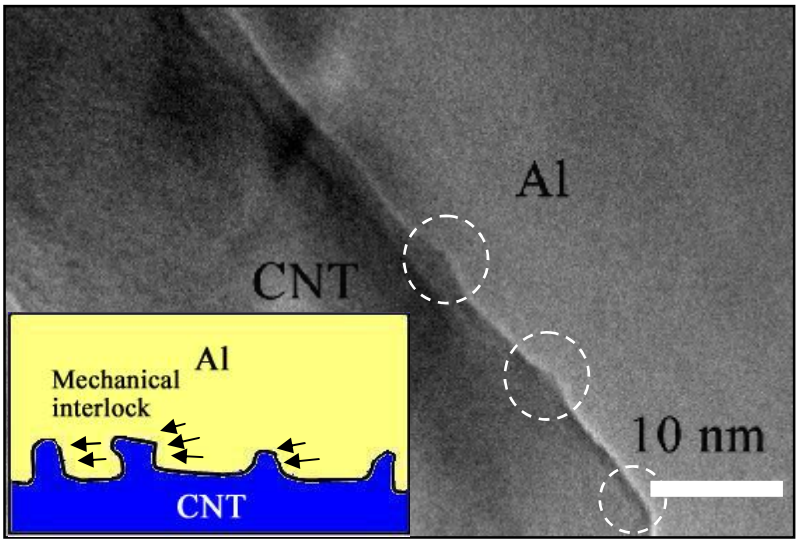

Figure 4-11. TEM image of CNT embedded in Al matrix. Non-uniform CNT diameter can be observed. There are protrusion on the CNT surface, which was beneficial to the micromechanical interlocking. Inset is the schematic illustration of the surface asperities that serve as mechanical anchors, locking the matrix.

Effects of Surrounding Matrix on Interfacial Bonding

Besides the CNT *per se*, the bonding strength also depends on the environment surrounding it, namely the stress around the reinforcing phase. As mentioned earlier, there exists a thermal mismatch of the CTE between the matrix and CNTs, when the composite cools down from the fabrication temperature. The radial stress, σ_{therm}, applied on the CNT surface, arising from thermal shrinkage, could be expressed as [112]:

$$s_{therm} = \frac{\left(a_f - a_m\right)\Delta T}{\frac{1+g_m}{2E_m} + \frac{1-2g_f}{E_f}} \qquad (4\text{-}3)$$

Where γ is the Poisson's ratio, E is elastic modulus and ΔT is the temperature difference. From Equation 4-3, it can be seen that: (i) if $\alpha_f > \alpha_m$, σ_{ther} would be positive, that means there is tensile stress on the interface; (ii) Conversely, if $\alpha_f < \alpha_m$, σ_{therm} would be negative and there is compressive stress on the interface [112]. The CNT reinforced Al matrix system is the second case. Thermal contraction of the matrix exerts a compressive stress (thermal shrinkage) on the particle surface. This radial compressive stress is beneficial to the enhancement of friction between CNTs and matrix phase.

CNTs also experienced physical constraint from the powder metallurgy and secondary operations, i.e. the hot extrusion and hot rolling; Composite experienced somewhat severe plastic deformation during the processing. Compressive stresses were obtained with the extreme reduction in area by both the extrusion and rolling operations. Experimental Raman spectroscopy as well as TEM studies lent support to this suggestion as follows.

Raman spectra were taken from ten different random points on the as-received CNTs and as-rolled Al-CNT composite, and the G-band position was calculated and presented in Figure 4-12. As stated previously, the Raman frequency shifts of CNT in a stressed state were associated with the variation of carbon-carbon bond distance. The apparent G-band shift of the as-rolled Al-CNT composite to a large wavenumber could be observed (G-band shift from 1572cm^{-1} of the as-received CNTs to 1604cm^{-1} of the as-rolled Al-CNT composite). This implied closer interatomic distance which can be interpreted to cause increasing vibration frequency (increasing wave number) in the CNTs. The closer interatomic distance indicated the pressure exerted on the CNTs. Such a contraction is suggested as a result from the processing by hot-extrusion and hot-rolling.

Besides the Raman spectra, another evidence of compression pressure CNT experiencing was the fractured cap of CNTs. This is presented in Figure 4-13, as fractured end of the CNT is clearly seen.

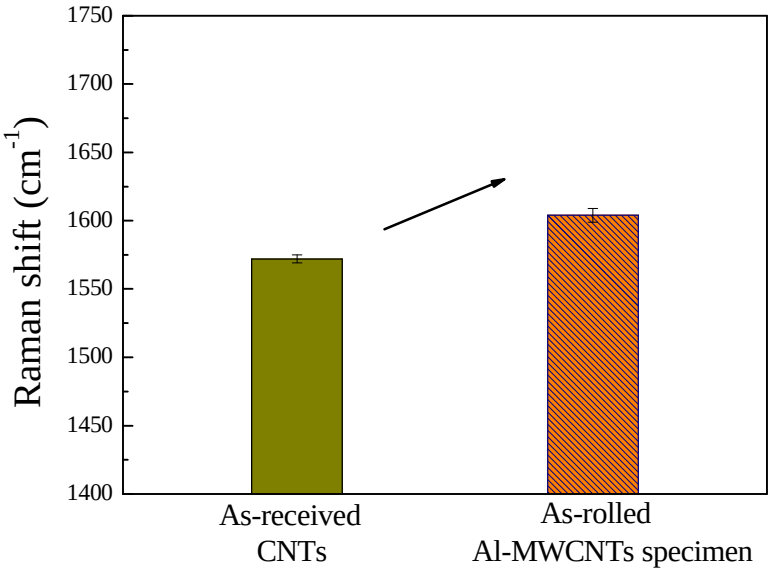

Figure 4-12. G-band position of the as-received CNTs and as-rolled Al-CNTs composite. Note that G-band shift to larger wavenumber in the as-rolled specimen, due to the compression stress CNTs experienced.

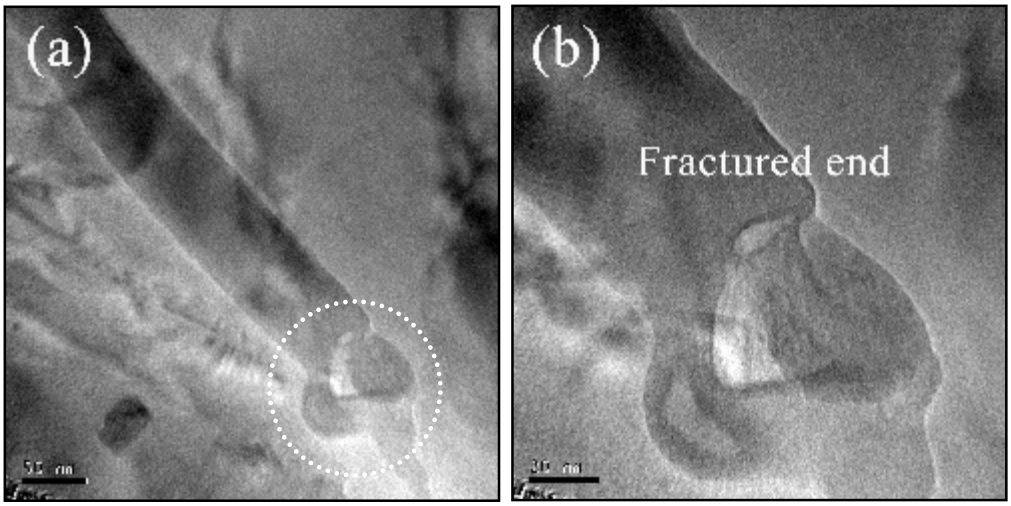

Figure 4-13. (a) TEM image of the fractured end CNT in the matrix due to the compression force resulting from fabrication. This compression force also introduced defects and irregularities in the tubes. The fractured end CNT contributed to the inner-wall pullout. (b) Magnification of the fractured end of (a).

The key mechanism to transfer the load from matrix to CNT is the interfacial bonding strength. Resistance to CNT pullout is caused by mechanical interlocking (surface roughness, friction interlocking and dovetail interlocking) between the matrix and the roughened CNTs. Taken together, the interfacial shear stress of an aggregate, τ, is hereby proposed as:

$$t = -m(s_{thermal} + s_{proces}) + t_{interlock} + C \quad (4\text{-}4)$$

Where μ is the interface friction coefficient; $\sigma_{thermal}$ and σ_{proces} are the normal stresses across the interface arising from thermal shrinkage and processing constraint, respectively; $\tau_{interlock}$ is the interlocking stress; C is the impact factor. It can be seen that the interfacial surface (contact surface) as well as its roughness, the compression force applied on it, are

responsible for the resulting force level. To illustrate this, a schematic of the stresses applied to a CNT in the matrix, and the CNT pullout process under an application of tensile force, is schematically shown in Figure 4-14.

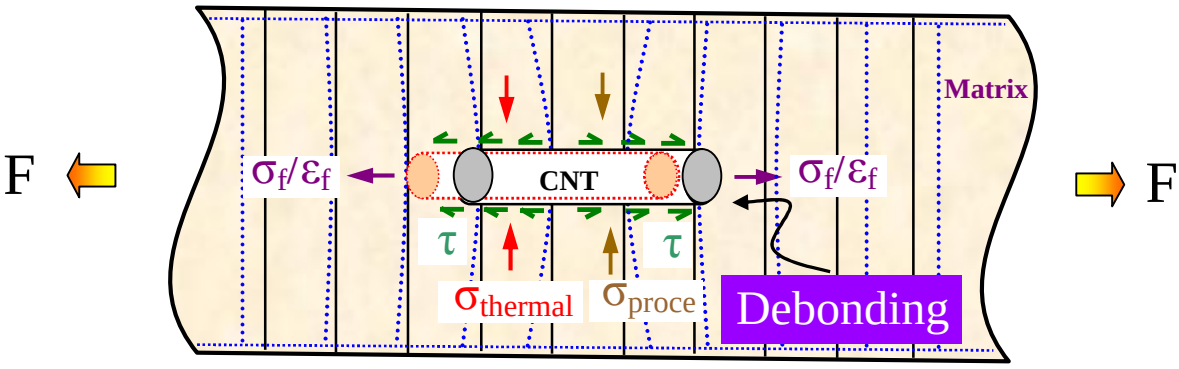

Figure 4-14. Schematic illustration of tensile-loading Al-CNT composite. Stresses acting on a CNT in the composite can be seen. CNT debonds with the matrix under the application of axial tensile load. Solid line: the material before tensile load; dashed line: the materials during tensile load. Compressive stress arising from thermal shrinkage (σ_{therm}) and processing constraint (σ_{proce}) were applied on the interface. Load transfer from matrix to CNT is through interfacial shear stress, τ, and CNT was stressed/strained ($\sigma_{f,}$ /ε_f).

4.5 Conclusions

(i) Al/Al-CNT composites were successfully synthesized using P/M technique combined with hot extrusion and hot rolling.

(ii) CNT incorporation into the Al matrix simultaneously improved the densification, hardness and ultimate tensile strength of the material. The improved yield strength

was discussed based on the load partition effect of CNT, thermal mismatch between matrix and CNT, and Orowan strengthening.

(iii) The amount of defects increased in the CNTs after powder mixing and sintering due to the physical compression force; whilst the graphitic structures were not damaged during the secondary processing.

(iv) CNTs were subjected to substantial compression stress not only in powder mixing but also in subsequent consolidation process due to constraint from the consolidation and shrinkage from thermal mismatch. These compressive stresses contribute to a sound CNT/matrix interfacial adhesion, but also facilitate the load transfer effect.

CHAPTER 5

A SIMPLE APPROACH TO PREPARE AL/CNT COMPOSITE: SPREAD-DISPERSION (SD) METHOD

5.1 Introduction

The dispersion of CNTs into matrix as well as the processing problems are the major challenges inhibiting the development of these composites. In order to reduce the agglomeration of CNTs, many control methods have been adopted. Hansang *et al* [19] dispersed the CNTs with Al powder using natural rubber as a mixing medium; and He *et al* [73] synthesized in-situ CNTs in Al powder. These Al-CNT mixtures were subsequently consolidated and good mechanical properties were obtained by comparison with the base matrix. Unfortunately, the complexity of these techniques, equipment constraint as well as high cost, restricts their further development. Therefore, the establishment of an appropriate and economical processing practice for CNT reinforced MMCs is still a challenge for researchers. In addition, in fiber composite, the alignment of the fiber is one of the important factors affecting the final quality of the product.

Accordingly, this study aims to produce CNT reinforced Al system composite with homogeneously distributed and aligned CNTs with low cost. In this chapter, the repeated pressing and rolling (RP&R) process was successfully applied to produce Al-CNT

composite. RP&R process was first reported by Yasuna *et al* [129-130] in 1997 for non-composite. In this process, several sheets of metal were accumulatively overlayed, pressed, and rolled to bond into one layer, with the purpose to produce metallic multilayers in a bulk form. The basic procedure of RP&R process was adopted in this study, but the main purpose is to spread CNTs in the matrix, therefore it has been named here as the Spread-Dispersion (SD) method. In the experiment, an enhancement of 66% of tensile strength of the CNT reinforced Al composite was obtained, with ultra-fine grain size of 20nm. Effort is made to understand the strengthening contributions in the composite.

5.2 Experimental

Aluminum composite with 0.5wt.% loading of CNT (Al-CNT) was fabricated by powder metallurgy technique as described in Chapter 4. The initial material was in the form of 0.6mm thick sheet. The schematic illustration of the Spread-Dispersion method is given in Figure 5-1. First, rectangle-shaped strips of 6mm × 1mm × 0.6mm (length × width × thickness) were machined from the master sheet for SD use. Before the SD process, the edges of the strips were trimmed to prevent cracks occurring during rolling. Six strips were stacked one over anther (Figure 5-1). Then the stacked assembly was pressed under 300MPa at room temperature to reduce the thickness by half. Subsequently the assembly was roll-bonded into a single strip with thickness of 0.6mm at 500°C using a hot-rolling machine (the assembly was secured at one end before rolling to avoid separation).

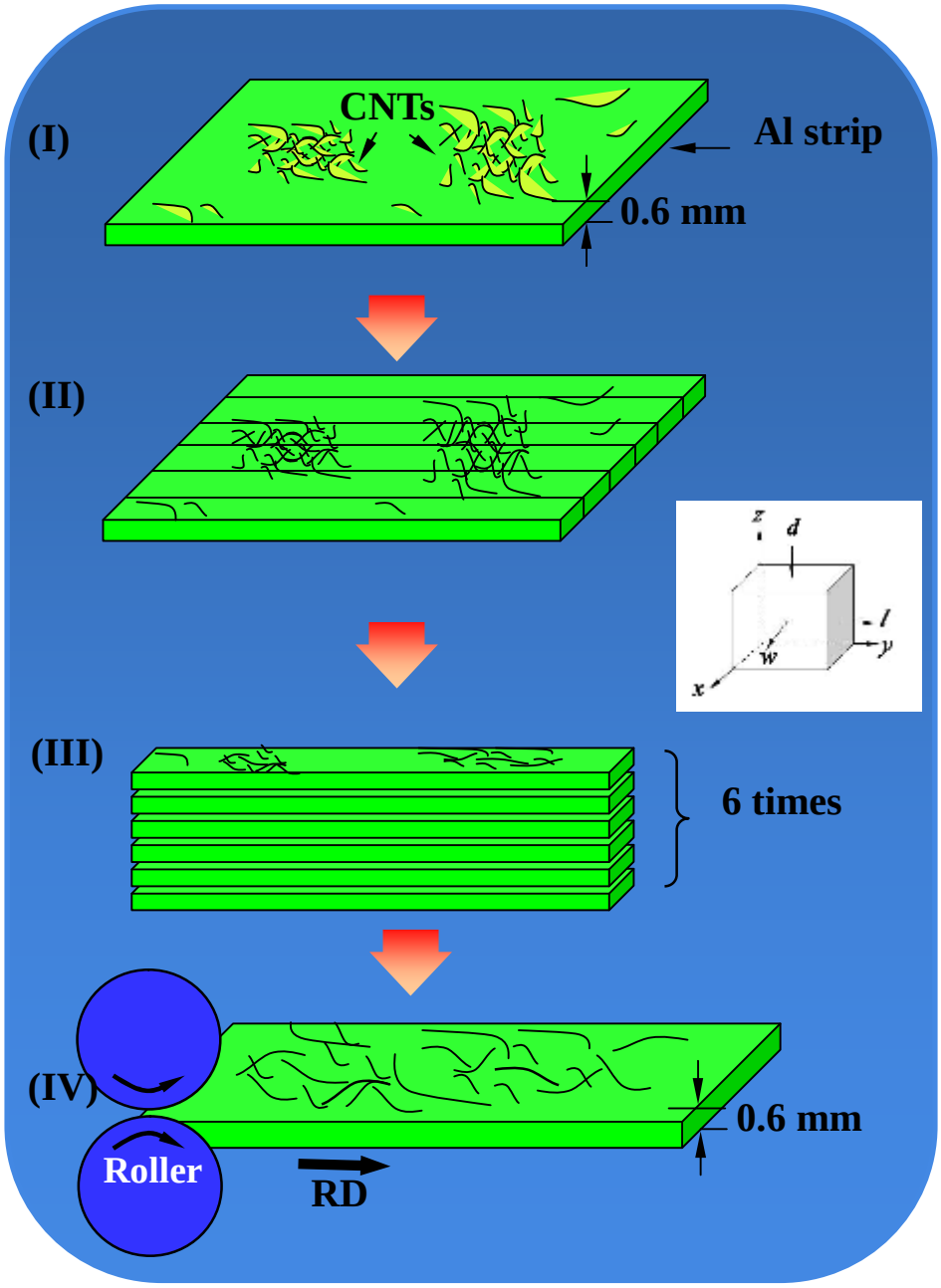

Figure 5-1. Schematic illustration of the spread-dispersion (SD) method. RD is rolling direction.

5.3 Results and Discussion

As the schematic of the Spread-Dispersion method shown in Figure 5-1, if the initial thickness of the single strip is d_0, then the thickness after SD process (stacked n times), d_f, becomes:

$$d_f = \frac{d_o}{n} \tag{5-1}$$

Considering volume conservation,

$$d_0 S_0 = d_f S_f \tag{5-2}$$

Then the final lateral area of the specimen after rolling is:

$$S_f = nS_o \tag{5-3}$$

where d_0 and S_0 are the initial thickness and plane area (x – y plane) of the strip (before SD process); d_f and S_f are the final thickness and area of the strip (after SD process); n is the number of the strips stacked together (Figure 5-1). In this study, n is 6. The initial thickness of the strip is reduced to 1/6 (Equation 5-1), and the achieved reduction is 83.33%. Because of volume conservation (Equation 5-2), the final specimen spread 6 times from the initial one (Equation 5-3). By this way, substantial plane spreading is realized and ultra-high plastic strain is introduced.

In traditional modeling, researchers only consider plane stress and strain change in plane rolling, that is the thickness reduction (z) and the longitudinal (rolling directional) spreading (y), whereas ignoring the lateral spreading (x). However, it should be noted that since the aspect ratio, R (width/thickness), adopted in this study is 13, the lateral spreading should be taken into account [131]. That is, the roll strip spread in both the rolling and lateral direction. The experimental thickness, width and length of the strip in

this study were recorded in Table 5-1. From Table 5-1, it can be seen that with reduction in thickness, the strip spread substantially in both rolling and transverse direction. It is expected that through substantial matrix deformation flow, CNTs could be homogeneously distributed and preferentially aligned. When processing with a large enough plastic deformation introduced, homogeneous distribution of reinforcements could be achieved regardless of the size difference between matrix powder and reinforcement particle [79]. The redistribution of reinforcement in metal matrix by hot-rolling has been reported elsewhere [113, 132-133]. It has also been reported that a rolling process is a good option to align reinforcement within MMCs [134-135].

Table 5-1. Dimension of the strip before and after SD process.

Single Strip	Thickness (*d*)	Length (*l*)	Width (*w*)
Before SD process (mm)	0.6	60	8
After SD process (mm)	0.1	192	15
Expansion (%)	- 83.33%	+ 220%	+ 87.5%

SD processing led to further structural refinement of the Al matrix. TEM observations show that fine equiaxed grains with average size of 20nm were obtained, and coarse grains were occasionally observed (see Figures 5-2(a) to (d)). Individual CNTs were found within the matrix grains (Figure 5-2(c)). Figure 5-3 presents the tensile stress-strain response of the samples before and after the SD process. It can be seen that though a small amount of CNTs (0.5 wt.%) was added to the matrix, the enhancement of tensile strength was evident. By comparing with the monolithic Al under the same processing, an enhancement of 66% in tensile strength was obtained in the SD Al-CNT composite. The

improved tensile strength in the SD composite was accompanied with decreased ductility. The decreased ductility is mainly due to the reduction of dislocation mobility.

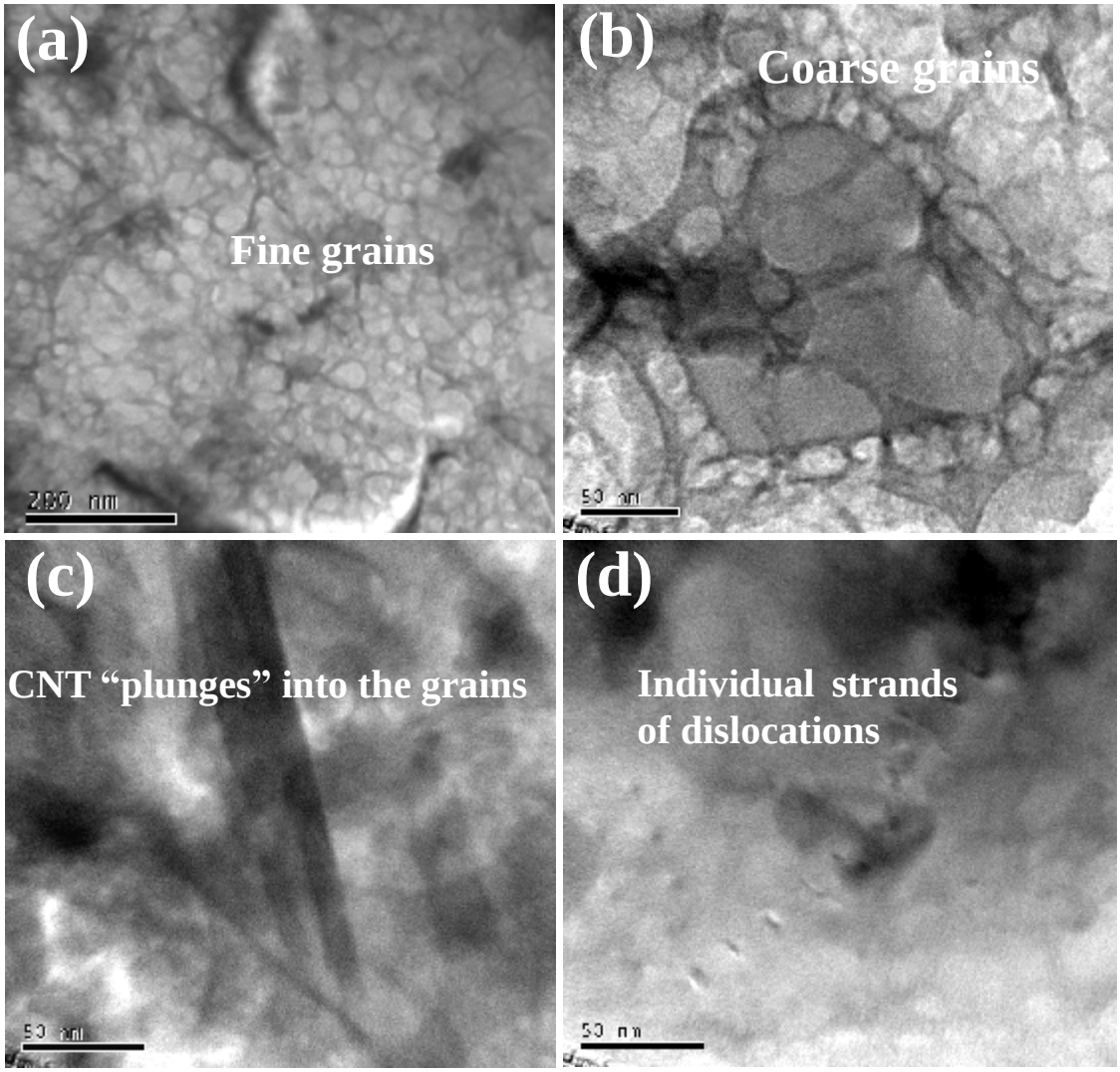

Figure 5-2. TEM micrographs of the SD Al-CNT composite: (a) fine grains with average size of 20nm; (b) coarse grains occasionally observed; (c) CNT passing through the grains; (d) individual strands of dislocations.

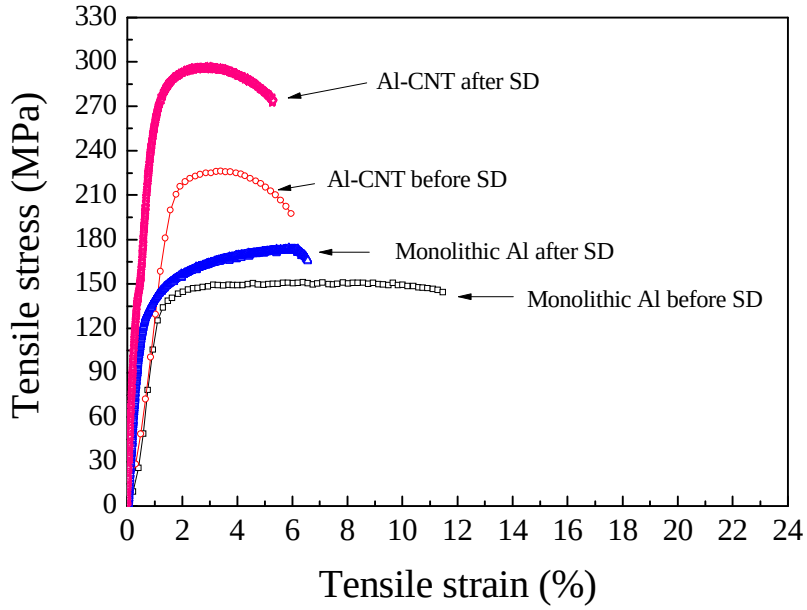

Figure 5-3. Uniaxial tensile stress-strain response of the samples before and after SD process.

If not taking into account of the strengthening effect from CNTs, it has been stated that strength variations in severely deformed materials are governed by the two main strengthening mechanisms: strain hardening by dislocations and grain refinement [133]. The dislocations and grain refinement strengthening of the SD material were evidenced by TEM (Figure 5-2(a) and 2(d)). In the present study, in view of the reinforcement (CNTs), the improved tensile strength is presumably due to a simultaneous combination of several contributing factors:

(i) The applied compressive and shear forces during deformation processing step, allowed the mobility of CNTs diffuse within the matrix, and this flow also facilitate the dis-integration and spreading of CNTs, leading to a more uniform distribution of the

CNTs. In addition, the stress concentration at the clustering CNTs would be reduced with the redistribution of CNTs, minimizing the void initiation sources.

(ii) The redistribution of CNTs with the metal flow led to the disappearance of CNT-free zones. The separated CNT would fill up the CNT-free zones in the matrix, making a more uniform distribution of CNTs.

(iii) The matrix and the reinforcement were brought into intimate contact with each other due to the rolling pressure, leading to a stronger bonding. A strong interface or good adhesion would definitely promote the load transfer efficiency, consequently, enhancing the strength of the composite.

Besides the above contributing factors, one important issue that should be noted is the graphitic structure of CNTs during rolling. It has been reported in micro-size particle reinforced MMCs, such as Al_2O_3 and SiC, considerable amount of damage to the particulates was associated to the cold or hot-rolling [113-114]. In present study, little evidence of CNT damage was found from the Raman spectra results: the I_D/I_G ratios of CNTs before and after SD process were 1.20 and 1.26, respectively, which indicated negligible damage of the CNTs due to the protection of the soft matrix.

Although till now there is no study on the influence of the plastic deformation on the uniformity of CNT distribution and mechanical properties of CNT reinforced metal matrix system, the present investigations suggested that the SD process would be effective in distributing CNTs and improving mechanical properties of the resultant composite. The process is simple, low cost and does not require any specialized

equipment, nor does it damage the graphitic structure of CNT. It is suggested that this SD method could also be applied to other nano-particle reinforced metallic/polymeric matrix composites.

5.4 Conclusions

Amongst the plethora of processing techniques, this study provides a simple technique to produce Al-CNT nanocomposite. Specimens with fine structure were produced by a Spread-Dispersion method. Compared with the monolithic Al, an enhancement in tensile strength of 66% of the Al-CNT nanocomposite was obtained with minor decreased ductility. The improved tensile strength was contributed to the segregation and uniform-distribution of clustered CNTs, disappearance of the CNT-free zones, stronger Al/CNT bonding and the retention of CNT graphitic structure.

CHAPTER 6

CARBON NANOTUBE EVOLUTION IN ALUMINUM MATRIX DURING COMPOSITE FABRICATION PROCESS

6.1 Introduction

In general the conventional powder metallurgy (P/M) route for making carbon nanotube (CNTs) metal matrix composites includes: (i) mixing and blending; (ii) consolidation; and (iii) secondary processing, as described in Chapter 4. Henceforth, one issue that should be considered is how the CNTs evolve in the P/M steps? How can CNTs be integrated into composite materials without losing their unique properties? The understanding CNTs evolution in the composites processing steps would give valuable information about the selection of proper methods to obtain the expected composite properties. To date, however, there is no report to trace and characterize the CNT evolution during the whole composite fabrication process. Presently, the greatest attention only focuses on the influence of mixing technique on CNTs [71, 127, 136]. It is noted that not only the apparent influence from the powder mixing process but also the subsequent processing steps are important.

Therefore, in this chapter CNT evolution during composite processing was precisely tracked by Raman spectroscopy assisted with SEM and TEM. Possible impacting factors were discussed. This chapter gives a clear picture of the CNT evolution in metal composite fabrication process.

6.2 Experimental

Aluminum powder and 0.5wt.% CNTs were used. The synthesis procedure has been elaborated in Chapter 4. Raman spectroscopy, SEM and TEM were used to characterize the materials.

6.3 Results and Discussion

6.3.1 Microstructure of the Powder Mixture and Composite

SEM image of the Al-CNTs mixture is presented in Figure 6-1(a). It can be seen that the individual CNTs were embedded within the Al powder. Some CNT clusters were still found amongst the Al powder.

Figure 6-1(b), (c) and (d) show the microstructure of the Al-CNT composite in the as-sintered, as-extruded and as-rolled condition, respectively. Equiaxed grains were observed in the as-sintered sample. These spherical grains were elongated as they were subjected to the severe plastic deformation in hot-extrusion process (Figure 6-1(c)). The plastic flow also led to the alignment of CNTs along the extrusion direction. The average size of the grains was further refined by hot-rolling, down to 0.2μm (Figure 6-1(d)). Plastic deformation not only refined the matrix grains, but also separated the CNT clusters and redistributed the CNTs; this would be explained later.

6.3.2 CNTs Evolution

Raman spectroscopy revealed complementary information on the evolution of CNTs.

Raman spectra of the as-received CNTs as well as those at the different fabrication stages are presented in Figure 6-1(e) (corresponding to Figure 6-1(b), (c) and (d)). By comparison, it can be seen that the intensity in the Raman spectra amplitude of the as-received CNTs was the highest, which gradually decreased for subsequent stages (see Figure 6-1(e)). This meant a dilution effect (good dispersion effect) of CNTs. Closer examination of the Raman spectra showed that the dispersion effect not only existed in the primary powder mixing operation, but was also present in the secondary processing. It indicated that the secondary processing also assisted in the redistribution of the reinforcements within the matrix as mentioned earlier. When secondary processing with a large enough deformation is introduced, homogeneous distribution of reinforcements could be achieved regardless of the size difference between matrix powder and reinforcement particle [79].

By comparison from the I_D/I_G ratios of these spectra (Figure 6-1(f)), it could be seen that this ratio varied, especially in the case of the as-received CNTs to the mixed and as-sintered one. The I_D/I_G ratio represents the defect density in graphitic structures. The amount of defects apparently increased in the CNTs after mixing due to the physical force and in the as-sintered state due to consolidation. Whereas the I_D/I_G ratio during hot-extrusion and hot-rolling did not differ much, indicating the amount of defects did not propagate during hot-extrusion and hot-rolling. It is supposed that the tubular-structure of CNTs was not damaged by the hot-deformation, due to the protection by the soft matrix.

The G-band position, on the other hand, gave information of the stress the CNTs experienced. G-band is related to the high-frequency in-plane stretching of the

carbon-carbon bonds [137]. Its vibration frequency is inversely dependent on the interatomic distance. When a strain is applied to them, the interatomic distances of the CNTs change, hence the vibrational frequencies of some of the normal modes change, resulting in a Raman peak shift [120]**.** The larger the strain the CNT experiences, the larger the Raman peak shifts [120]. At the "mixed" state, G-band shift of the CNTs to a large wavenumber could be observed (Figure 6-1(g)). This higher frequency or wavenumber shift was explained by the reduced carbon-carbon distance resulting from the compression stress nanotubes experienced. On closer observation in Figure 6-1(g), it could be found that the stress in the as-sintered nanotubes was also substantial. It is easy to deduce that the compression stress of the mixed CNTs resulted from the physical force during blending, but what contributed to the compression stress in the as-sintered stage? Here, two factors are suggested: (i) constraint from the consolidation, and (ii) shrinkage from thermal mismatch. The composite underwent plastic deformation during the sintering and secondary processing. Compressive stress field was obtained with the reduction in area by both extrusion and rolling operations. Another contributing factor is the thermal shrinkage. CNTs have a coefficient of thermal expansion approximately of ~1×10^{-6} K^{-1}; while commercial purity Al exhibits a much greater coefficient of thermal expansion of 23.6×10^{-6} K^{-1}. Therefore, substantial thermal contraction of the Al matrix exerted a compressive stress on the CNT surface when cooling down during fabrication.

It is noted that when the composite was subjected to heating again, i.e. hot-extrusion and hot-rolling, the thermal mismatch stress in the composite would be relaxed. When re-cooling down from the processing temperature, thermal shrinkage again occurred. This can explain the slight G-band shift of the as-extruded and as-rolled composites compared

with the as-sintered one (Figure 6-1(g)).

To further understand the CNT within the matrix, TEM was used. Though it is well-known that Al/CNT wettability is poor, TEM examinations of the interface indicated that the CNTs were in intimate contact with the Al matrix. No physical gaps on the CNT and Al interface can be observed, suggesting good adherence between them (Figure 6-2). In addition, SEM observation of the fracture mode (after acid etching) showed that the individual CNTs were embedded in the matrix, implying the successful incorporation of CNTs (Figure 6-3).

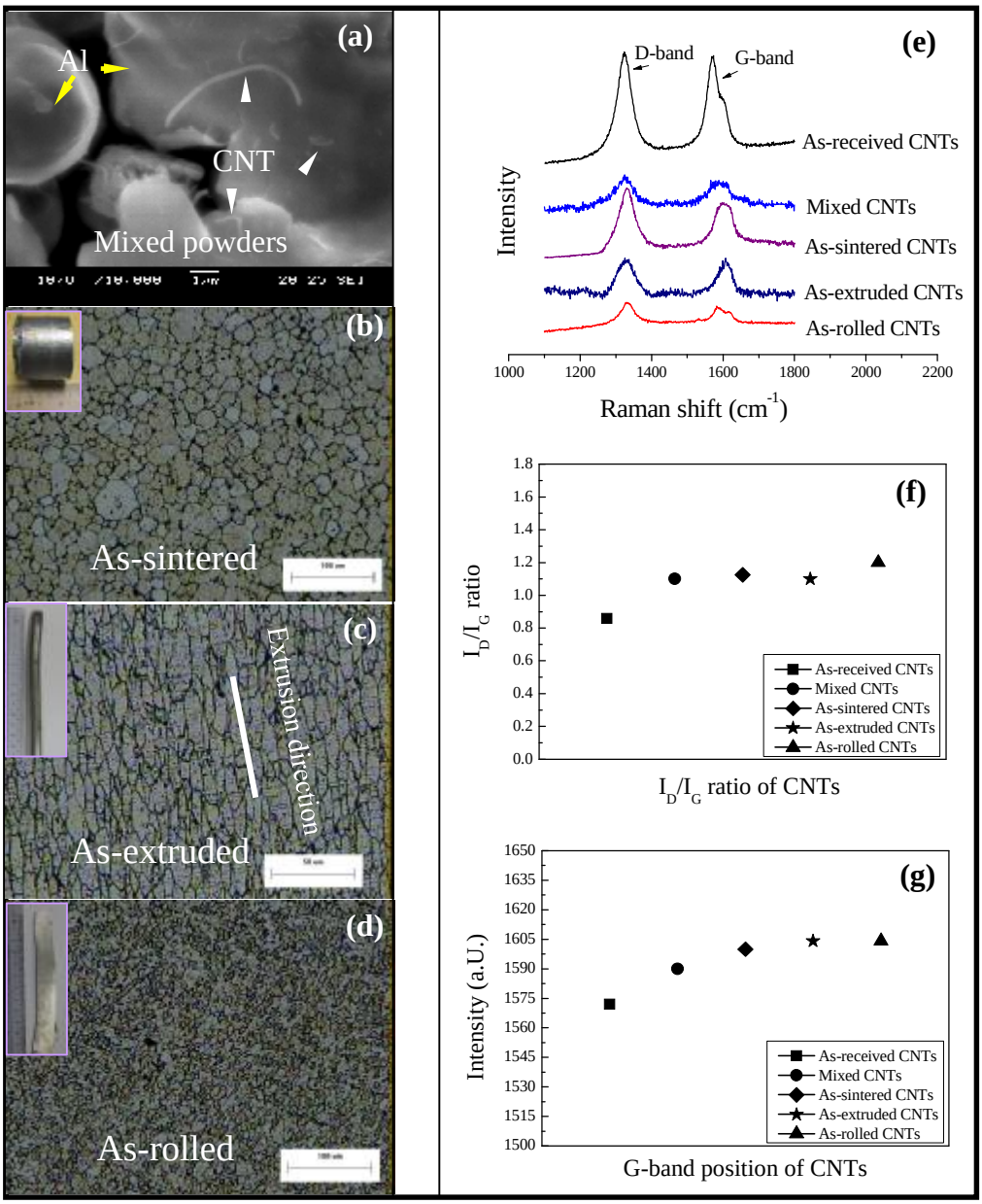

Figure 6-1. (a) SEM image of the Al-CNT mixture; microstructures of the consolidated Al-CNT composite at (b) as-sintered, (c) as-extruded and (d) as-rolled conditions; (e) Raman spectroscopy of the CNTs; (f) I_D/I_G ratio and (g) G-band shift.

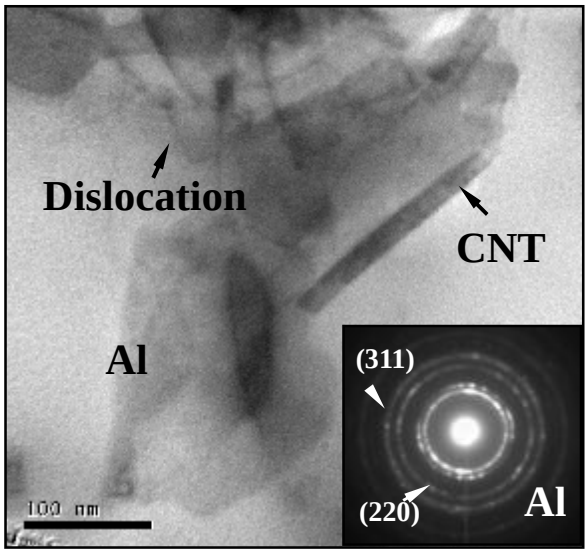

Figure 6-2. TEM image of CNT imbedded in the Al matrix. Inset is SADP pattern of Al.

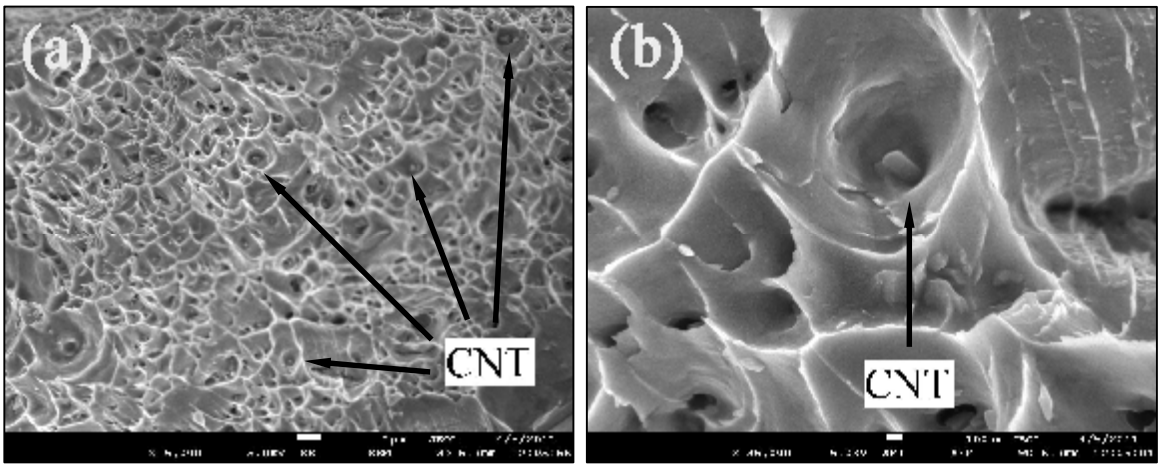

Figure 6-3. (a) Low magnification and (b) high magnification SEM fractographs of the tensile fractured Al-CNT composite. Scattered individual CNT was observed on the fracture surface.

6.4 Conclusions

Al-CNT composite was fabricated by P/M technique, and the evolution of CNTs within the matrix was characterized.

(i) The separation of CNTs was affected by both the powder mixing operation and the secondary processing. Secondary processing with a large enough deformation could homogeneously redistribute the reinforcements.

(ii) The Raman spectroscopy results showed that the amount of defects increased in the CNTs after mixing and sintering due to the physical compression force; whilst the graphitic structures were not damaged during the secondary processing, due to the protection by the soft matrix.

(iii) CNTs were subjected to substantial compression stress not only during powder mixing but whilst sintering, due to constraint from the consolidation and shrinkage from thermal mismatch.

CHAPTER 7

NANOINDENTATION OF AL/CNT COMPOSITES

7.1. Introduction

Previous work has devoted to fabricating Al-CNT composites then extracting their mechanical properties using conventional macroscopic mechanical tests, such as hardness and elastic modulus. The conventional macroscopic mechanical tests (i.e. tensile and compressive test), however, are constrained by the result accuracy, the specimen size, and the local mechanical properties of the specimen cannot characterize precisely. For example, the measurement of strain may not be accurate due to the deformation from the grip zone in the conventional tensile test.

By comparison with the conventional mechanical tests, nanoindentation technique has many advantages. In indentation, a force as small as several nN and displacement of several $\mathring{A}$ can be accurately measured [139]. With its high resolution load and depth sensing capabilities, nanoindentation is able to characterize the mechanical properties at specified locations in a broad range of material systems with heterogeneous microstructures [140]. For example, nanoindentation has been used to investigate the mechanical behavior near grain boundary [141] and on different crystallite planes [142]. Additionally it can avoid the sample size effect, since the sample size is comparable to the indent size.

Most the previous work on Al-CNT composites used conventional mechanical tests to characterize their mechanical properties. Less attention, however, was paid to their mechanical properties under nanoindentation. In this work nanoindentation load-displacement results, elastic moduli, and hardness values of the as-extruded Al-CNT specimens (easier to prepare the sample than the as-rolled one) were investigated. In addition, local mechanical properties of the tensile-fractured specimens over longitudinal and transverse direction were studied.

7.2 Experimental

The after tension test fractured specimen was divided into five regions for nanoindentation test. The region was marked as section N1, N2, N3, N4 and N5 (Figure 7-1). Five indents were made on each region for statistical analysis. Nanoindentation was made at both the longitudinal and transverse of each region. Nanoindentation tests were carried out on a MTS Nanoindenter XP with a diamond pyramidal-shaped Berkovich tip. Continuous Stiffness method (CSM) was used. In the nanoindentation test target strain rate is 0.05/s, up to a peak depth of 1500nm, with holding time 20s.

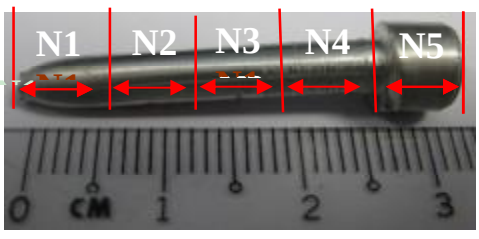

Figure 7-1. Nanoindentation test specimen. Five regions were divided. Nanoindentation test was carried out on both the longitudinal and transverse section.

7.3 Results and Discussion

Nanoindentation hardness is calculated as the indentation load divided by the projected contact area of the indentation at peak load, then following Oliver & Pharr's analysis [143] and the elastic modulus is calculated by using the relation:

$$\frac{1}{E_r} = \frac{(1-u^2)}{E} + \frac{(1-u_i^2)}{E_i} \tag{7-1}$$

where E and v are Young's modulus and Poisson's ratio for the specimen and E_i and v_i are the same parameters for the indenter. E_r is reduced modulus, obtained from measurement data related only to the instrument. For the diamond indenter, E_i = 1141 GPa, v_i = 0.07. The Poisson ratio for Al is 0.33.

The representative load-displacement curves of the nanoindentation made on the as-extruded monolithic Al and Al-CNT specimens are shown in Figure 7-2(a). It is apparent that the slope of the unloading curve is very steep, which indicates the good ductility of the specimens. The corresponding local mechanical properties, i.e. H and E, of these as-extruded specimens are shown in Figure 7-2(b). There is a significant mechanical property enhancement in the Al-CNT composites properties at the content of 0.5 wt.% of CNTs. These results are in good agreement with conventional tensile and HV hardness test results, as shown in Figure 7-3 and 7-4. By comparison with the HV and nanoindentation hardness, the Vickers hardness of the extruded samples is ~ 50% of that of the nano-hardness. This is because nanoindentation analysis utilizes the projected contact area at the peak load instead of the residual projected area [144].

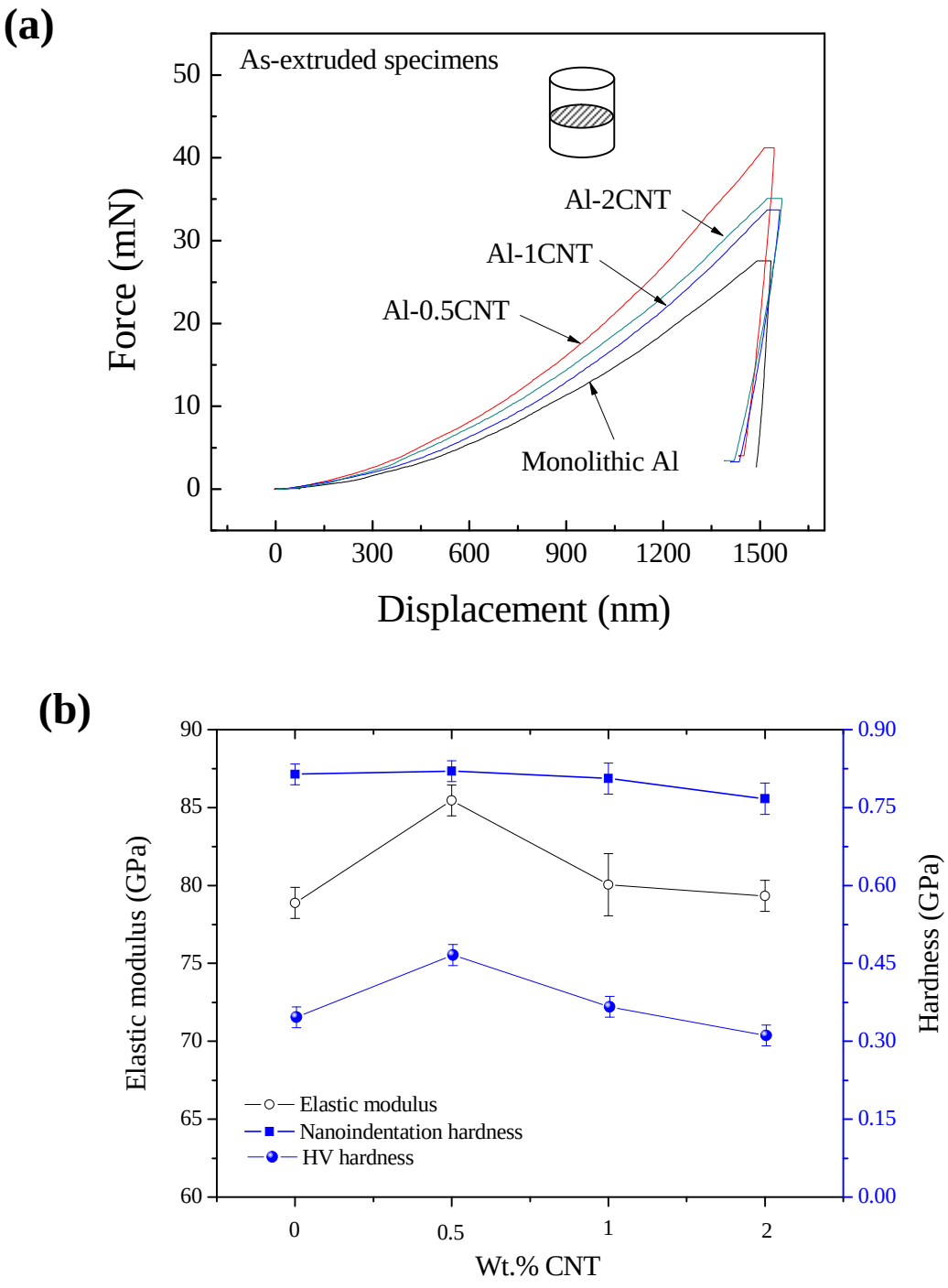

Figure 7-2. Nanoindentation load-displacement of the (a) as-extruded monolithic Al and Al-CNT composites, and (b) their corresponding HV hardness, nanoindentation H and E. Based on the continuous stiffness method, constant depth 1500nm.

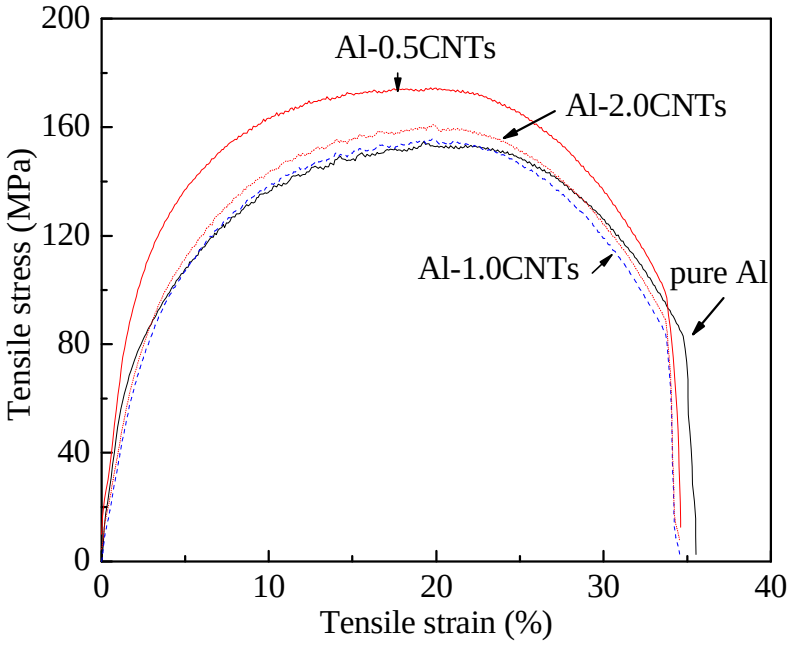

Figure 7-3. Uniaxial tensile stress-strain response of the as-extruded samples.

The H and V of the five regions of the tensile-fractured monolithic Al and Al-CNT specimens are shown in Figure 7-5(a). From Figure 7-5(a), there is a clear trend that E in the necking region is highest, then decreases as towards the undeformed region (N1 → N5). Whilst for H, its value varies in the five regions, but a general trend was observed that H decreases from the necking to grip region. The plastic deformation in the tensile process resulting in strain hardening, plays a significant contribution to the total strength of the fractured specimens. Strain hardening is highest in the localized necking region, then decrease towards the undeformed grip region, likewise values of H are highest in the necking region, then have a trend to decrease from localized deformed region (necking part) to the undeformed region.

By comparing the two sections of the same region tested, E of the longitudinal section (L)

are higher than those of the transverse section (T), see Figure 7-5(a). Thus, the selective maximum force (F) applied on the different regions of the Al-0.5CNT specimen at peak depth is shown in Figure 7-5(b). It can be seen that F is much higher in L than that in the T section (Figure 7-5(b)), which indicates higher mechanical strength in the L section.

As it is common in Al and other FCC extruded alloys, the texture comprises two well-defined fiber texture components, namely, the <111> and the <100>, where the fiber axis is that of the extrusion direction [145]. In the present specimen, apparent geometrical orientation of elongated grains in the extrusion axis was observed (Figure 7-6(a)). The extrusion axis is predominated by slip planes which have comparatively closer interatomic distance (close-packed). Closer interatomic distance leads to larger E. Thus E showed higher in the L section as a result of having high <111> <100> texture in the extrusion axis.

Additionally, the effect of alignment of reinforcement (CNT), in the matrix is another main factor attributed to the anisotropic mechanical properties in L and T sections. In the hot extrusion process, the CNTs embedded in the matrix were aligned along the extrusion axis, accompanying with the matrix flow. The alignment of CNT was examined by TEM (Figure 7-6(b)). From the SEM fracture surface of the Al-0.5CNT specimen (Figure 7-6(c)), the CNTs can be observed to be pulled out from the dimples. It is well known that the degree of fiber alignment is crucial in determining the mechanical properties. Aligned fibers lead to the maximum stiffness and strength in the direction of alignment.

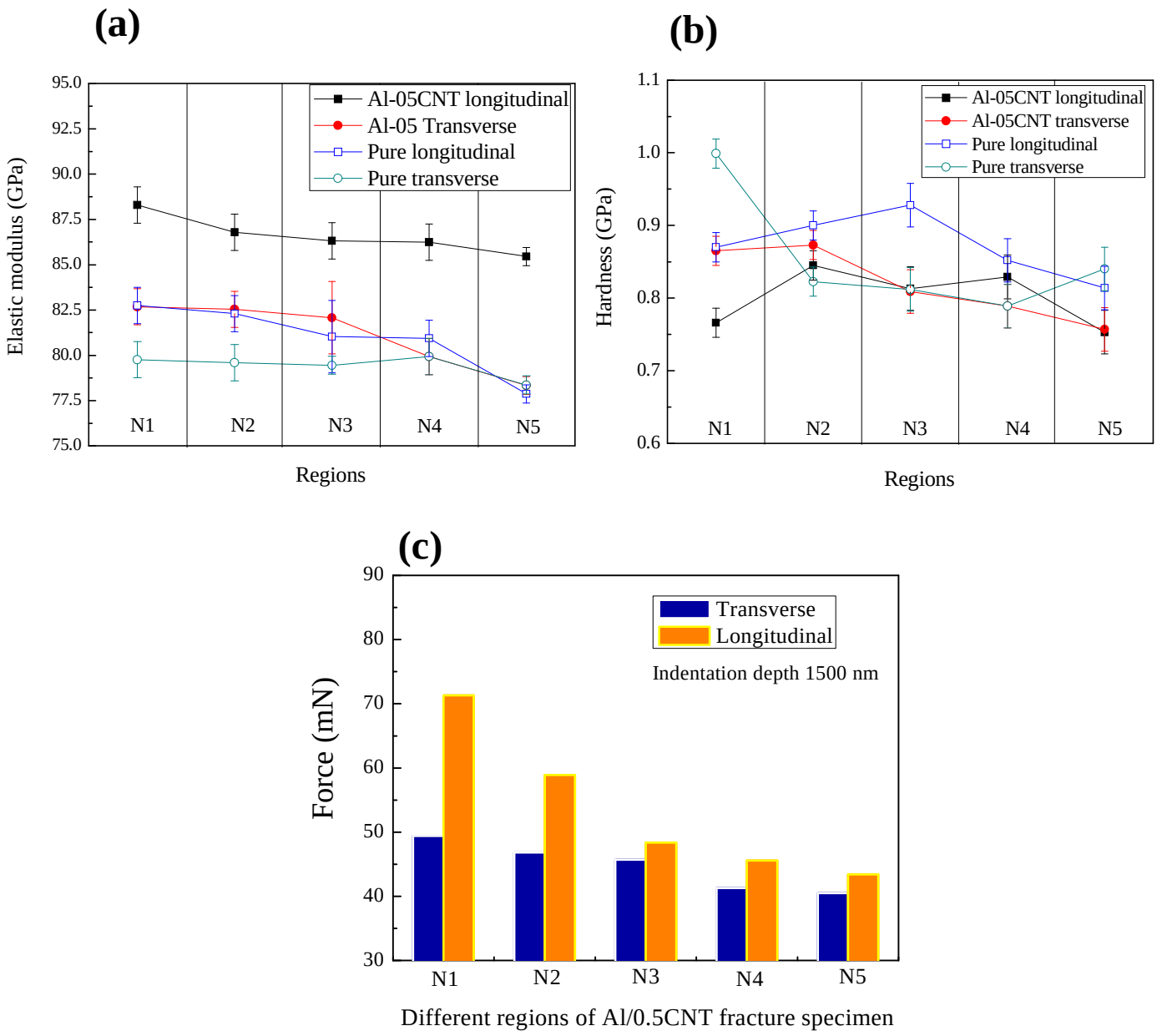

Figure 7-4. (a) Nanoindentation elastic modulus, and (b) nanoindentation hardness of the five regions of the tensile-fractured monolithic Al and Al-0.5CNT specimens, and (c) maximum force applied on the different regions of the Al-0.5CNT specimen when obtaining the peak depth.

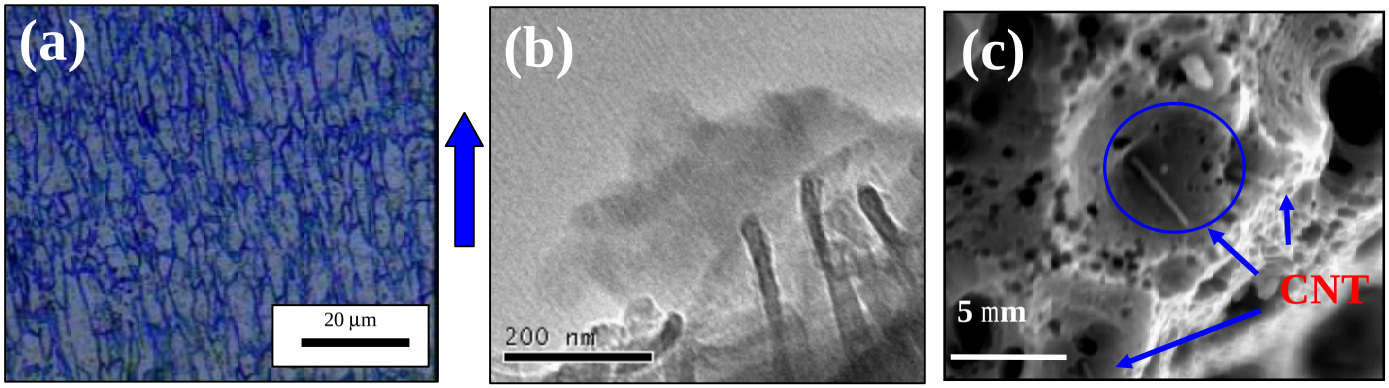

Figure 7-5. (a) Microstructure of the as-extruded Al-2.0 CNT composite, and (b) TEM image of the as-extruded Al-0.5CNT composite showing alignment of CNTs along the extrusion direction. Arrow indicates the extrusion direction. (c) fractograph of the Al-0.5CNT specimen. CNTs were pulled out from the dimples.

7.4 Conclusions

Nanoindentation tests were applied to detect the local mechanical properties of Al-CNT specimens. Different local regions of the as-extruded and tensile-fractured specimen over the longitudinal and transverse section were studied.

(i) In the as-extruded specimen the values of hardness (H) and elastic modulus (E) reached maximum at the 0.5wt.% CNT adding Al samples, which corresponded well with those obtained from conventional macro- and microscopic tests.

(ii) E was highest in the necking region then decreased with increasing distance from the localized deformed region. This variation was due to different degrees of strain hardening.

(iii) H and E in the transverse direction were less than those in the longitudinal direction. This anisotropy was due to texture hardening of the Al matrix and the alignment of CNT.

CHAPTER 8

ELEVATED-TEMPERATURE TENSION PROPERTIES OF AL/CNT COMPOSITES

8.1 Introduction

Metal matrix composites with aluminum as the matrix material (AMCs) are being used or considered for use in a variety of applications such as automotive, aerospace, electronics packaging and industrial/commercial products. The potential engineering applications of Al-CNT composites require these materials with high strength and stiffness as well as good elevated temperature properties, since AMCs have high potential for use in structural applications operating at elevated temperatures. At present, however, the measurements of the mechanical properties of Al-CNT composites were mainly studied by tension tests at room temperature [19, 50, 73, 102, 138]. To the best of authors' knowledge, no studies have been made on the elevated-temperature tension behavior of Al–CNT composites. Accordingly, the present investigation was undertaken with objective to study the elevated-temperature tension behavior of the Al matrix composite reinforced with CNTs.

8.2 Experimental

Aluminum composite with 0.5wt.% loading of CNT (Al-CNT) was fabricated by powder

metallurgy technique as described in Chapter 4. Tensile dog-bone shaped specimens of 11mm × 4mm × 1.5mm (length × width × thickness) were machined from the master sheet for elevated tensile testing purpose. The details of the elevated temperature tension tests were described in Chapter 3.

8.3 Results

Figure 8-1 shows the engineering stress–strain curves for monolithic Al and Al-CNT composites tested at different temperatures. The dependences of temperature on the tensile strength and strain of Al/Al-CNT composites are demonstrated in Figure 8-2.

As seen in Figure 8-2(a) and 2(b), generally, at elevated temperatures total elongation of the monolithic Al increased with increasing temperature, accompanied with decreasing strength. Except at 500℃, the fraction elongation of the monolithic Al decreased to 15%. The drop of ductility for monolithic Al at 500℃ is attributed to the cavity formation on grain boundaries causing local necking. This case was also reported in fcc pure copper previously [146]. By comparison, it can be seen that the incorporation of CNT raised the overall stress level at all the testing temperature range compared with the unreinforced counterparts (see Figure 8-2(a). An enhancement as high as 102% was obtained at 200℃. This is due to the strengthening effect of CNTs which has been elaborated elsewhere [5]. However, it is worthy noting that the tensile strain of the CNT composite continuously decreased with the increasing testing temperature (hot embrittlement), as contrary to the monolithic Al (Figure 8-2(c)).

The SEM fractographs of Al-CNT composite tested at different elevated temperature are shown in Figure 8-3. Dominant micro-dimples were observed on the fracture surface at 200℃. With temperature increasing to 300℃, the composite experienced semi-brittle failure mode, as the semi-cleavage was present. At higher testing temperature, 400℃ and 500℃, micro-cracks and cavities were evident with small dimples surrounded, indicating the rupture failure with local ductile fracture. The presence of large cavitations and the resultant high temperature embrittlement of the composite are suggested to be contributed to the interfacial separation of CNT and matrix, which would be discussed below.

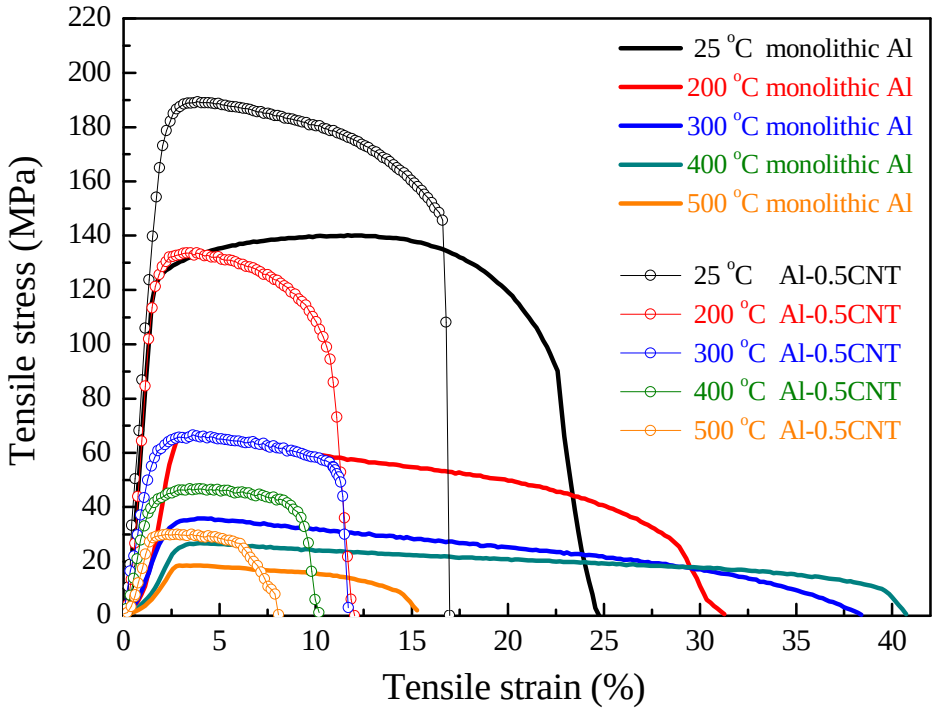

Figure 8-1. Engineering stress–strain curves for Al/Al-CNT tested at different temperatures.

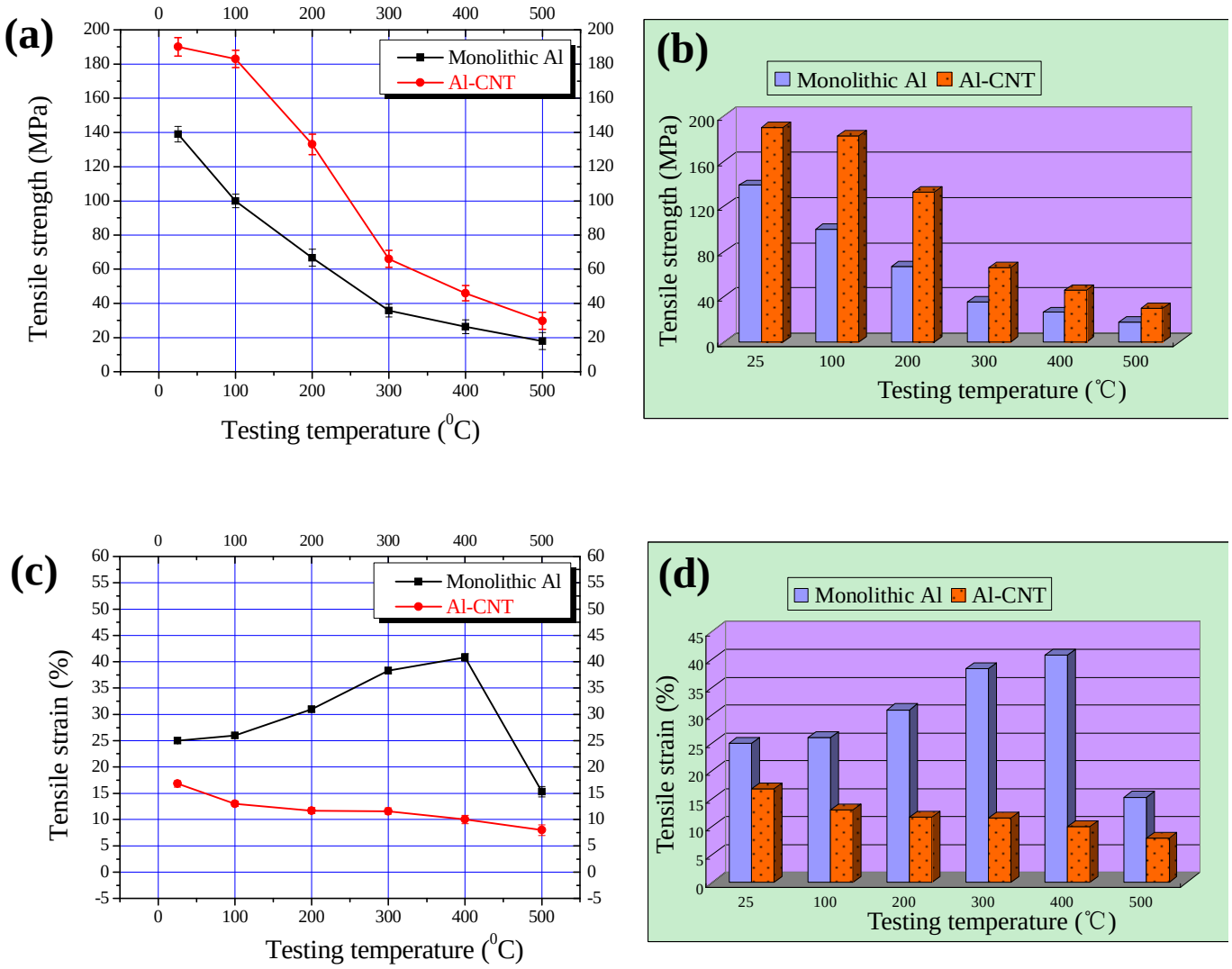

Figure 8-2. Dependence of (a) (b) the tensile strength, and (c) (d) tensile strain on temperature for Al/Al-CNT composite.

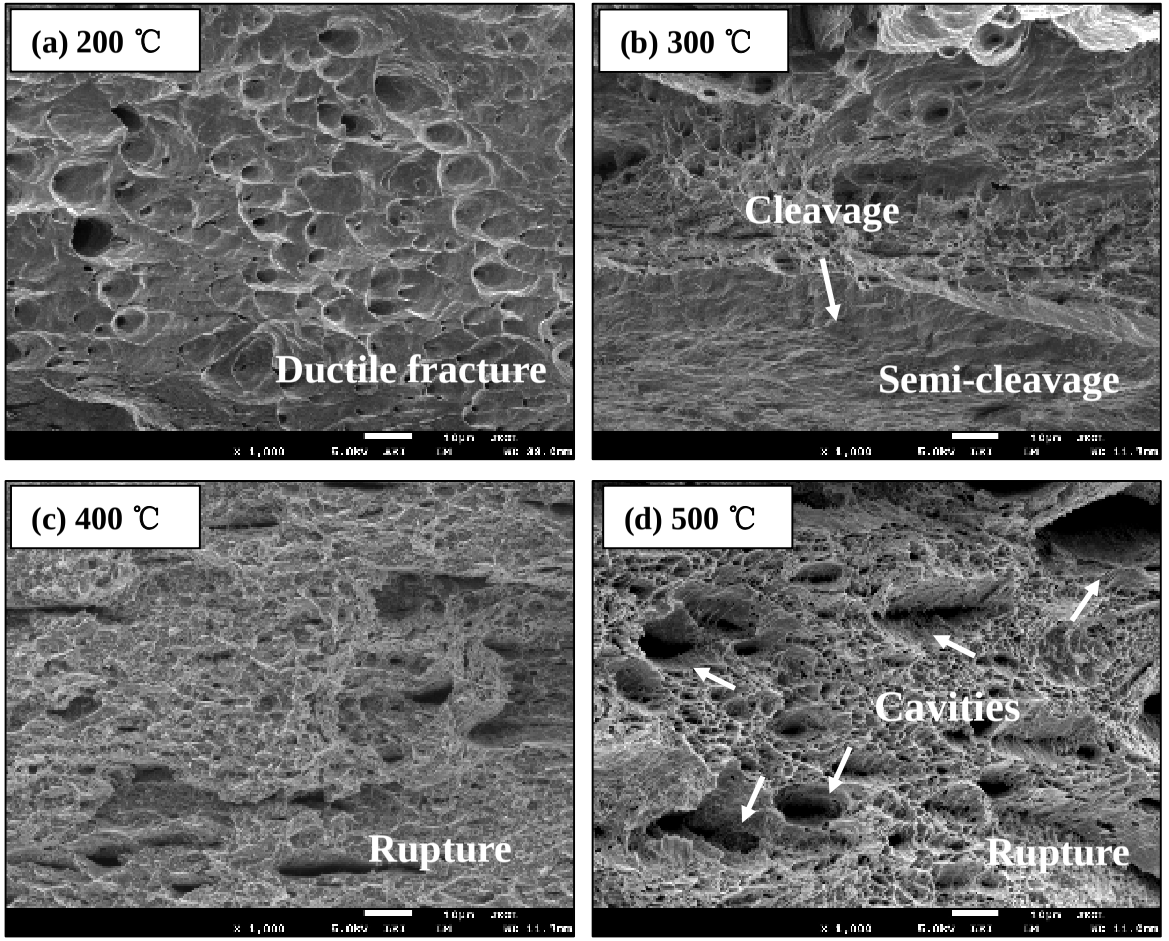

Figure 8-3. SEM fractographs of the Al-0.5CNT composite tensile tested at different temperatures: (a) 200°C, (b) 300°C, (c) 400°C, and (d) 500°C.

8.4 Discussion

Generally for aluminum composites, there are three failure mechanisms of the composites: (i) breakage of reinforcement; (ii) fracture of the matrix; and (iii) reinforcement/matrix interfacial de-bonding. The failure mode of the CNTs in the Al matrix, viz. pullout or fracture, was predicted by Kelly-Tyson Equation [147]:

$$\frac{l_c}{d_f} = \frac{s_f}{2t_{my}} \tag{8-1}$$

where l_c is the critical length; d_f and σ_f is the diameter and strength of CNT respectively; τ_{my} is the shear stress of the matrix, l is the actual length of CNT. The following values were used in the calculation of the critical length l_c: σ_f = 100GPa, d_f = 80nm, τ_{my} = 91MPa. The calculated value of l_c is 45μm while the actual length of CNT in this experiment is around 10μm. The $l_c > l$, demonstrates that there is not sufficient embedded length to generate a stress equal to the fiber strength. In this case, failure occurs by matrix yielding or de-bonding rather than fiber fracture ($l_c < l$). The pullout CNTs from the tensile fracture Al-CNT composite was shown by SEM, as presented in Figure 8-5.

The composite also did not fail by matrix fracture, because the fracture surface of the CNT composite were dominated by semi- and brittle mode at elevated temperature, i.e. cleavage and micro-cavities (see Figure 8-4), rather than dimples-controlled ductile mode which is normally exhibited in pure aluminum.

It is suggested that the presence of large cavitations was caused by the interfacial separation of CNT and matrix. The elastic modulus of CNT and Al is 1TPa and 70GPa approximately. Therefore, there is a large elastic modulus mismatch between them. In the

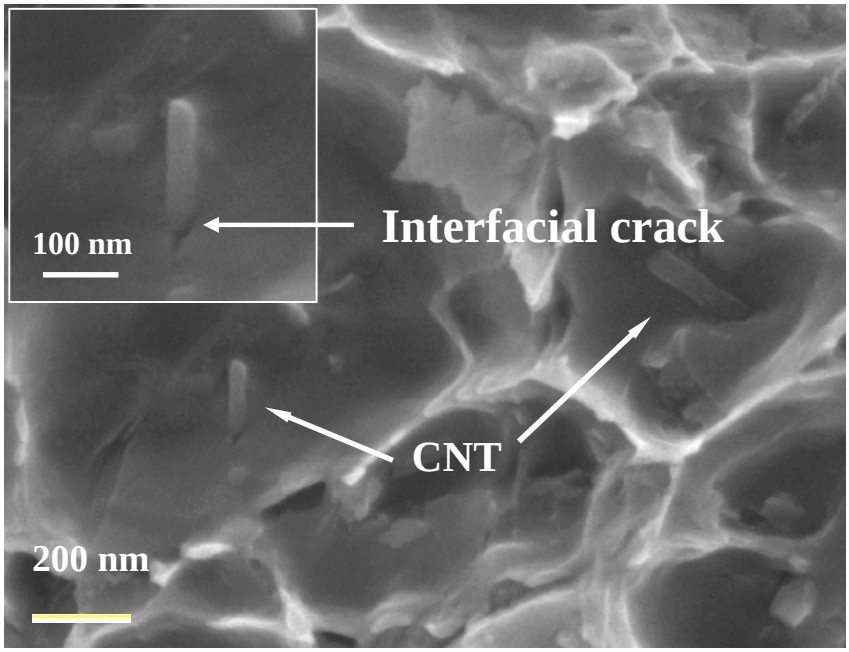

Figure 8-4. Pullout CNTs and interfacial crack was observed.

high temperature tensile test case, the easier plastic deformation flow of the soft Al matrix was obstructed by the stiff CNTs. The weak interfacial bonding at high temperature would lead to CNT slippage, giving rise to void initiation. With the further matrix plastic deformation, these voids propagated and coalesced, leading to premature failure of the composite. The pullout CNTs and the CNT slippage can be seen in Figure 8-5, and matrix cavitations are easily observed in the fracture surface as shown in Figure 8-4(c) and 4(d).

The slippage of CNT with the plastic deformation of the matrix has been reported by Mu *et al* [148]. They reported that, effective stress transfer to CNTs is limited to a small strain regime ($\varepsilon < 0.2\%$)，which is accompanied by elastic deformation. At higher strains, the stress on the CNTs decreases due to the slippage at the nanotube/matrix interface. At the

strain to break, the slippage at the CNT/matrix interface leads to easy separation of the CNT from the matrix. In this study, by careful examination, CNT/Al interfacial crack could be observed in the pullout CNTs, which indicated the CNT slippage and separation from the matrix (Figure 8-5). The poor reinforcement/matrix interface leading to premature failure at the interface during high temperature tensile loading have also been reported in Al-graphite [149], SiC/Al-Fe-V-Si [150] composites in previous studies elsewhere.

CNTs possess an enormous specific surface area (SSA) being several orders of magnitude larger than conventional macro- and mico-fillers [47]. An external SSA of CNTs is as high as 178m^2/g [125]. It should be noted that the high surface area in contact is an advantage for load transfer, but it would become a shortcoming at high temperature, leading to higher possibility of interfacial defects. Further, the defect initiation would be exacerbated if CNTs are rich along the grain boundaries. Another parameter strongly affecting ductility is the clusters of CNT due to the strong van der Waals forces of attraction between them. The weak adhesion between the CNT-CNT in the clusters inevitably act as void nucleation sites under loading and lead to premature failure of the composite. The void defects initiated by CNT clusters were examined by TEM as shown in Figure 8-6.

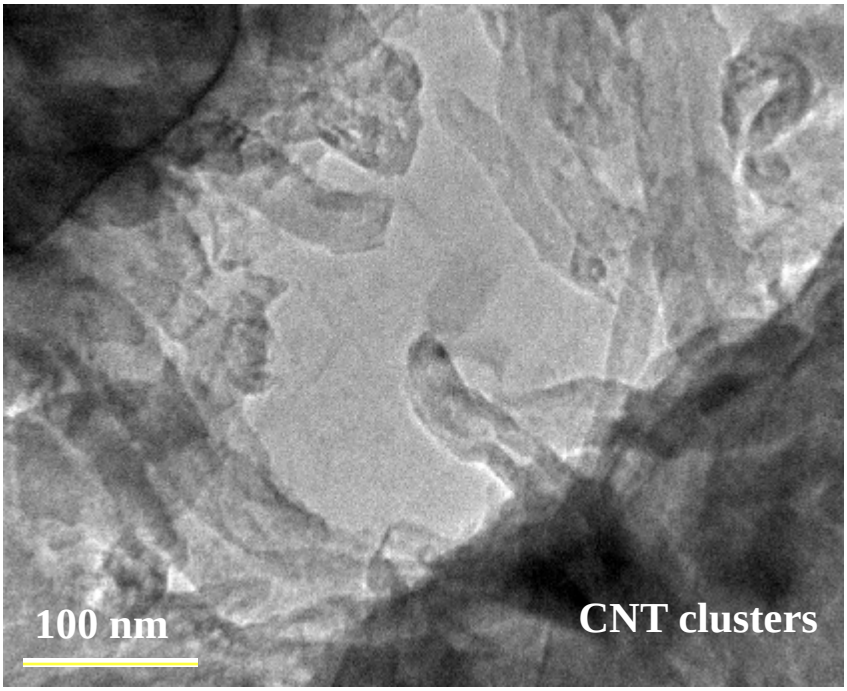

Figure 8-5. Defects initiated from the CNT clusters.

It is noted that with the increasing temperature, the monolithic Al exhibited increase ductility (Figure 8-4(b)), due to the easier plastic deformation of the matrix. And this, on the other hand, would exacerbate the Al/CNT interfacial separation. This deduction is corresponding well with the experimental results, that is, with increasing temperature the loss of ductility of the CNT composite increase (see Figure 8-3), and the fracture mode became more brittle (see Figure 8-4 (a) - (d)).

8.5 Conclusions

The elevated-temperature tensile behavior of Al/Al-CNT composites fabricated by P/M technique was studied. Tensile tests were performed in air at temperature ranging from 25-500°C.

(i) The incorporation of CNTs raised the overall stress level at all the temperature range with respect to the unreinforced counterparts. An enhancement as high as 102% was obtained at 200℃.

(ii) Fracture properties of the composite were affected by the tensile temperature. The CNT slippage and Al/CNT separation were observed. The tensile strain of the CNT composite continuously decreased with the increasing testing temperature (hot embrittlement), contrary to the monolithic Al. The causes of such hot embrittlement were suggested to be attributed to the interfacial segregation, large surface contact area of matrix/CNT and CNT clusters.

CHAPTER 9

TENSION-TENSION FATIGUE PROPERTIES OF AL-CNT COMPOSITES

9.1 Introduction

Fatigue and durability are main concerns for structural materials. For the structural members in aerospace or conductor applications, continuous fiber reinforced aluminum matrix composites would be subjected to vibration and other fluctuating loads, which can cause fatigue degradation of the materials [151]. Up to date, the mechanical studies on CNT reinforced Al composites mainly centered on their strength under monotonic tension loading [17-20, 22, 73]. To the authors' best knowledge, no published research work on the fatigue behavior of Al-CNT composites is available.

Accordingly, the main objective of this work is to study the fatigue behavior of Al-CNT composites under cyclic loading. The Al composites consisting of 0-2wt.% CNT were prepared by powder metallurgy (P/M) technique. Tension-tension fatigue tests were conducted. Experimental results showed that the incorporation of CNTs could improve the fatigue resistance of the composites compared with the unreinforced counterparts. An attempt was made to correlate the CNTs content and distribution effects on the fatigue crack paths in the Al matrix.

9.2 Experimental

Aluminum composites reinforced with 0, 0.5, 1 and 2wt.% CNTs were synthesized by powder metallurgy technique as described in Chapter 4. Flat I-shape fatigue specimen with gauge length of 11mm was used. The preparation of the specimen was according to ASTM E466 [152]. The details of the fatigue tests were described in Chapter 3.

9.3 Results and Discussion

9.3.1 Monotonic Tensile Strength

The monotonic tensile properties of Al/Al-CNT composites were described in Chapter 4 earlier. A simultaneous increase in 0.2% yield and ultimate tensile strength, elastic modulus and hardness was found for the CNT reinforced composites. The tensile strength increased with increasing fraction of CNTs. The strength reached maximum when the 2.0wt.% CNTs were added, an enhancement as high as 45% was obtained compared with the monolithic Al. The possible strengthening mechanism has been discussed in Chapter 4.

9.3.2 Fatigue Behavior

9.3.2.1 Fatigue Life (S-N) Diagrams

Figure 9-1 shows the dependence of fatigue properties on maximum stress (S–N or Wöhler curve) of the Al/Al-CNT composites. All the specimens showed a

stress-dependent fatigue behavior. With a variation in stress amplitude the fatigue life reduces as maximum stress increases. It can be observed that the additive of CNTs significantly increased the number of load cycles to failure.

It is noted that with increasing weight fraction of CNTs, the fatigue life declined. The most superior fatigue resistance is found in the Al-0.5CNT. Whilst for tensile properties, the Al-0.5CNT does not possess the highest tensile strength (refer to Chapter 4). On the other hand, there is a large scatter in the composite especially at high CNT weight fraction (2wt.%), see Figure 9-1. This degradation and scatter of the fatigue life with increasing content of CNT were attributed to the matrix cracking from inferior CNT distribution. Microscopic evidence of these damage mechanisms would be further discussed in later.

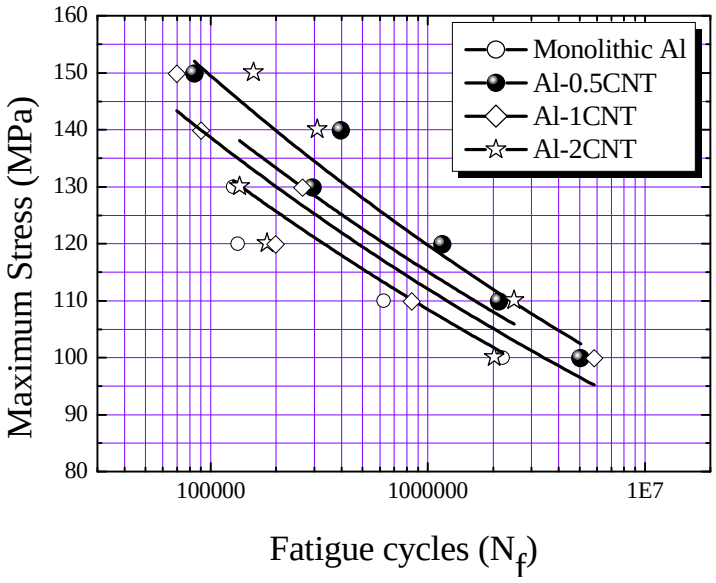

Figure 9-1. Stress–life (S-N) diagram for Al/Al-CNT composites. R=0.1, frequency=5. Fatigue life based on maximum stress.

9.3.2.2 Fatigue Damage Modes

Damage and failure modes of Al/Al-CNT composites were examined under FESEM. The fatigue-fracture surfaces of Al/Al-CNT cycled at a maximum stress of 120MPa are shown in Figure 9-2. It can be seen that initiation, propagation and catastrophic rupture regions are distinct on the fracture surface. The propagation-rupture transition regions of the specimens are highlighted in Figure 9-2(b), (d), (f) and (h). It is evident that with increasing weight fraction CNTs, the composites experienced semi-brittle failure mode. The propagation regions are characterized by cleavage steps for Al composite reinforced with higher weight fraction of CNTs (1wt.% and 2wt.%), see Figure 9-2(f) and 2(h). On the other hand, in the rupture regions, obvious difference was observed. Dominant dimples were observed of the fracture surface of monolithic Al, whilst micro-cracks and cavities were evident in the specimens with 1wt.% and 2wt.% CNTs, indicating brittleness of the composite.

Close examination of the CNT reinforced composites, crack bridging and subsequent CNT pullout in the wake of the crack tip was clearly shown, see Figure 9-3 and Figure 9-4. The propagation of the crack is driven by the cyclic loading and impeded by the resistance of the matrix and the reinforcement. The presence of CNT bridging play a crack resistance function, hindering matrix crack propagation under tension-tension fatigue loading. The adhesion of CNT to the matrix is one of the major issues concerning the sliding pullout CNT in Al composites. Previous work by our group has shown that the CNTs were subjected to substantial compression stress not only in powder mixing, but also sintering process, due to constraint from the consolidation and shrinkage from thermal mismatch (refer to Chapter 5). As the crack advances, energy is dissipated by the

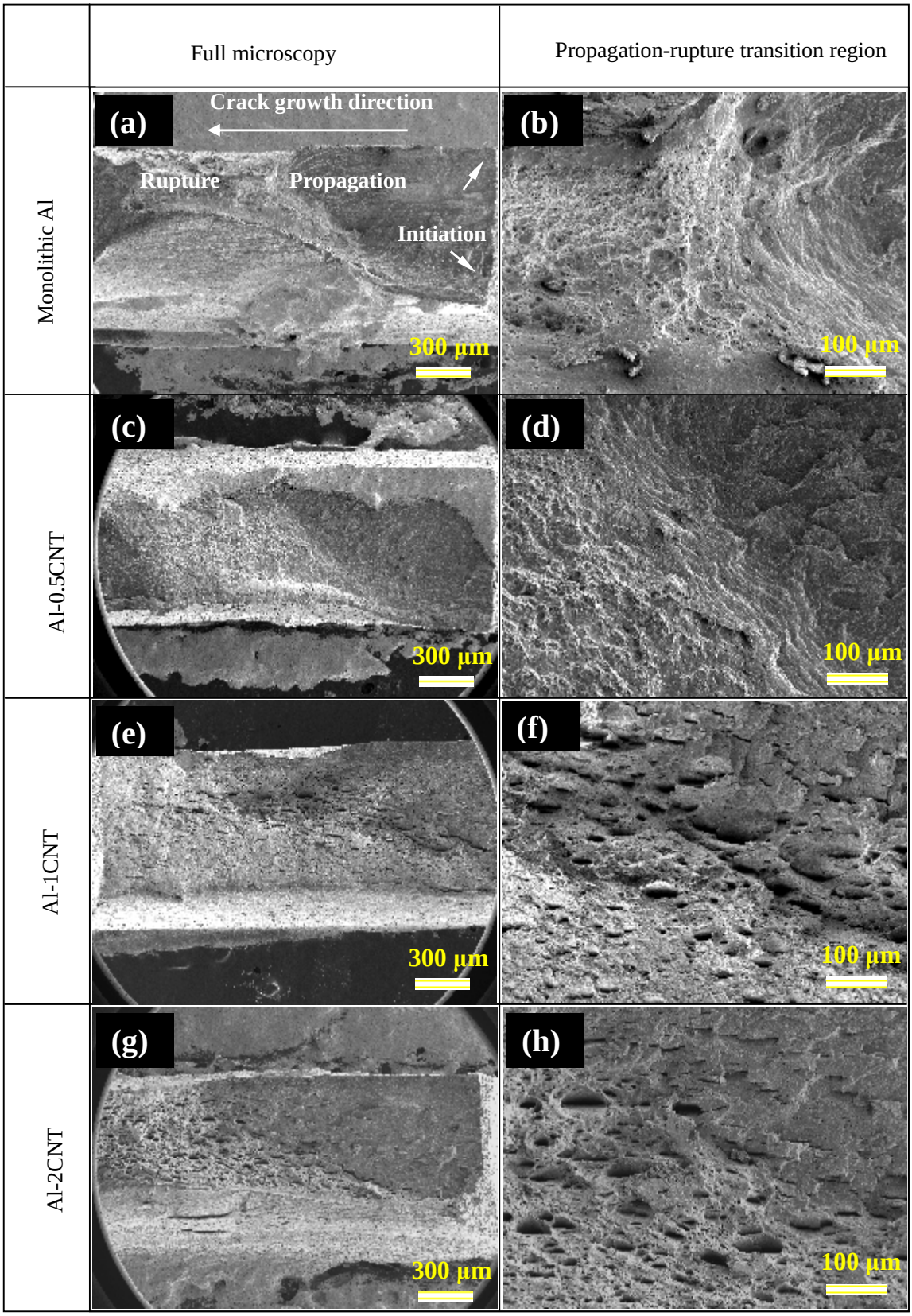

Figure 9-2. Fatigue-fracture surfaces of Al/Al-CNT composites cycled at a maximum stress of 120MPa, (a) (b) monolithic Al, (c) (d) Al-0.5CNT, (e) (f) Al-1CNT, and (g) (h) Al-2CNT.

frictional pull-out of the bridging CNTs from the matrix, reducing cyclic crack propagation rate. The compressive stresses formed during composite fabrication process can enhance the above frictional forces associated with CNT pullout, improving the reinforcing efficiency. Similar suggestions were also made by Mehdi *et al* [153] in CNT reinforced alumina ceramic composites. It is noted that from the cracks, both CNT pullout and fracture were observed, see Figure 9-5. It is suggested that short CNTs were pulled out and long CNT were broken. The CNT pullout and CNT breaking can both dissipate the energy and enhance the fracture toughness of the composite.

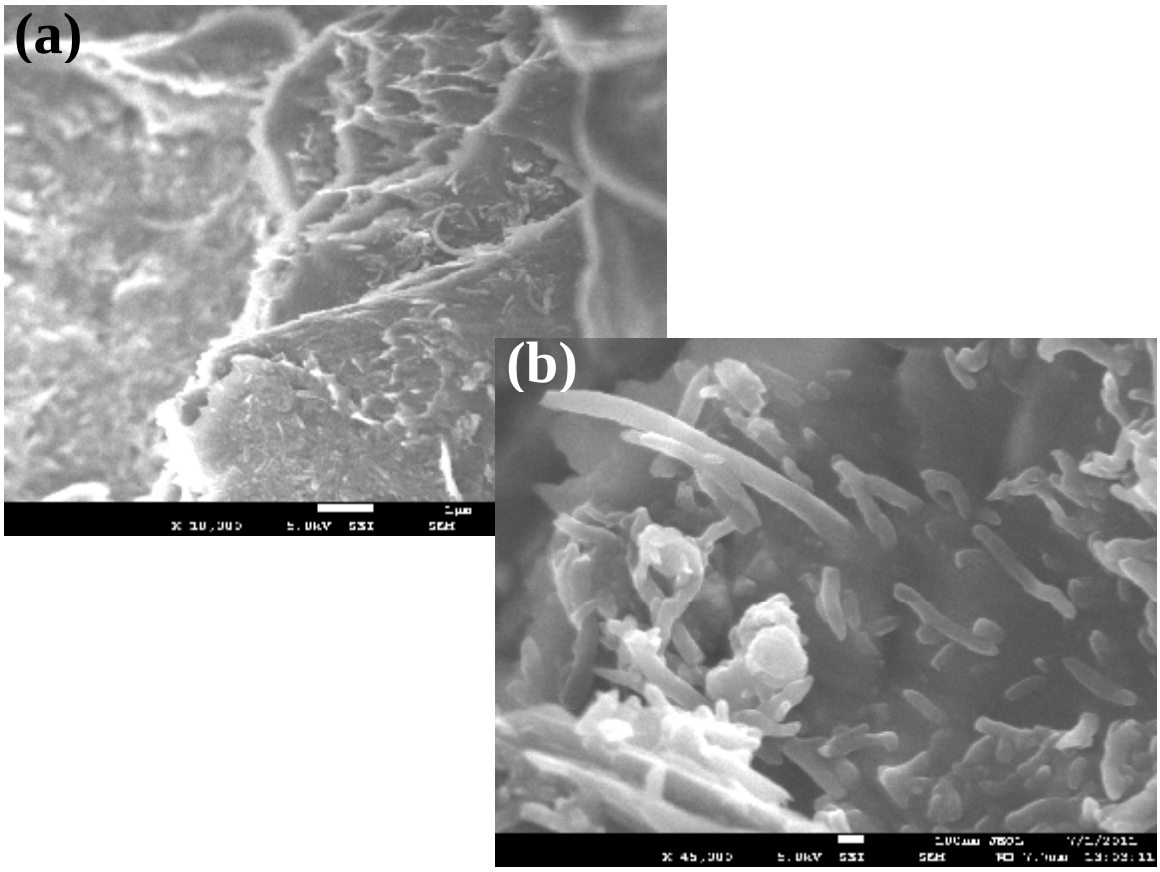

Figure 9-3. Pullout CNTs were observed in the fracture surface (side view) of the Al-CNT composites: (a) low magnification, and (b) high magnification.

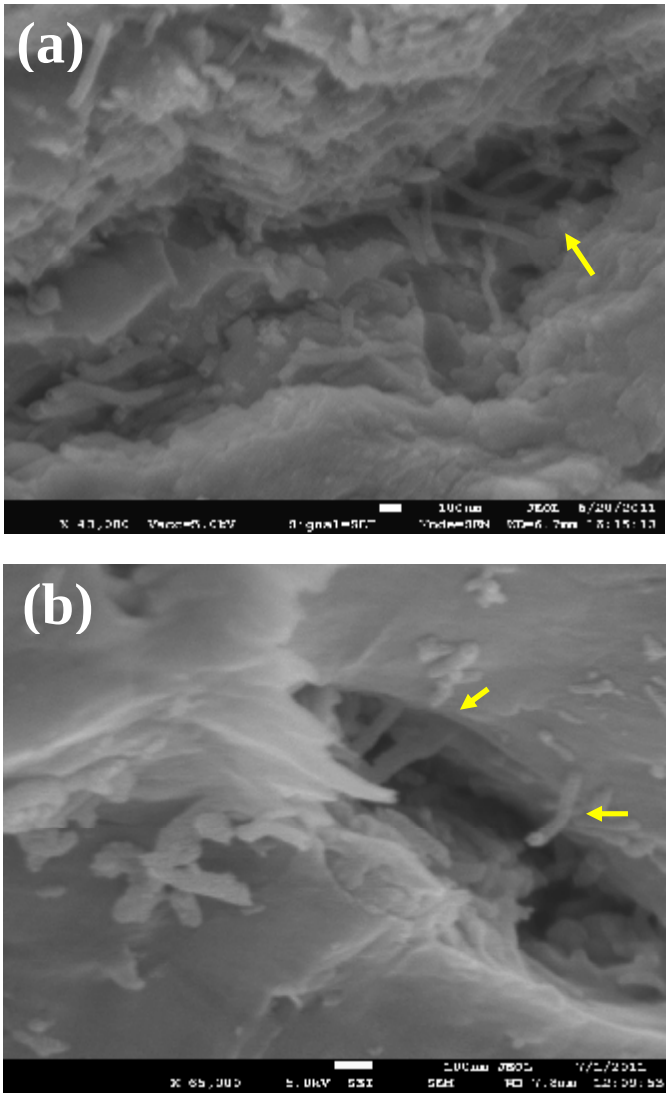

Figure 9-4. (a) and (b) Fatigue crack was bridged by high aspect ratio CNTs which generate a fiber-bridging zone in the wake of the crack tip.

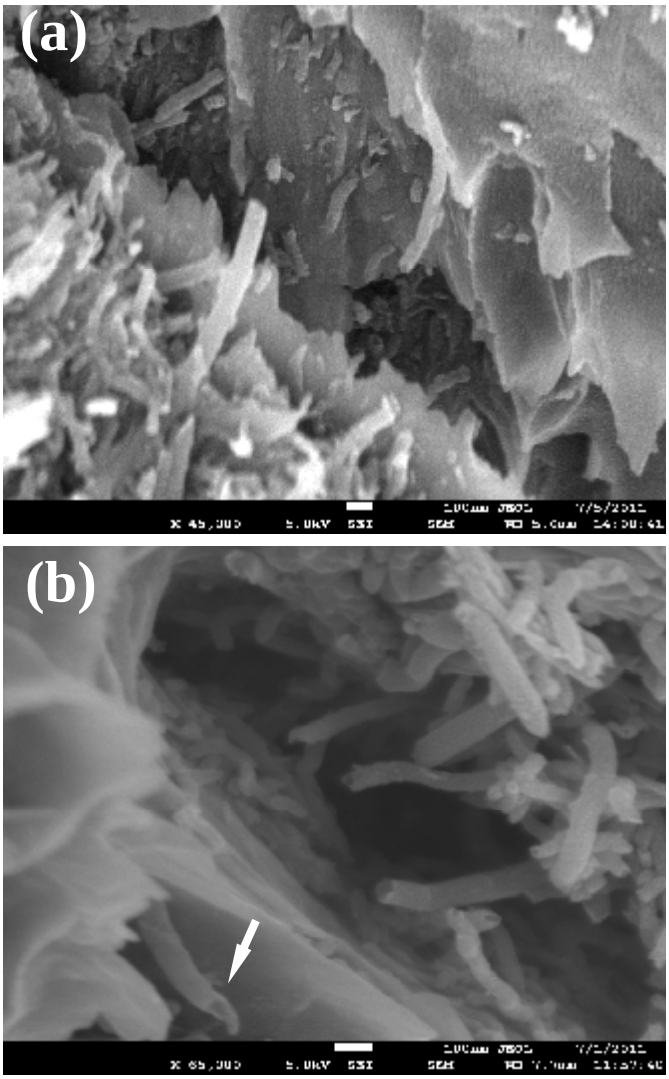

Figure 9-5. (a) (b) Both pullout and fractured CNTs were observed. It is suggested that short CNTs were pulled out and long CNTs were broken.

9.3.2.3 Fatigue Crack Paths

Several studies have shown that increasing volume fraction resulted in enhanced fatigue resistance [154]. However, in this study, the fatigue life declined as increasing weight fraction of CNTs (see Figure 9-1) as described earlier. The deterioration in fatigue resistance with increasing CNT content is attributed to the small clusters of CNTs at high reinforcement content. These small clusters did not pose a problem in the tensile tests of Al-CNT composites, but they would become detrimental for the material under cyclic loading.

The dispersion quality of the CNT reinforced samples were examined by FESEM on the fracture surface, as shown in Figures 9-6. In the lower CNT content composite (Al-0.5CNT), a high density of micro-cracks were observed and CNT clusters in the crack were hardly found (Figure 9-6(a)). Whereas, the clusters of CNTs increased from the fracture surface with higher CNT content. Clusters of CNTs were easily visible in the composite reinforced with 2.0 wt.% CNTs and the multitude cracks became larger (Figure 9-6(b)). Because higher CNT volume content naturally leads to the formation of agglomerates caused by the narrow separation [15]. The reinforcements are elastically loaded while the soft matrix plastically flow; due to the elastic modulus mismatch. Therefore, the initiation of the fatigue crack is always in the reinforcement clusters. It is suspected that fatigue cracks initiated and propagated along these clusters in the Al-2CNT composite.

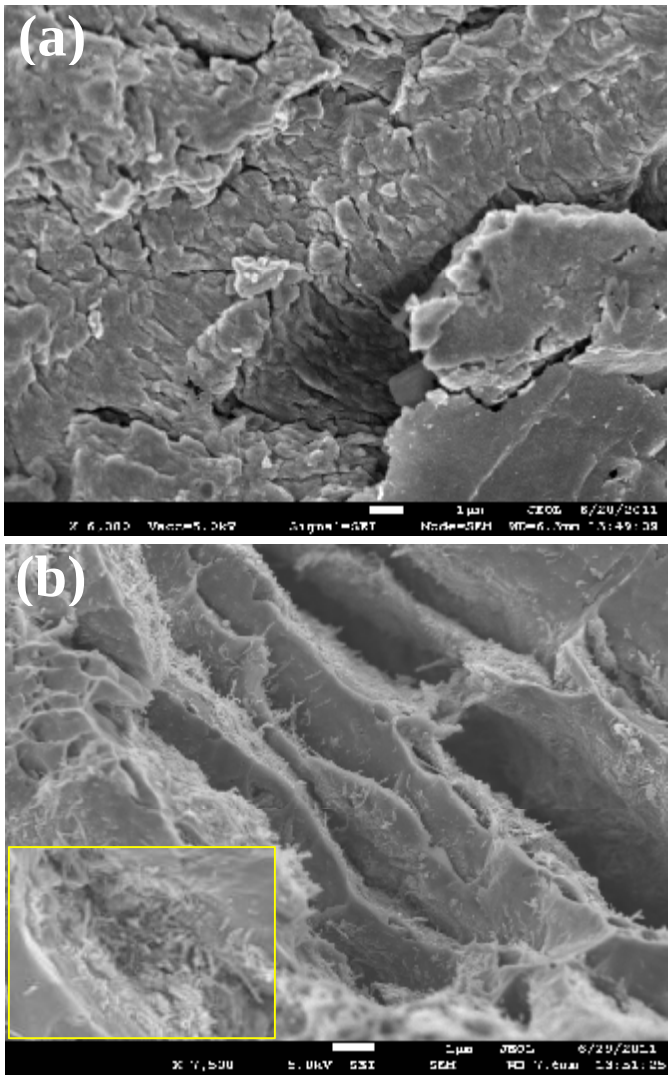

Figure 9-6. (a) CNT clusters in the crack were hardly observed in the Al-0.5CNT composites; (b) clusters of CNTs were easily visible in the composite with 2.0wt.% CNTs. Inset (b) is a high magnification of the CNT clusters.

SEM observation of the fatigue fracture surface can provide qualitative information on the crack growth mechanism. Figures 9-7 to 9-9 show the fatigue propagation regions of the fracture surface. In the propagation area, the striation of the monolithic Al (Figure 9-7) is more coarse and clearer than that of CNT composite (Figure 9-10 and 9-11). On the other hand, there are multitude of cracks in the propagation zone of the Al-0.5CNT specimen (crack always propagation parallel with the striations), whereas the monolithic Al is comparatively smooth, multitude cracks free. With higher CNT contents, Al-2CNT specimen, the multitude cracks became larger, and striations were hardly observed (see Figure 9-9).

In our previous study, it has been showed that Al-0.5CNT composite possess more homogeneous distribution of CNTs, and the possibility of CNT agglomeration and clumping would enhance with high content of CNT. On the other hand, in this study, only few CNTs in the fatigue crack were observed in the Al-0.5CNT. The small fraction of CNT decrease the possibility to observe them is one reason. Another reason is that cracks propagated following tortuous paths to avoid the CNTs, resulting in an absence of CNTs and a rougher surface. This crack deflection served as energy absorbing mechanism, since more micro surface will be created and long distance the crack come through, more energy is believed to be dissipated, which is beneficial to fracture toughness improvement. Whereas, in the fracture surface of materials with higher CNT content (2wt.%), the possibility of CNT agglomeration and clumping would enhance and the agglomerated CNTs were easily observed. The CNT clusters debonded ahead of the crack tip and subsequently crack growth, link and coalesce with the debonded CNT clusters. The growth of fatigue cracks along CNT clusters in the Al-2CNT were confirmed by SEM,

see Figure 9-11, which would lead to pre-failure of the composite under cyclic loading.

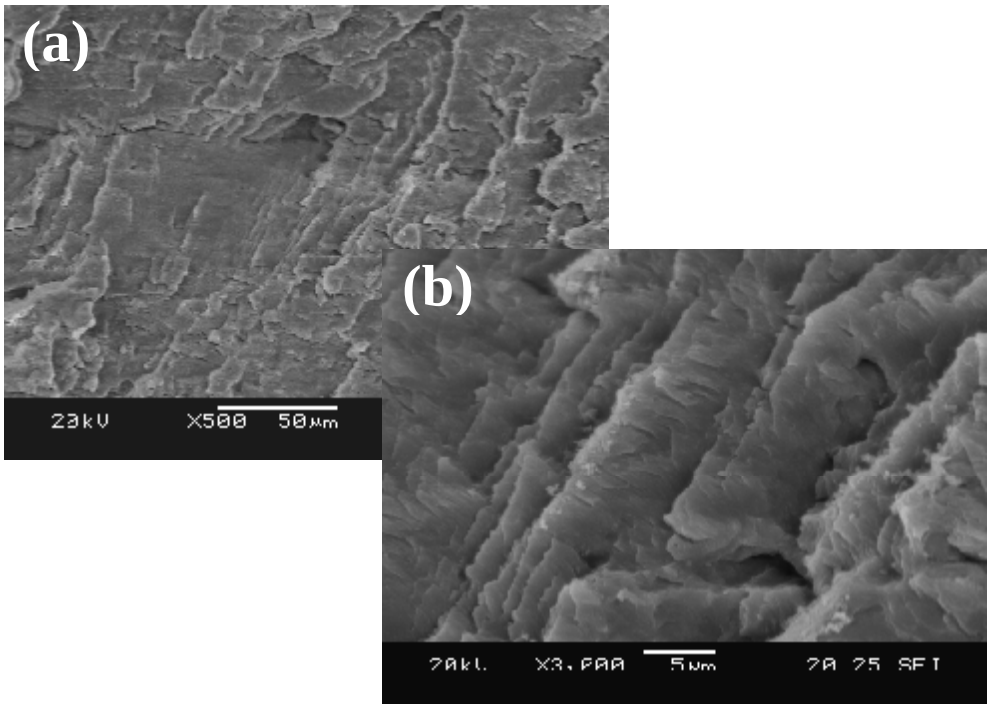

Figure 9-7. Coarse fatigue striations in the fracture surface of monolithic Al: (a) low magnification and (b) high magnification.

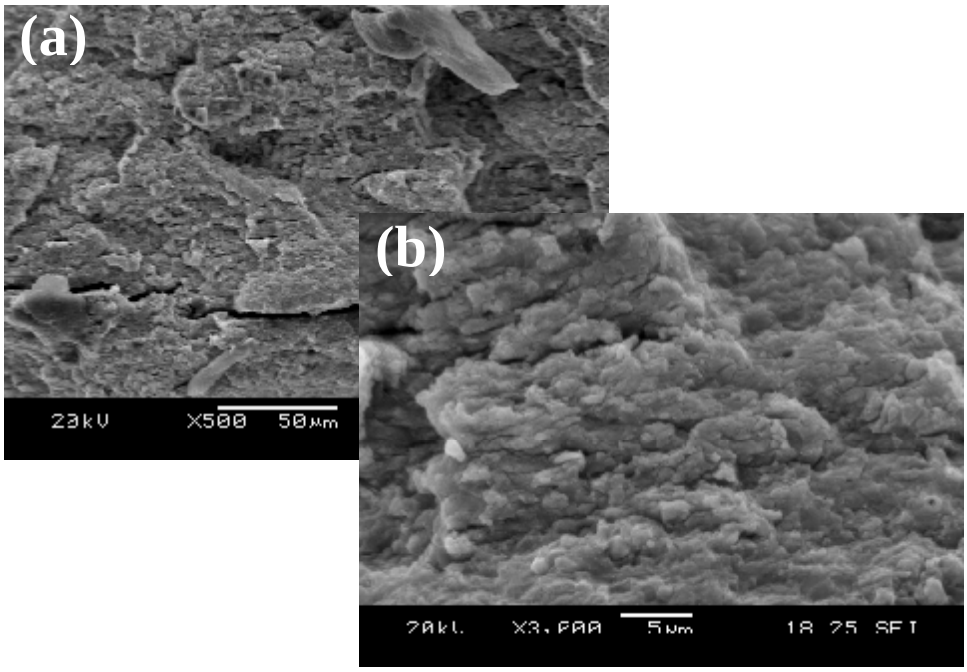

Figure 9-8. Fatigue striations in Al-0.5CNT composite fatigued at a maximum stress of 120MPa: (a) low magnification, and (b) high magnification.

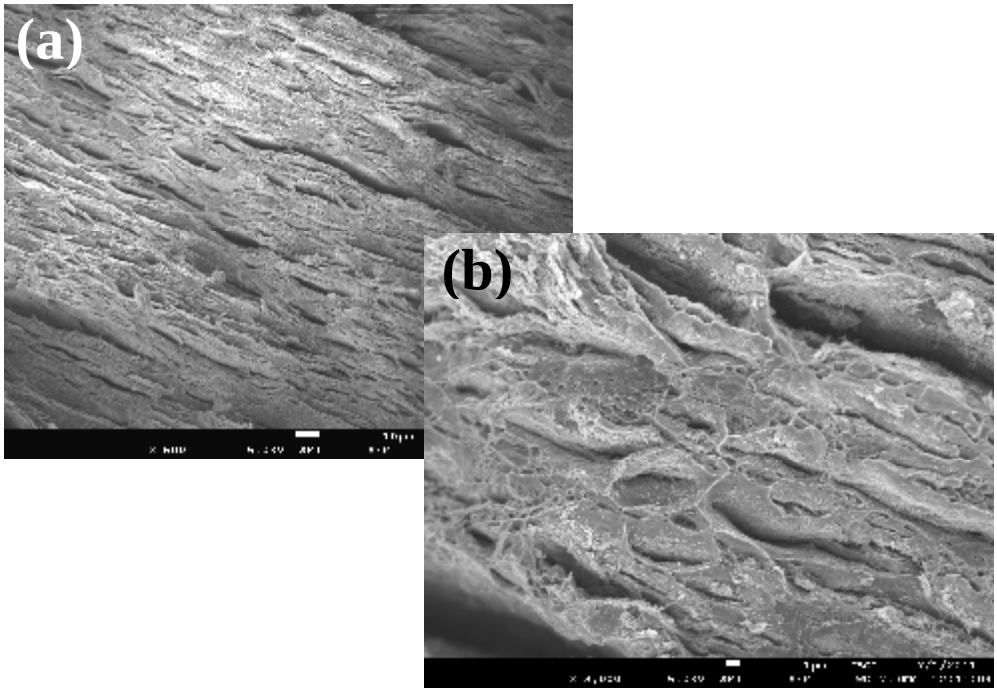

Figure 9-9. Fatigue striations in Al-2CNT composite fatigued at a maximum stress of 120MPa: (a) low magnification, and (b) high magnification.

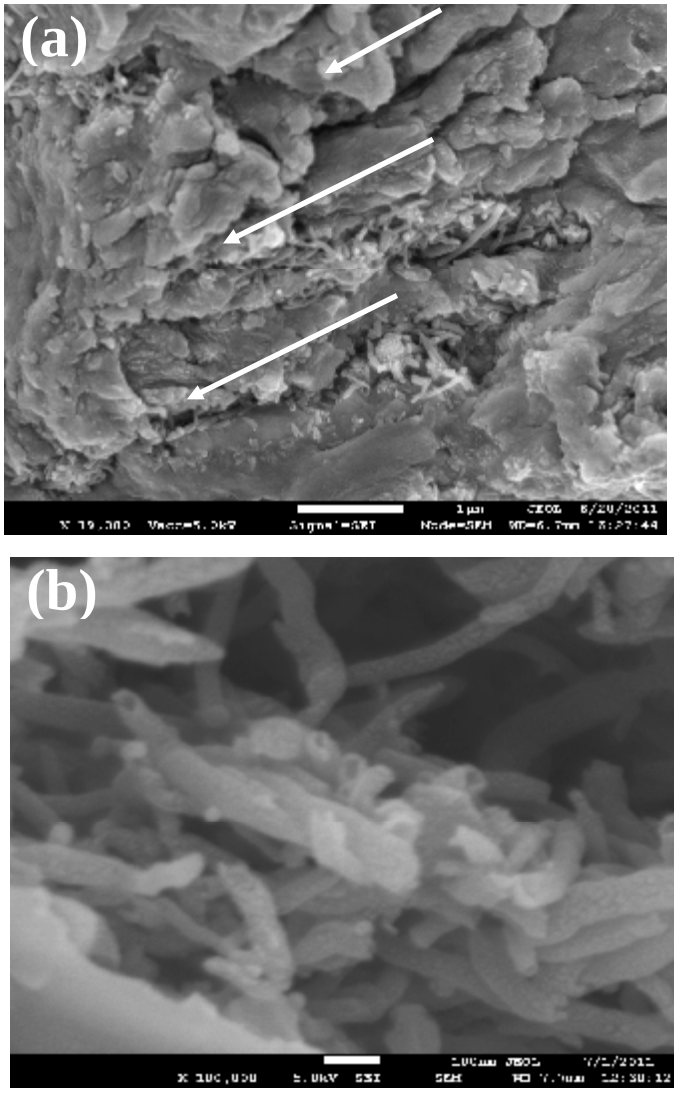

Figure 9-10. (a) SEM observation showed that the CNT clusters appeared favorable to be void initiation sources, and crack grew along these clusters. Arrows indicate the crack growth path; (b) CNT clusters.

The suggested fatigue crack paths were schematically illustrated in Figures 9-11(a) to (c). Figure 9-11(a) corresponds to the monolithic Al, and (b) and (c) corresponds to the composites with a CNT weight fraction of 0.5% and 2%, respectively. In 0.5wt.% CNT composite, the fatigue crack propagated following tortuous paths to avoid the CNTs, resulting a rougher surface. As it can be seen, for a given cyclic load amplitude, the crack would need more number of cycles to grow and coalescence in the materials with obstacle (Figure 9-11(b)) than those without obstacles (Figure 9-11(a)). When the weight fraction of CNT increases, the possibility of CNT agglomeration increases. The CNT clusters were favorable to be void initiation sources, and crack grew along these clusters, then the cracks links and coalescence. This would deteriorate to the fatigue life.

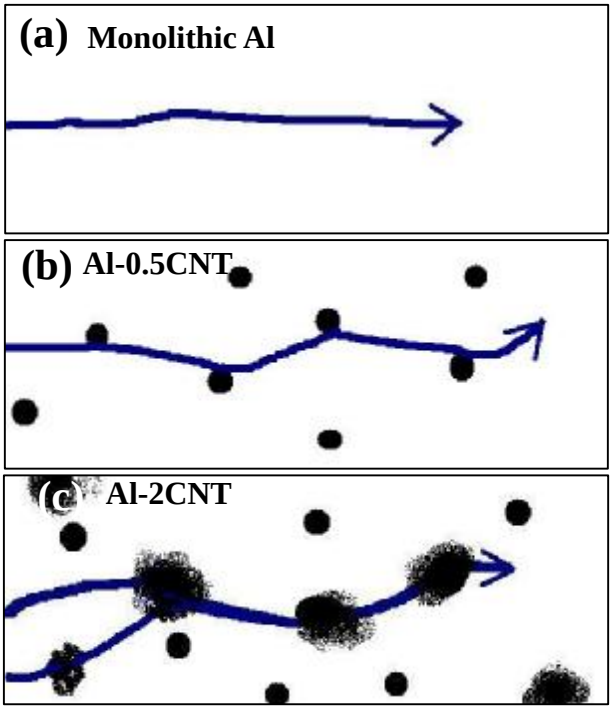

Figure 9-11. Schematic depictions of fatigue crack paths in Al/Al-CNT composites. (a) Monolithic Al; (b) Al-0.5CNT, cracks propagate avoiding the CNTs; and (c) Al-2CNT, cracks grow along the CNT clusters, link and coalescence.

9.4 Conclusions

Based on fatigue investigation on the Al/Al-CNT composites synthesized by P/M technique, the following conclusions can be made:

(i) The CNT participation improved the material damage resistance under cyclic loading. It was found that CNT could suppress fatigue crack propagation by crack-bridging, CNT pullout and breakage mechanism.

(ii) With increasing content of CNTs, the fatigue life declined. It was demonstrated that high yield and ultimate tensile strength of the Al-CNT composites under monotonic loading did not reflect high fatigue strength under cyclic loading. The most superior fatigue resistance was found in the Al-0.5CNT. At lower CNT content composite (0.5%), the cracks grew tortuously to avoid CNTs, whilst they grew along CNT cluster at higher CNT content (2wt.%). The possibility of CNT agglomeration and clumping would enhance with high content of CNT. The CNT clusters favored large crack initiation, link and coalesce, which led to decrease of fatigue life.

CHAPTER 10

CONCLUSIONS

In this work, a sequential study on the fabrication, microstructure and mechanical properties of the Al/Al-CNTs composites was conducted. Significant amount of work involves CNT dispersion, composite processing, mechanical testing and electron microscopy characterization. Special attention was given to the room- and elevated-temperature tension, nanoindentation and fatigue properties evaluation.

1. Processing

Al/Al-CNT composites were synthesized using the powder metallurgy (P/M) technique followed by hot extrusion and hot rolling. 0-2.0wt.% of CNTs were added as reinforcements. CNT incorporation into the Al matrix simultaneously improved the densification, hardness and ultimate tensile strength of the materials. The improved yield strength is contributed to the load partition effect of CNT, thermal mismatch between matrix and CNT, and Orowan strengthening. CNTs were subjected to substantial compression stress not only in powder mixing but also in subsequent consolidation process due to constraint from the consolidation and shrinkage from thermal mismatch. These compressive stresses not only contributed to a sound CNT/matrix interfacial adhesion, but also facilitated the load transfer effect.

Amongst the plethora of processing techniques, this study provided a simple technique to

produce Al-CNT nanocomposite. Specimens with fine structure were produced by a Spread-Dispersion method. Compared with the monolithic Al, an enhancement in tensile strength of 66% of the Al-CNT nanocomposite was obtained with minor decrease in ductility. The improved tensile strength was contributed to the segregation and uniform-distribution of clustered CNTs, disappearance of the CNT-free zones, stronger Al/CNT bonding and the retention of CNT graphitic structure.

2. CNT Evolution during Composite Processing

One important issue that should be noted is the graphitic structure of CNTs during the P/M steps. The CNT evolution during composite processing was precisely tracked by Raman spectroscopy assisted with SEM and TEM. The separation of CNTs was affected by both the powder mixing operation and the secondary processing. Secondary processing with a large enough deformation could homogeneously redistribute the reinforcements. The amount of defects increased in the CNTs after mixing and sintering due to the physical compression force; whilst the graphitic structures were not damaged during the secondary processing. CNTs were subjected to substantial compression stress not only in powder mixing during powder mixing but whilst sintering, due to constraint from the consolidation and shrinkage from thermal mismatch.

3. Nanoindentation, Elevated-temperature Tension and Fatigue Properties

3.1 Nanoindentation

Nanoindentation test was applied to detect the local mechanical properties of Al/Al-CNT specimens. Different local regions of the as-extruded and tensile-fractured specimen over

the longitudinal and transverse section were studied.

(i) In the as-extruded specimen the values of nanoindentation hardness (H) and elastic modulus (E) obtained reached maximum at the 0.5wt.% CNT adding Al samples, which corresponded well with those obtained from conventional macro- and microscopic tests previously reported.

(ii) Elastic modulus was highest in the necking region then decreased with increasing distance from the localized deformed region. This variation was due to different degrees of strain hardening.

(iii) Nanoindentation hardness and elastic modulus of the transverse direction were less than those of the longitudinal direction. This anisotropy was due to texture hardening of the Al matrix and the alignment of CNT.

3.2 Elevated-temperature Tension

Elevated-temperature tensile tests on Al/Al-CNT composites were performed in air at temperature from 25 to 500 °C, with a stresses rate of 1×10^{-3}/s.

(i) The incorporation of CNT raised the overall stress level at the all temperature range, respect to the unreinforced counterparts. An enhancement as high as 102% was obtained at 200℃.

(ii) Fracture properties of the composite were affected by the tensile temperature. The CNT slippage and Al/CNT separation were observed. The tensile strain of the CNT composite continuously decreased with the increasing testing temperature (hot embrittlement), as a contrary of the monolithic Al. The causes of such hot embrittlement were suggested to be attributed to the interfacial

segregation, large surface contact area of matrix/CNT, and CNT clusters.

3.3 Fatigue

Tension-tension fatigue tests on Al/Al-CNT composites were performed using a sinusoidal wave function at a stress ratio $R = \sigma_{min}/\sigma_{max} = 0.1$ and at a frequency of 5Hz. The maximum stresses applied were 100, 110, 120, 130, 140 and 150MPa.

(i) The CNT participation improved the material damage resistance under cyclic loading. It was found that CNT could suppress fatigue crack propagation by crack-bridging, CNT pullout and breakage mechanism.

(ii) With increasing content of CNTs, the fatigue life declined. It was demonstrated that high yield and ultimate tensile strength of the Al-CNT composites under monotonic loading did not reflect high fatigue strength under cyclic loading. The most superior fatigue resistance was found in the Al-0.5CNT. At lower CNT content composite (0.5%), the cracks grew tortuously to avoid CNTs, whilst grew along CNT cluster at higher CNT content (2wt.%). The possibility of CNT agglomeration and clumping would enhance with high content of CNT. The CNT clusters favored large crack initiation, link and coalesce, which led to decrease of fatigue life.

CHAPTER 11

SUGGESTIONS FOR FUTURE WORK

1. Diameter and Length Dependent Strength of CNT Reinforced Metal Composites

It is expected that for a given length, smaller CNT diameters would result in greater total interfacial bonding area thus the greater resultant strength of the composite. On the other hand, for a given diameter, the longer CNT (higher aspect ratio) would share load better. But it was recently reported by Esawi *et al* [126] that compared to the larger diameter CNTs, the smaller-diametered ones were more difficult to disperse with increasing CNT content. This would subsequently decrease the tensile properties and hardness of the composites. Another issue is that longer CNTs may lead to more entanglement of the nanotubes. Up to date, there has been limited report on the effect of CNT diameter and length on the metal composites [126]. Effectiveness of composites evaluated in terms of various dimensions like diameter and length of CNT is of value.

2. CNT Reinforced Al Alloys Based Composites

In this study, commercial pure Al powder was used as the matrix material, and for the available literature on CNT reinforced Al based composites, most of the matrices used were pure Al. Only a few researchers used Al alloys as the matrices, like Al2024 [127, 155], Al2124 [156], Al60601 [156]. Additional insight on the Al alloys based composite can be study, especially the 2xxx (Al-Cu/Al-Cu-Mg) and 6xxx (Al-Mg-Si alloys) series

aluminum alloys, which have recently found increased application in construction, automotive (for body panels and bumbers) and aerospace (for fuselage skins and other applications) industries because of their attractive combinations of properties. Furthermore, the influence of heat treatment on the strength of these Al alloy composites with CNTs is of great interest too. It is expected that the addition of a reinforcing phase to a metal alloy could significantly increase the dislocation density in the matrix when cooling down from the solution heat-treatment temperature [157]. CNT reinforced Al alloys based composites are worthy of investigation.

3. Hybrid Composites

Hybrid composites are engineering combinations of two or more reinforcements. Hybrid composites are expected to possess better properties compared with singular reinforced composites as they combine the advantages of their constituent reinforcements, which provides a rather high degree of freedom in material design [158]. There have been some studies on the hybrid Al composites, like Al/SiC_p/SiC_w [158], Al/graphite nanofiber (GNF)/alumina short fiber (Al_2O_3sf) [159], Al/SiC/graphite hybrid composites [160], and improved tensile strength and wear resistance were obtained. Addition of micro-scale ceramic reinforcements such as SiC, Al_2O_3, TiC, B_4C and ZrO_2, with the nano-scale CNT into metal matrix are expected to improve strength, hardness and thermal shock resistance of the composites. There has been report on the magnesium based hybrid composites containing nano-sized SiC and CNTs [161], however, the Al based hybrid composite with CNT and other reinforcements has not been reported. Further studies conducted on Al based SiC/Al_2O_3/TiC-CNT micro/nano hybrid composites are of great significance.

REFERENCES

[1] Alexander E, Christopher SM, Andreas M (2003) Metal matrix composites in industry: an introduction and a survey. Springer, Dordrecht

[2] Antonio M (1993) Metal matrix composites: proceedings of the Ninth International Conference on Composites (ICCM/9) Woodhead Publishing, Madrid

[3] Iijima S (1991) Nature 354:56

[4] Noguchi T, Magario A, Fukazawa S, Shimizu S, Beppu J, Seki M (2004) Mater Trans 45:602

[5] George R, Kashyap KT, Rahul R, Yamdagni S (2005) Scripta Mater 53:1159

[6] Bakshi SR, Singh V, Seal S, Agarwal A (2009) Surf Coat Technol 203:1544

[7] Xu CL, Wei BQ, Ma RZ, Liang J, Ma XK, Wu DH (1999) Carbon 37:855

[8] Huang JY, Chen S, Wang ZQ, Kempa K, Wang YM, Jo SH, Chen G, Dresselhaus MS, Ren ZF (2006) Nature 439:281

[9] Bhalerao GM, Sinha AK, Sathe V (2008) Physica E 41:54

[10] Enomoto K, Kitakata S, Yasuhara T, Ohtake N, Kuzumaki T, Mitsuda Y (2006) Appl Phys Lett 88: 153115

[11] Baughman RH, Zakhidov AA, de Heer WA (2002) Science 297:787

[12] Ajayan PM (1993) Nature 361:333

[13] Ajayan PM, Ebbesen TW, Ichihashi T, Iijima S, Tanigaki K, Hiura H (1993) Nature 362:522

[14] Ajayan PM, Redlich P, Rühle M (1997) J Microscopy 185:275

[15] Morsi K, Esawi AMK, Lanka S, Sayed A, Taher M (2010) Composites Part A 41:322

[16] Li QQ, Rottmair CA, Singer RF (2010) Compos Sci Technol 70:2242

[17] Kwon H, Park DH, Silvain JF, Kawasaki A (2010) Compos Sci Technol 70:546

[18] Kwon H, Kawasaki A (2009) J Nanosci Nanotechnol 9:6542

[19] Kwon H, Estili M, Takagi K, Miyazaki T, Kawasaki A (2009) Carbon 47:570

[20] Joo SH, Yoon SC, Lee CS, Nam DH, Hong SH, Kim HS (2010) J Mater Sci 45:4652

[21] Esawi AMK, Morsi K, Sayed A, Taher M, Lanka S (2010) Compos Sci Technol 70:2237

[22] Deng CF, Ma YX, Xue XB, Zhang XX, Wang DZ (2010) Mater Sci Technol 18:229

[23] Choi HJ, Lee SM, Bae DH (2010) Wear 270:12

[24] Choi HJ, Shin JH, Min BH, Bae DH (2010) Composites Part A 41:327

[25] Choi HJ, Shin JH, Min BH, Park JS, Bae DH (2009) J Mater Res 24:2610

[26] Bakshi SR, Lahiri D, Agarwal A (2010) Int Mater Rev 55:41

[27] Wang L, Choi H, Myoung JM, Lee W (2009) Carbon 47:3427

[28] Lim DK, Shibayanagi T, Gerlich AP (2009) Mater Sci Eng A 507:194

[29] Paramsothy M, Hassan SF, Srikanth N, Gupta M (2009) Composites Part A 40:1490

[30] Torralba JM, da Costa CE, Velasco F (2003) J Mater Process Technol 133:203

[31] Esawi AMK, Borady MAE (2008) Compos Sci Technol 68:486

[32] Esawi AMK, Morsi K, Sayed A, Gawad AA, Borah P (2009) Mater Sci Eng A 508:167

[33] Pérez-Bustamantea R, Estrada-Guel I, Amézaga-Madrid P, Miki-Yoshida M, Herrera-Ramírez M, Martínez-Sánchez R (2009) Mater Sci Eng A 502:159

[34] Hasan H (2006) Aluminum. The Rosen Publishing Group, New York

[35] Joseph RD & ASM International Handbook Committee (1993) Aluminum and aluminum alloys. ASM International

[36] Rosso M (2006) J Mater Process Technol 175:364

[37] Pal TK (2005) Mater Manuf Processes 20: 717

[38] Marikani A (2009) Engineering Physics. Asoke K. Ghosh, PHI Learning Private Limited, New Delhi

[39] Iijima S, Ichihashi T (1993) Nature 363:603

[40] Bethune DS (1993) Nature 363:605

[41] Dai LM (2006) Carbon nanotechnology: recent developments in chemistry, physics, materials science and device applications. Elsevier, Netherlands

[42] Cheng WW, Lin ZQ, Wei BF, et al. (2011) Int J Biochem Cell Biol 43:564

[43] Ci LJ, Rao ZL, Zhou ZP, Tang DS, Yan YQ, Liang YX, Liu DF, Yuan HJ, Zhou WY, Wang G, Liu W, Xie SS (2002) Chem Phys Lett 359:63

[44] Suresh A (2007) Processing and properties of nanocomposites. World Scientific Publishing, Delaware

[45] Ajayan PM, Tour JM (2007) Nature 447:1066

[46] Huang JY, Chen S, Wang ZQ, Kempa K, Wang YM, Jo SH, Chen G, Dresselhaus MS, Ren ZF (2006) Nature 439:281

[47] Fiedler B, Gojny FH, Wichmann MHG, Nolte MCM, Schulte K (2006) Compos Sci Technol 66:3115

[48] Bakshi SR, Agarwal A (2011) Carbon 49:533

[49] Morsi K, Esawi AMK, Borah P, Lanka S, Sayed A, Taher M (2010) Mater Sci Eng A 527:5686

[50] Morsi K, Esawi AMK, Borah P, Lanka S, Sayed A (2010) J Compos Mater

44:1991

[51] Tjong SC (2009) Carbon nanotube reinforced composites: metal and ceramic matrices. Wiley-VCH,

[52] Yuuki J, Kwon H, Kawasaki A, Magario A, Noguchi T, Beppu J, Seki M (2007) Mat Sci Forum 534-536:889

[53] Laha T, Y Liu, A Agarwal (2007) Journal of Nanoscience and Nanotechnology 7:515

[54] Rul S, Lefèvreschlick F, Capria E, Laurent C, Peigney A (2004) Acta Mater 52:1061

[55] Sun J, Gao LA, Jin XH (2005) Ceram Int 31:893

[56] Ye F, Liu LM, Wang YJ, Zhou Y, Peng B, Meng QC (2006) Scripta Matall 55:911

[57] Xia Z, Riester L, Curtin WA, Li H, Sheldon BW, Liang J, Chang B, Xu JM. (2004) Acta Mater 52:931

[58] Curtin WA, Sheldon BW (2004) Mater Today 7:44

[59] Kumari L, Zhang T, Du GH, Li WZ, Wang QW, Datye A, Wu KH (2008) Compos Sci Technol 68:2178

[60] Ionescu E, Francis A, Riedel R (2009) J Mater Sci 44:2055

[61] Wei T, Fan ZJ, Luo GH, Wei F, Zhao DQ, Fan JP (2008) Mater Res Bull 43:2806

[62] Peigney A, Flahaut E, Laurent C, Chastel F, Rousset A (2002) Chem Phys Lett 352:20

[63] Spigarelli S, Cabibbo M, Evangelista E, Langdon TG (2002) Mater Sci Eng A 328:39

[64] Li Y, Langdon TG (1997) Acta Mater 45:4797

[65] Rupesh K, Suryasarathi B (2005) J Miner Mater Char Eng 4:31

[66] Neubauer E, Kitzmantel M, Hulman M, Angerer P (2010) Compos Sci Technol 70:2228

[67] Pérez-Bustamante R, Estrada-Guel I, Amézaga-Madrid P, Miki-Yoshida M, Herrera-Ramírez JM, Martínez-Sánchez R (2009) J Alloys Compd 495:399

[68] Li QQ, Viereckl A, Rottmair CA, Singer RF (2009) Compos Sci Technol 69:1193

[69] Salimi S, Izadi H, Gerlich A (2011) J Mater Sci 46:409

[70] Kwon H, Park DH, Silvain JF, Kawasaki A (2010) Compos Sci Technol 70:546

[71] Wu YF, Kim GY, Russell AM (2012) Mater Sci Eng A 532:558

[72] Choi HJ, Shin JH, Bae DH (2011) Compos Sci Technol 71:1699

[73] He C, Zhao N, Shi C, et al. (2007) Adv Mater 19:1128

[74] Kuzumaki T, Miyazawa K, Ichinose H, Ito K (1998) J Mater Res 13:2445

[75] Takashi Y, Nobuyuki K, Satoshi N, Koichi U, Ken T (2006) Electrochemistry, 74:233

[76] Bakshi SR, Singh V, Balani K, McCartney DG, Seal S, Agarwal A (2008) Surf Coat Technol 202:5162

[77] Bak JH, Kim YD, Hong SS, et al. (2008) Nature Mater 7:459

[78] Ci LJ, Ryu ZY, Jin-Phillip NY, Ruhle M (2006) Acta Mater 54:5367

[79] Tan MJ, Zhang X (1998) Mater Sci Eng A 244:80

[80] Deng CF, Zhang XX, Wang DZ, Lin Q, Li AB (2007) Mater Lett 61:1725

[81] Choi HJ, Bae DH (2011) Mater Sci Eng A 528:2412

[82] Angelo PC, Subramanian R (2008) Powder Metallurgy: Science, Technology And Applications. PHI.

[83] Yoshio S, Tatami J, Yamakawa T, Wakihara T, Komeya K, Meguro T, Aramaki K, Yasuda K (2011) Carbon 49:4131

[84] Ahn JH, Wang Y, Kim YJ, Kim SJ, Chung H (2007) Mater Sci Forum 539-543:860

[85] Inam F, Yan H, Reece MJ, Peijs T (2008) Nanotechnol 19

[86] Lau KT (2005) Compos Sci Technol 65:719

[87] Suryanarayana C (2004) Mechanical alloying and milling. Marcel Dekker, New York

[88] Xia K (2010) Adv Eng Mater 12:724

[89] Koch CC (2002) Nanostructured materials: processing, properties and potential applications. Noyes Publications, William Andrew Publishing

[90] Deng CF, Zhang XX, Ma Y, Wang D (2007) Rare Met 26:450

[91] Lahiri D, Bakshi SR, Keshri AK, Liu Y, Agarwal A (2009) Mater Sci Eng A 523:263

[92] Li YH, Housten W, Zhao YM (2007) Nanotechnol 18

[93] Zhang Z, Chen DL (2006) Scripta Mater 54:1321

[94] Thostenson ET, Li CY, Chou TW (2005) Compos Sci Technol 65:491

[95] Chou YC, Hsieh TF, Hsieh YC, Lin CP, Shu CM (2010) J Therm Anal Calorim 102:641

[96] Saito Y, H Utsunomiya, N Tsuji, T Sakai (1999) Acta Mater 47:579

[97] Quadir MZ, Ferry M, Al-Buhamad O, Munroe PR (2009) Acta Mater 57:29

[98] Quadir MZ, Wolz A, Hoffman M, Ferry M (2008) Scripta Mater 58:959

[99] Eizadjou M, Kazemi TA, Danesh MH, Shakur SH, Janghorban K (2008) Compos Sci Technol 68:2003

[100] Laha T, Agarwal A, McKechnie T, Seal S (2004) Mater Sci Eng A 381:249

[101] Laha T, S Kuchibhatla, S Seal, W Li, A Agarwal (2007) Acta Mater 55:1059

[102] Laha T, Chen Y, Lahiri D, Agarwal A (2009) Composites Part A 40:589

[103] Laha T, Agarwal A (2008) Mater Sci Eng A 480:323

[104] Zhou SM, Zhang XB, Ding ZP, Min CY, Xu GL, Zhu WM (2007) Composites Part A 38:301

[105] Nalwa HS (2002) Handbook of thin film materials: Nanomaterials and magnetic thin films. Academica press,

[106] Kim I, Lee JH, Lee GS, Baik SH, Kim YJ, Lee YZ (2009) Wear 267:593

[107] Vidal-Sétif MH, Lancin M, Marhic C, et al. (1999) Mater Sci Eng A 272:321

[108] Xia Z, Curtin WA (2004) Phys Rev B, Condens Matter 69

[109] Ebbesen TW, Takada T (1995) Carbon 33:973

[110] Chandra N, Namilae S (2006) Mech Adv Mater Struct 13:115

[111] Kelly PM (1972) Scr Mater 6:647

[112] Xia K (1994) J Mater Sci 29:5219

[113] Lee JC, Subramanian KN (1992) Mater Sci Eng A 159:43

[114] Mitra R, Chalapathi RVS, Maiti R, Chakraborty M (2004) Mater Sci Eng A 379:391

[115] Pierard N, Fonseca A, Colomer JF, Bossuot C, Benoit JM, Tendeloo GV (2004) Carbon 42:1691

[116] Coleman JN, Khan U, Gun'ko YK (2006) Adv Mater 18:689

[117] Subramoney S (1998) Adv Mater 10:1157

[118] Rao CNT (2001) Chem Phys 2:78

[119] Wong EW (1997) Science 277:1971

[120] Schadler LS (1998) Appl Phys Lett 73:3842

[121] Kelly PM (1972) Scr Metall 6:647

[122] Arsenault RJ, Shi N (1986) Mat Sci Eng 81:175

[123] Joachim R, Harald H, Martin B (2007) Mechanical behaviour of engineering materials: metals, ceramics, polymers, and composites. Springer Berlin Heidelberg, New York

[124] Hari SN (2002) Handbook of thin film materials: Nanomaterials and magnetic thin films. Academica press, Michigan

[125] Inoue S, Ichikuni N, Susuki T, Uematsu T, Kaneko K (1998) J Phys Chem B 102:4689

[126] Esawi AMK, Morsi K, Sayed A, Taher M, Lanka S (2011) Composites Part A 42:234

[127] Pérez-Bustamante R, Pérez-Bustamante F, Estrada-Guel I, et al. (2011) Powder Technol In Press, Corrected Proof, doi: 10.1016/j.powtec.2011.06.007

[128] So KP, Lee IH, Duong DL, Kim TH, Lim SC, An KH, Lee YH (2011) Acta Materialia 59:3313

[129] Yasuna K, Terauchi M, Otsuki A, shihara KN, Shingu PH (1997) J Appl Phys 82:2435

[130] Yasuna K, Terauchi M, Otsuki A, Ishihara KN, Shingu PH (2000) Mater Sci Eng A 285:412

[131] Helmi A, Alexander JM (1968) Iron Steel Inst 206:1110

[132] Lee JC, Subramanian KN (1995) Mat Sci Eng A 196:71

[133] Jamaati R, Toroghinejad MR (2010) Mater Des 31:4816

[134] Kim KT, Cha SI, Hong SH (2006) Mater Sci Eng A 430:27

[135] Dong SR, Tu JP, Zhang XB (2001) Mater Sci Eng A 313:83

[136] Morsi K, Esawi A (2007) J Mater Sci 42:4954

[137] Dresselhaus MS (2000) Adv Phys 49:705

[138] Sridhar I, Karthic N (2009) J Mater Sci 44:1750

[139] Liu L (2008) Mech Res Commns 35:256

[140] Pathak S, Stojakovic D, Kalidindi SR (2009) Acta Mater 57:3020

[141] Soer WA, De Hosson J (2005) Mater Lett 59:3192

[142] Li Y, Kang R, Gao H, Wang J, Lang Y (2009) Rare Met 28:570

[143] Oliver WC, Pharr GM (1992) J Mater Res 7:1564

[144] Yao C, Srinivasa RB, Arvind A (2009) ACS Appl Mater Interfaces 1:235

[145] Borrego A, Fernández R, María D, Ibáñez J, González-Doncel G (2002) Comp Sci Technol 62:731

[146] Davies PW, Dunstan GR, Evans RW, Wilshire B (1971) J Inst Met 99:195

[147] Kelly A, Tyson WR (1965) J Mech Phys 13:329

[148] Mu M, Osswald S, Gogotsi Y, Winey KI (2009) Nanotechnology 20

[149] Modi OP, Singh AK, Yegneswaran AH, Rohatgi PK (1992) J Mater Sci Lett 11:1466

[150] He YQ, Qiao B, Wang N, et al (2009) Chinese J Nonferrous Met 20:469

[151] Zhang WL, Gu MY, Chen JY, Wu ZG, Zhang F, Deve HE (2003) Mater Sci Eng A 341:9

[152] ASTM (2007) Standard Practice for Conducting Force Controlled Constant Amplitude Axial Fatigue Tests of Metallic Materials, ASTM International

[153] Estili M, Kawasaki A, Sakamoto H, Mekuchi Y, Kuno M, Tsukada T (2008) Acta Mater 56:4070

[154] Chawla N, Shen YL (2001) Adv Eng Mater 3:357

[155] Choi HJ, Min BH, Shin JH, Bae DH Composites Part A In Press, Corrected Proof

[156] Saheb N (2011) Adv Mater Res 239-242:759

[157] Oguocha INA, Yannacopoulos S (1996) J Mater Sci 31:3145

[158] Zhang XN, Geng L, Wang GS (2006) J Mater Process Technol 176:146

[159] Babu JSS, Kang CG, Kim HH (2011) Mater Des 32:3920

[160] Guo MLT, Tsao CYA (2000) Compos Sci Technol 60:65

[161] Thakur S, Kwee G, Gupta M (2007) J Mater Sci 42:10040

APPENDIX

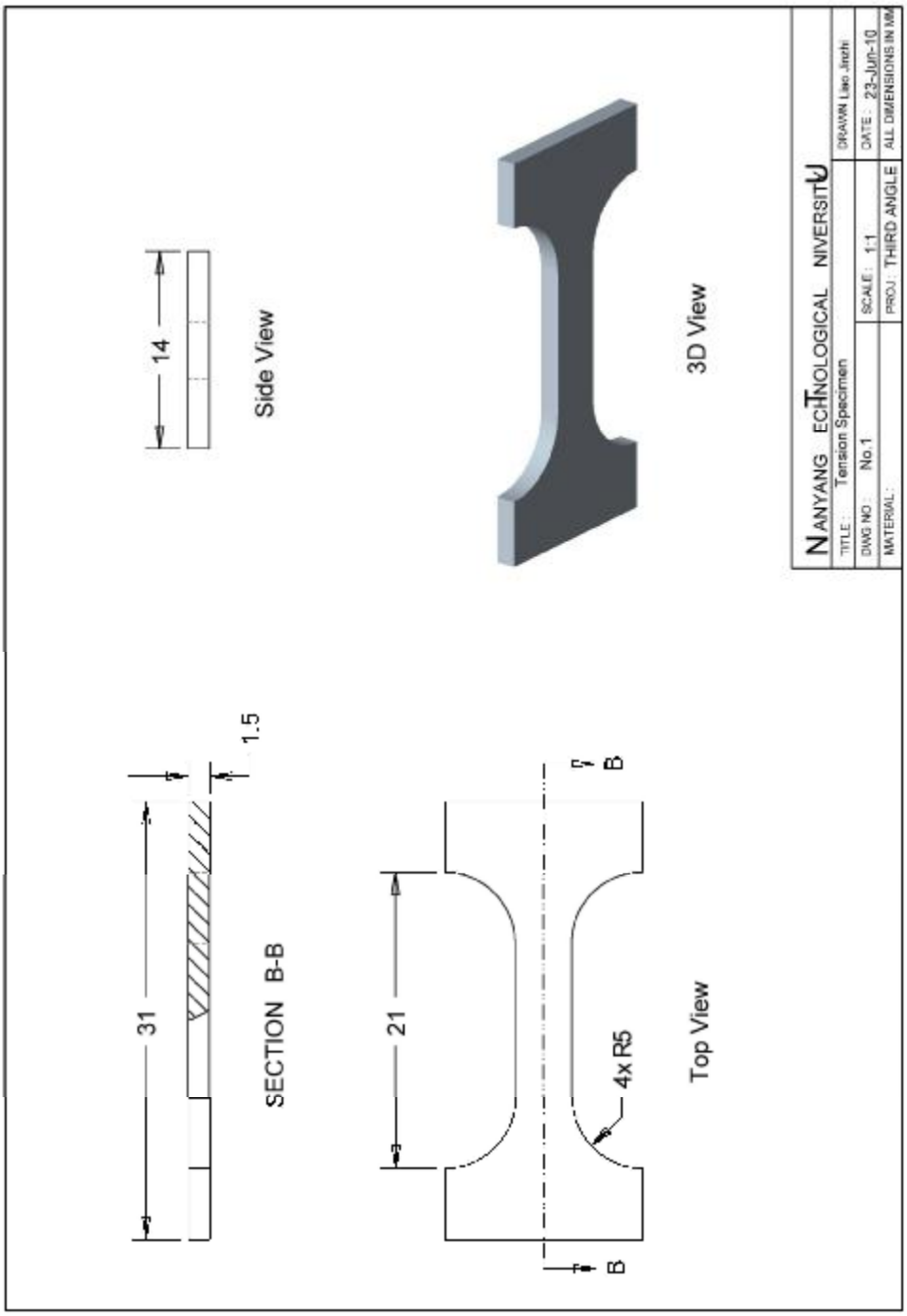

Appendix I. Illustration of the tensile testing specimen (used at room and elevated temperature).

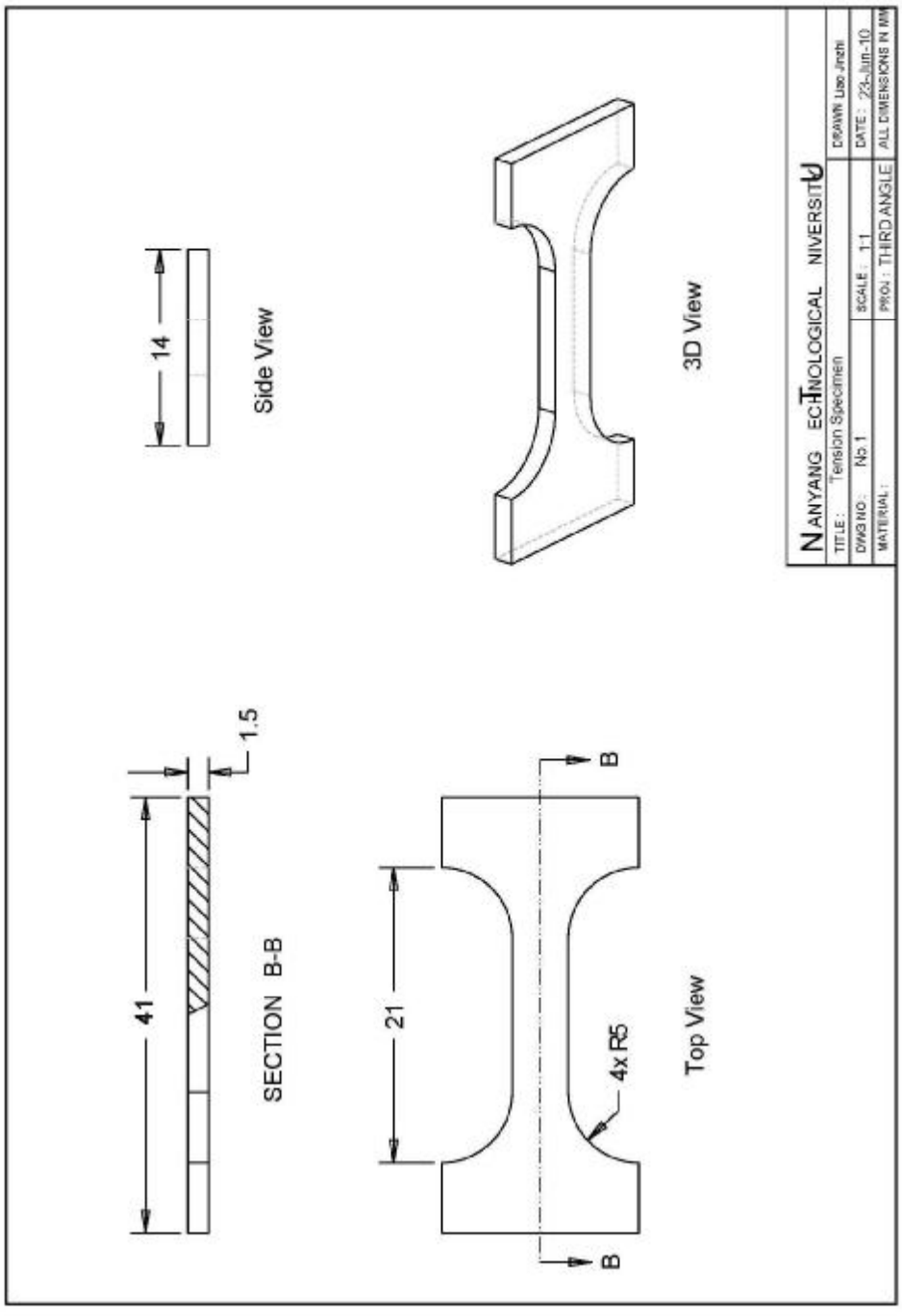

Appendix II. Illustration of the fatigue testing specimen geometry.

PUBLICATIONS

Journal papers:

2010

[1] J.Z. Liao, M.J. Tan, I. Sridhar. Spark plasma sintered multi-wall carbon nanotube reinforced aluminum matrix composites. Materials and Design, 2010;31(S1):S96-S100.

[2] J.Z. Liao, J.J. Pang, M.J. Tan. Nanoindentation of Multi-wall CNT Reinforced Al Composites. Key Engineering Materials, 2010;447-448:549-53.

2011

[3] J.Z. Liao, M.J. Tan. Mixing of carbon nanotubes (CNTs) and aluminum powder for powder metallurgy use. Powder Technology. 2011;208(1):42-8.

[4] J.Z. Liao, M.J. Tan. Carbon nanotube evolution in aluminum matrix during composite fabrication process. Materials Science Forum, 2011;690:294-7.

[5] J.Z. Liao, M.J. Tan. A simple approach to prepare Al/CNT composite: Spread-Dispersion (SD) method. Materials Letter, 2011;65:2742-44.

[6] J.Z. Liao, M.J. Tan, A. Santoso, High strength aluminum nanocomposites reinforced with multi-walled carbon nanotubes. Advance Materials Research, 2011;311-313:80-83.

2012

[7] J.Z. Liao, M.J. Tan. Improved tensile strength of carbon nanotube reinforced aluminum composites processed by powder metallurgy. Advance Materials Research, 2012;500:651-656.

Conference papers:

2009

[1] J.Z. Liao, M.J. Tan, I. Sridhar. Fabrication and superplasticity of MWCNTs/Al composites, International Conference on Materials for Advanced Technologies (ICMAT 2009), Singapore.

2010

[2] J.Z. Liao, M.J. Tan, I. Sridhar. Nanoindentation of multi-wall CNT reinforced Al composites, International Conference on Precision Engineering ICoPE 2010 & 13th ICPE (ICoPE), Singapore.

[3] J.Z. Liao, M.J. Tan, et al., Novel carbon nanotube reinforced aluminum composite assisted by polymer-binder, in Materials Science & Technology Conference & Exhibition 2010: Houston, Texas, US. Vol 4, p. 2263-2267.

2011

[4] J.Z. Liao, M.J. Tan. Preparation of carbon nanotube reinforced aluminum composite by Spread-Dispersion (SD) method, in East Asian Postgraduate Workshop on Nanoscience and Technology (pgws2011), Hong Kong.

[5] J.Z. Liao, M.J. Tan. Wear resistance of carbon nanotube reinforced aluminum composites, International Conference on Materials for Advanced Technologies (ICMAT 2011), Singapore.

[6] J.Z. Liao, M.J. Tan, A. Santoso. High strength aluminum nanocomposites reinforced with multi-walled carbon nanotubes, The 2011 International Conference on Advanced

Design and Manufacturing Engineering (ADME 2011), Guangzhou, China.

[7] J.Z. Liao, M.J. Tan. Fatigue behavior of Al/CNT composite, in Materials Science & Technology Conference & Exhibition 2011: Columbus, Ohio, US.

2012

[8] J.Z. Liao, M.J. Tan, Improved tensile strength of carbon nanotube reinforced aluminum composites processed by powder metallurgy. The 10th Asia-Pacific Conference on Materials Processing (APCMP2012), Jinan, China.